

AD710775

August 1970
Report 1341-26F

APPLICATIONS OF CUMULATIVE DAMAGE IN THE PREPARATION
OF PARAMETRIC GRAIN DESIGN CURVES AND THE
PREDICTION OF GRAIN FAILURES ON PRESSURIZATION

FINAL REPORT

1 April 1969 through 28 February 1970

VOLUME II - APPENDICES A THROUGH M

By

K. W. Bills, Jr., D. M. Campbell, R. D. Steele and
J. D. McConnell

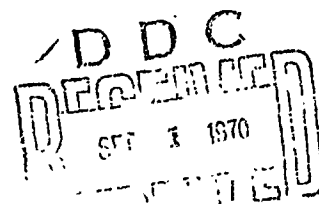
Aerojet Solid Propulsion Company
Sacramento, California

and

Consultants: L. R. Herrmann, University of California and
R. J. Farris, University of Utah

Prepared For

Department of the Navy
Naval Ordnance Systems Command (ORD-0331)
Contract No. N00017-69-C-4423



THIS DOCUMENT CONTAINED
BLANK PAGES THAT HAVE
BEEN DELETED

BEST AVAILABLE COPY

NOTICE TO USERS

Portions of this document have been judged by the Clearinghouse to be of poor reproduction quality and not fully legible. However, in an effort to make as much information as possible available to the public, the Clearinghouse sells this document with the understanding that if the user is not satisfied, the document may be returned for refund.

If you return this document, please include this notice together with the IBM order card (label) to:

Clearinghouse
Attn: 152.12
Springfield, Va. 22151

Report 1341-26F

APPLICATIONS OF CUMULATIVE DAMAGE IN THE PREPARATION
OF PARAMETRIC DESIGN CURVES AND THE PREDICTION OF
GRAIN FAILURES ON PRESSURIZATION

VOLUME II - APPENDICES A THRU M

PREPARED FOR

DEPARTMENT OF THE NAVY
NAVAL ORDNANCE SYSTEMS COMMAND (ORD-0331)
CONTRACT NO. N00017-69-C-4423

Prepared by:

K. W. Bills, Jr.
K. W. Bills, Jr.
Associate Scientist
Propellant Physics

Approved by:

G. J. Svob
G. J. Svob, Manager
Integrated Grain Design
and Weights, Department 4320

Aerojet Solid Propulsion Company

Report 1341-26F

VOLUME II

TABLE OF CONTENTS

APPENDIX A	Modulus Data Input for the Computer
APPENDIX B	Parameter Study for History 1
APPENDIX C	Parameter Study for History 2
APPENDIX D	A New Normalized Relation for the Relaxation Modulus
APPENDIX E	Incremental Analysis Procedure
APPENDIX F	Prony Series Curve Fit Analysis
APPENDIX G	Inclusion of Non-Zero Thickness Stresses in Plane Stress Analyses
APPENDIX H	A Computer Program for Viscoelastic Solids of Revolution Subjected to Time-Varying Thermal and Mechanical Load Environments - Version 2.1
APPENDIX I	Non-Linear Analyses Based on Propellant Dilatation
APPENDIX J	Basic Cumulative Damage Equations
APPENDIX K	Study of Propellant Failure Under Pressure
APPENDIX L	Effects of Previous Damage
APPENDIX M	Input Data for Pressurization Tests on a PBAN Propellant

APPENDICES

APPENDIX A

MODULUS DATA INPUT FOR THE COMPUTER

Aerojet Solid Propulsion Company

Report 1341-26F

Appendix A

MODULUS DATA INPUT FOR THE COMPUTER

The relaxation modulus was represented by a sixteen-term Prony series. This relation for the tensile modulus, $E(t)$, is

$$E(t) = A_0 + \sum_{i=1}^m A_i e^{-\beta_i t} \quad (A-1)$$

where A_0 , A_i , and β_i are constants.

For an incompressible material the relaxation modulus in shear, $\mu(t)$, is given by

$$\mu(t) = \frac{E(t)}{3} = \frac{A_c}{3} + \sum_{i=1}^m \frac{A_i}{3} e^{-\beta_i t} \quad (A-2)$$

The viscoelastic stress analyses requires the shear modulus representation.

The Prony series constants employed in the present parameter study are given in Table A-1, for the CTPB propellant, and in Table A-2, for the HTPB propellant.

To complete the viscoelastic description the time-temperature shift function, a_T , is required. Hence, also listed in Tables A-1 and A-2 are the logarithms of a_T at 12 different temperatures from -100° to $+200^\circ\text{F}$, for the two referenced propellants.

Aerojet Solid Propulsion Company

Report 1341-26F

TABLE A-2

MODULUS INPUT FOR THE HTPB PROPELLANT

Prony Series Parameters					
$\log (t/a_T)$ (min)	E psi	β_i (hr ⁻¹)	A_i	$A_i/3$	i
			80	26.67	0
-8	10000	3×10^9	4376.65	1458.9	1
-7	7000	3×10^8	3697.78	1232.6	2
-6	4000	3×10^7	2056.49	685.50	3
-5	2400	3×10^6	896.865	298.96	4
-4	1600	3×10^5	665.701	221.90	5
-3	1050	3×10^4	384.337	128.11	6
-2	720	3×10^3	250.028	83.343	7
-1	500	3×10^2	180.589	60.196	8
0	350	3×10^1	106.550	35.517	9
1	260	3×10^0	67.0877	22.363	10
2	205	3×10^{-1}	35.8845	11.962	11
3	170	3×10^{-2}	39.3243	11.441	12
4	140	3×10^{-3}	24.4644	8.155	13
5	120	3×10^{-4}	15.1300	5.043	14
6	110	3×10^{-5}	-2.4636	-0.8212	15
7	100	3×10^{-6}	33.0018	11.001	16

Time-Temperature Shift Function

Temp., °F	$\log_{10} a_T$
-75	6.90
-50	4.93
-25	3.41
0	2.35
25	1.48
50	0.72
77	0
100	-0.46
125	-0.90
150	-1.24
170	-1.47

APPENDIX B
PARAMETER STUDY FOR HISTORY 1

Aerojet Solid Propulsion Company

Report 1341-26F

APPENDIX B

PARAMETER STUDY FOR HISTORY 1

The results of a series of one-dimensional, thermoviscoelastic analyses are presented graphically in this appendix. All of the analyses were based upon the environmental temperature history described in the text and shown separately in each figure. The data for the CTPB propellant are presented in Figures B-1 to B-6, while those for the HTPB propellant are given in Figures B-7 to B-12.

No analyses of the results are made here.

A. CTPB PROPELLANT

The following graphs give the thermoviscoelastic solutions for these grain designs.

PARAMETER STUDY OF INNER-BORE HOOP STRAINS
CTPB PROPELLANT - HISTORY 1
(B = 4 in.)

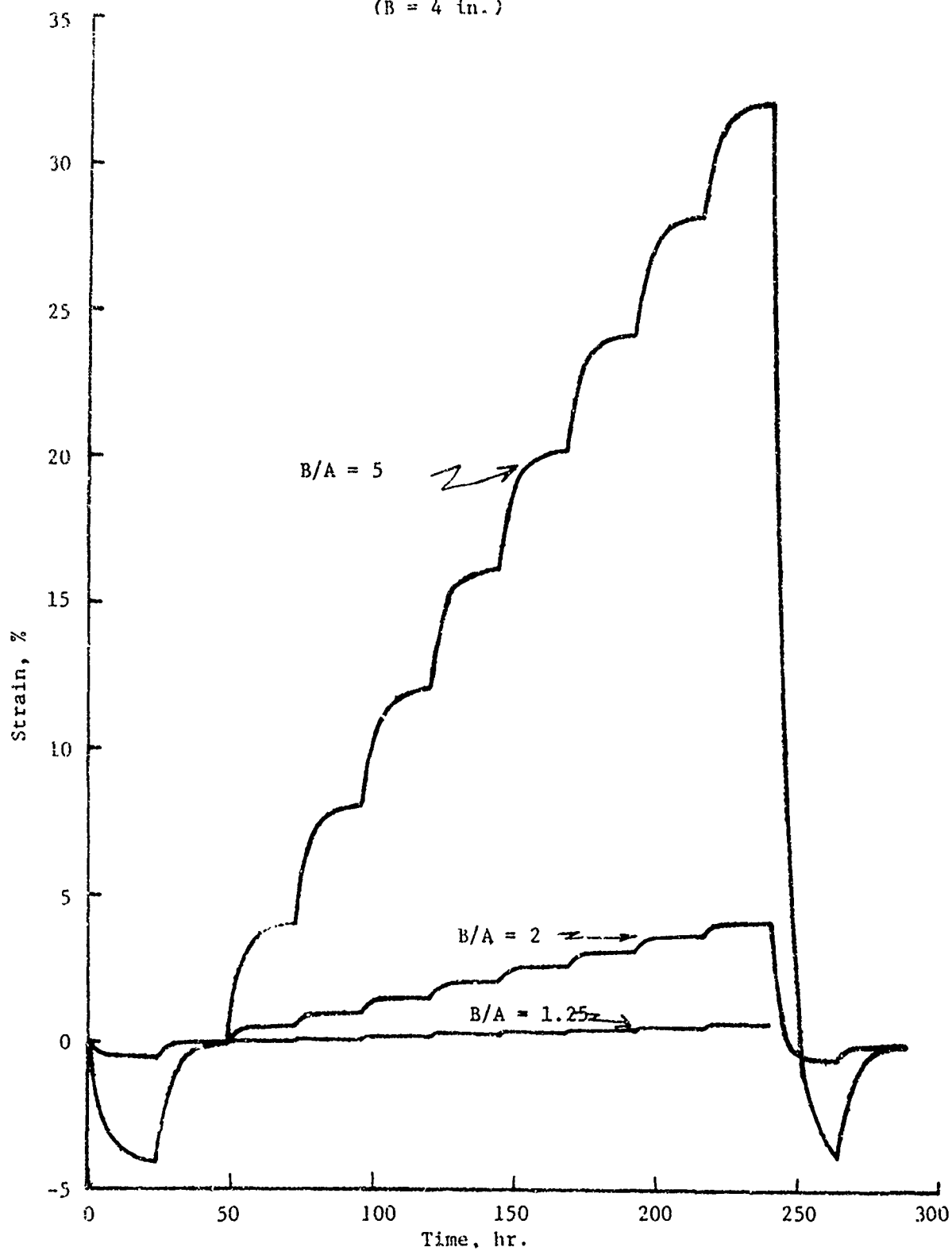


Figure B-1

PARAMETER STUDY OF INNER-BORE HOOP STRAINS
CTPB PROPELLANT - HISTORY 1
(B = 8 in.)

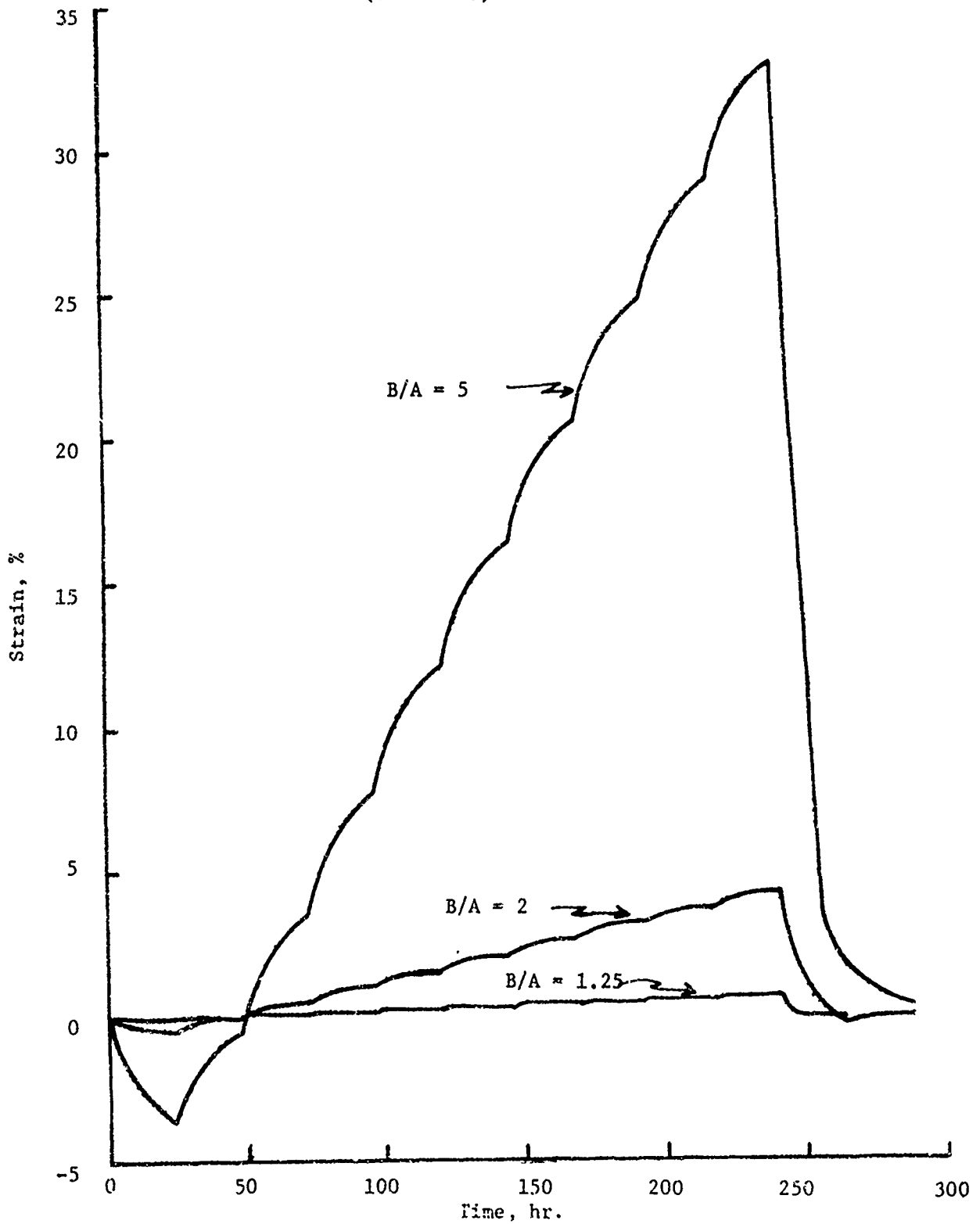
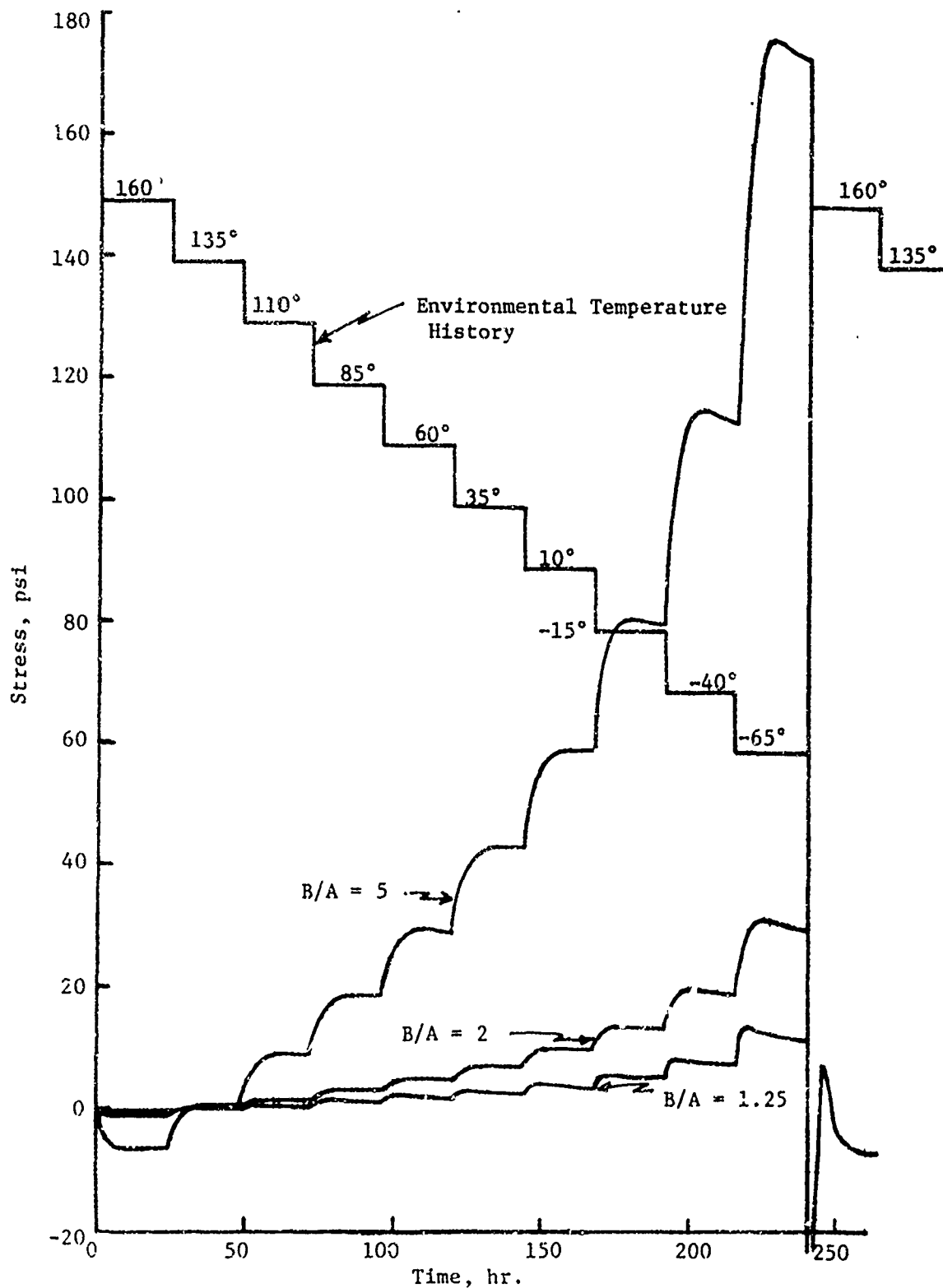


Figure B-2

PARAMETER STUDY OF INNER-BORE HOOP STRESS SOLUTIONS
CTPB PROPELLANT - HISTORY 1
(B = 4 in.)



PARAMETER STUDY OF INNER-BORE HOOP STRESS SOLUTIONS
CTPB PROPELLANT - HISTORY 1
(B = 8 in.)

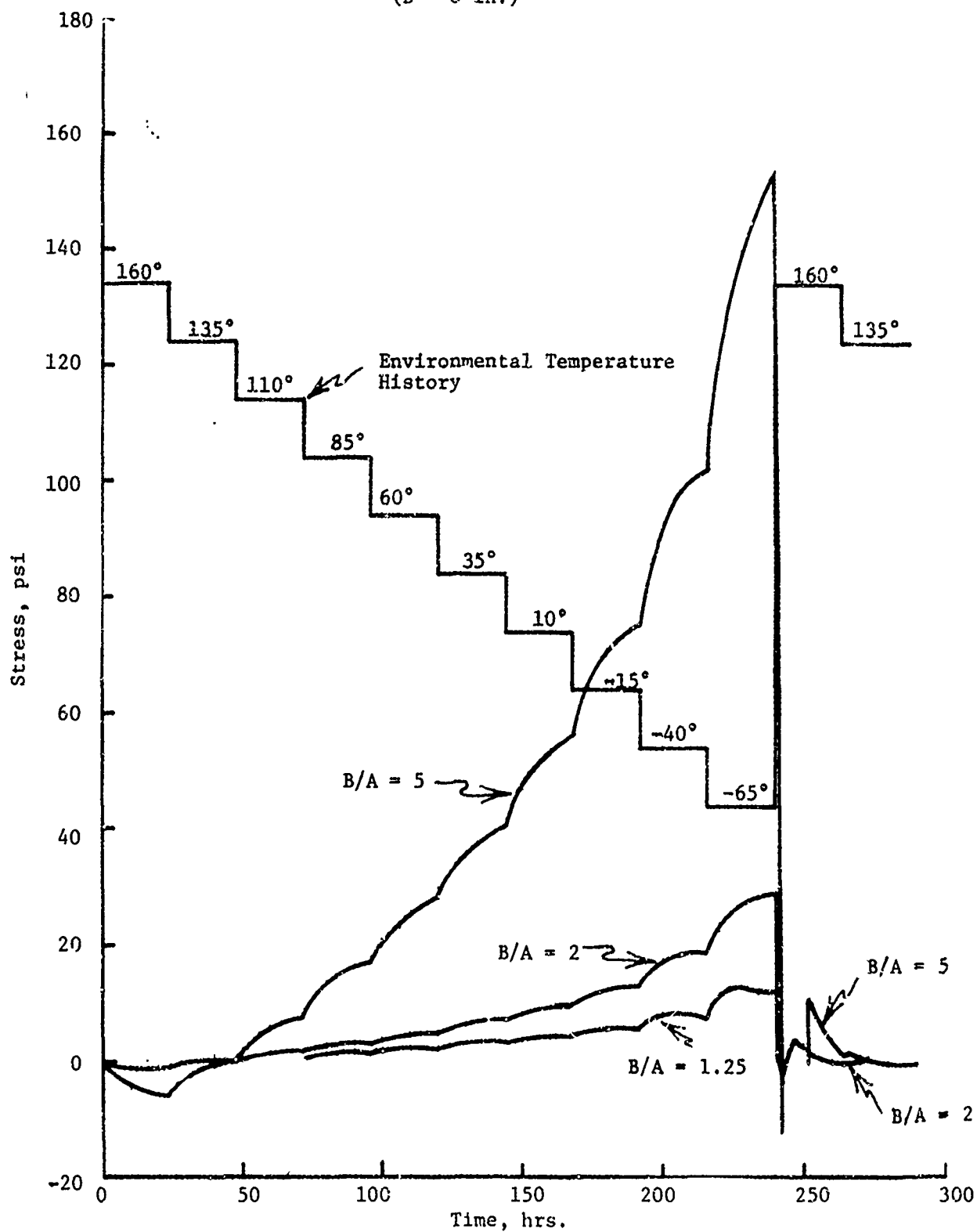


Figure B-4

PARAMETER STUDY OF RADIAL BOND STRESS SOLUTIONS
CTPB PROPELLANT - HISTORY 1

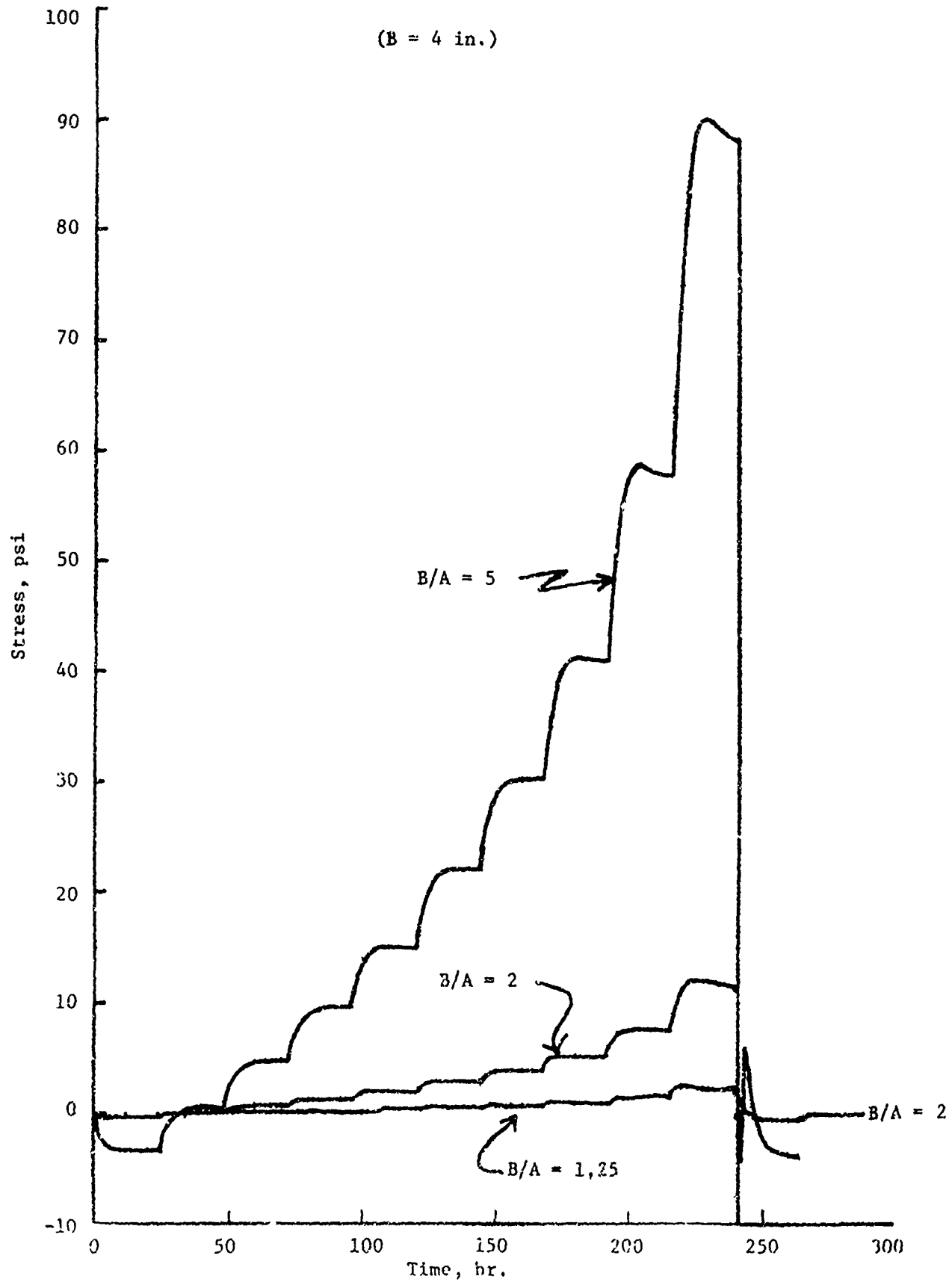


Figure B-5

PARAMETER STUDY OF RADIAL BOND STRESS SOLUTIONS
CTPB PROPELLANT - HISTORY 1

(B = 8 in.)

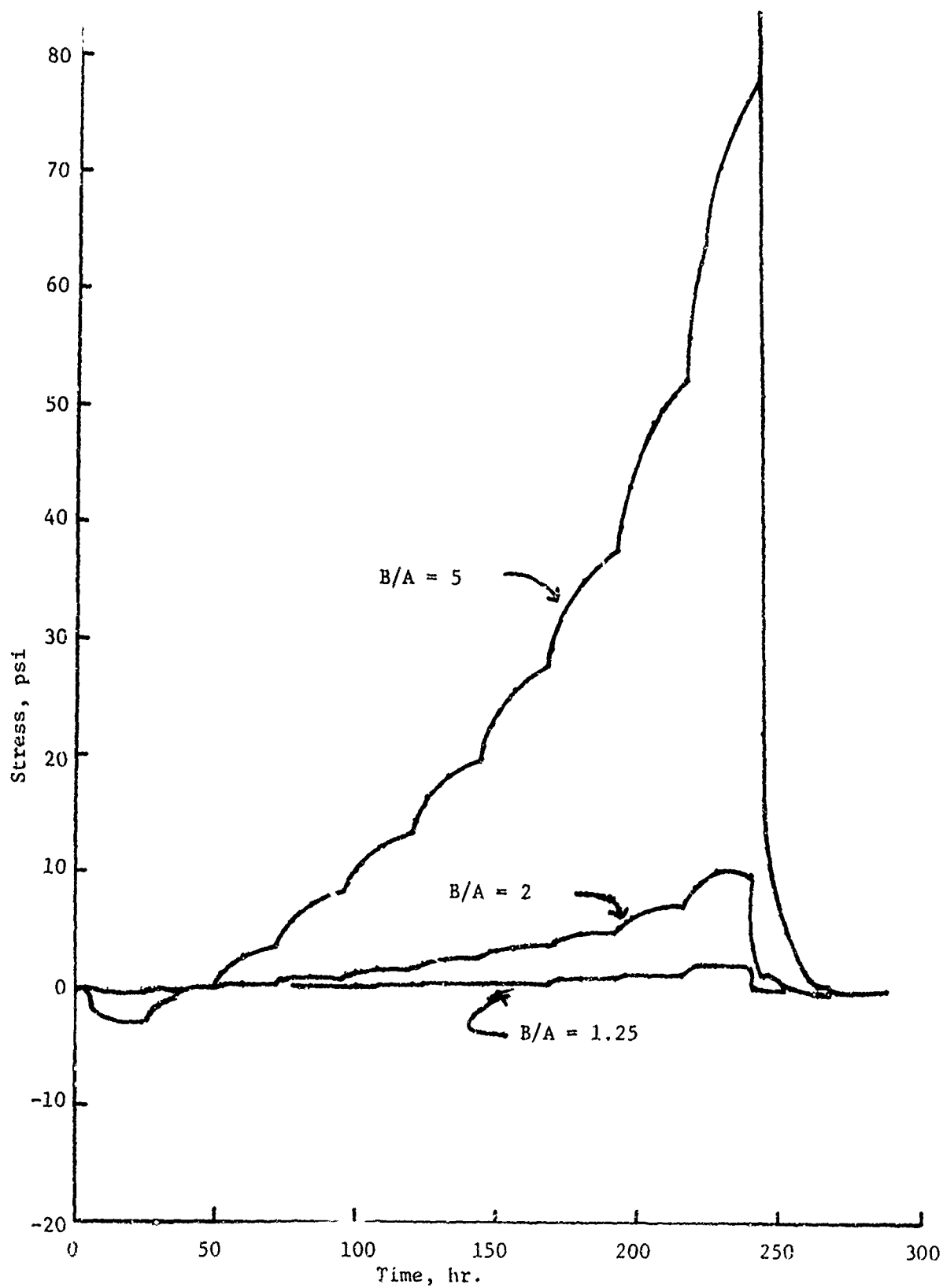


Figure B-6

Aerojet Solid Propulsion Company

Report 1341-26F

Appendix B

B. HTPB PROPELLANT

The following graphs give the thermoviscoelastic solutions for these grain designs.

PARAMETER STUDY OF INNER-BORE HOOP STRAINS
HTPB PROPELLANT - HISTORY 1

(B = 4 in.)

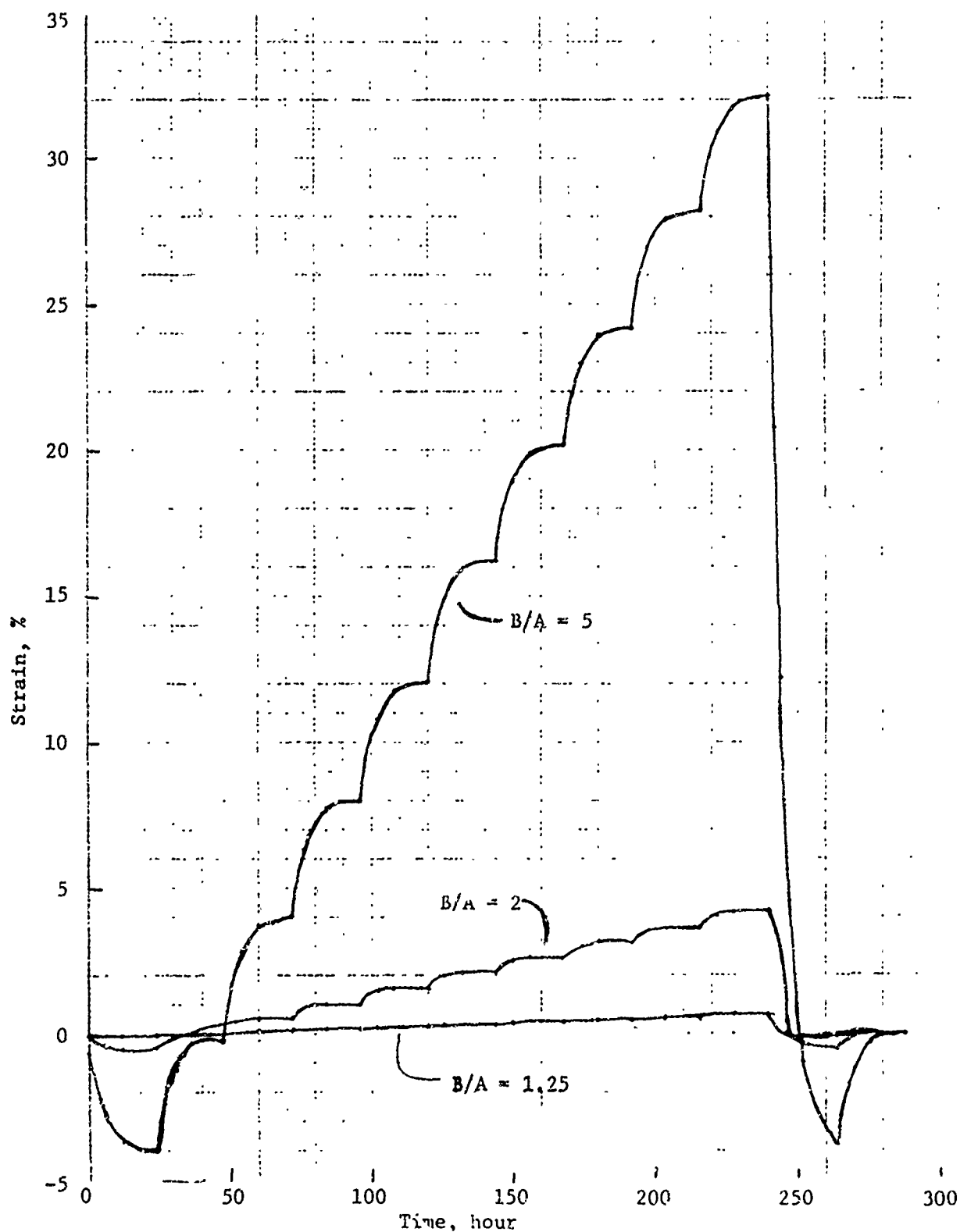


Figure B-7

Aerojet Solid Propulsion Company
Report 1341-267

PARAMETER STUDY OF INNER-BORE HOOP STRAINS
HTPB PROPELLANT - HISTORY 1

Appendix B

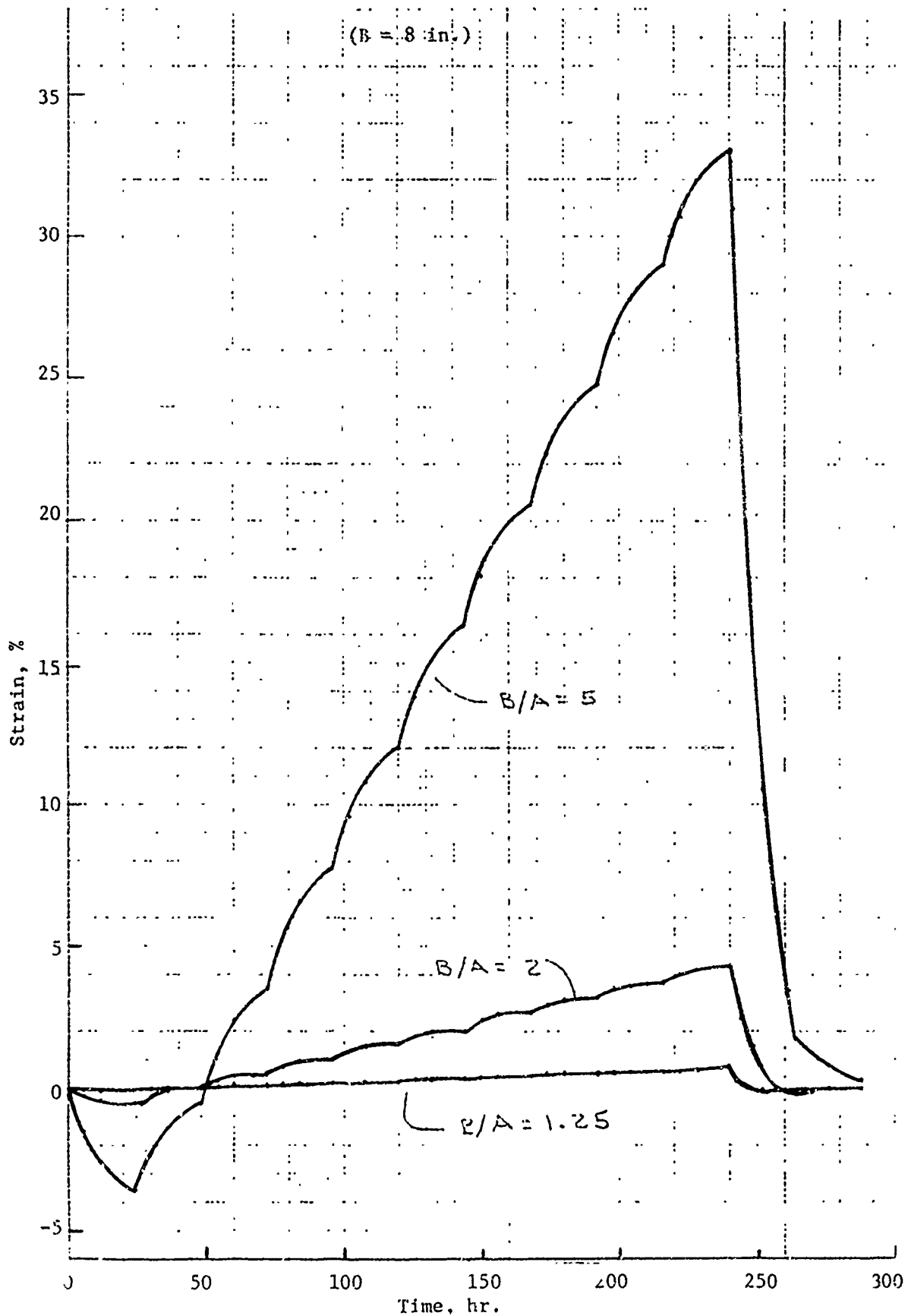


Figure B-8

PARAMETER STUDY OF INNER-BORE HOOP STRESS SOLUTIONS
HTPB PROPELLANT - HISTORY 1

(B = 4 in.)

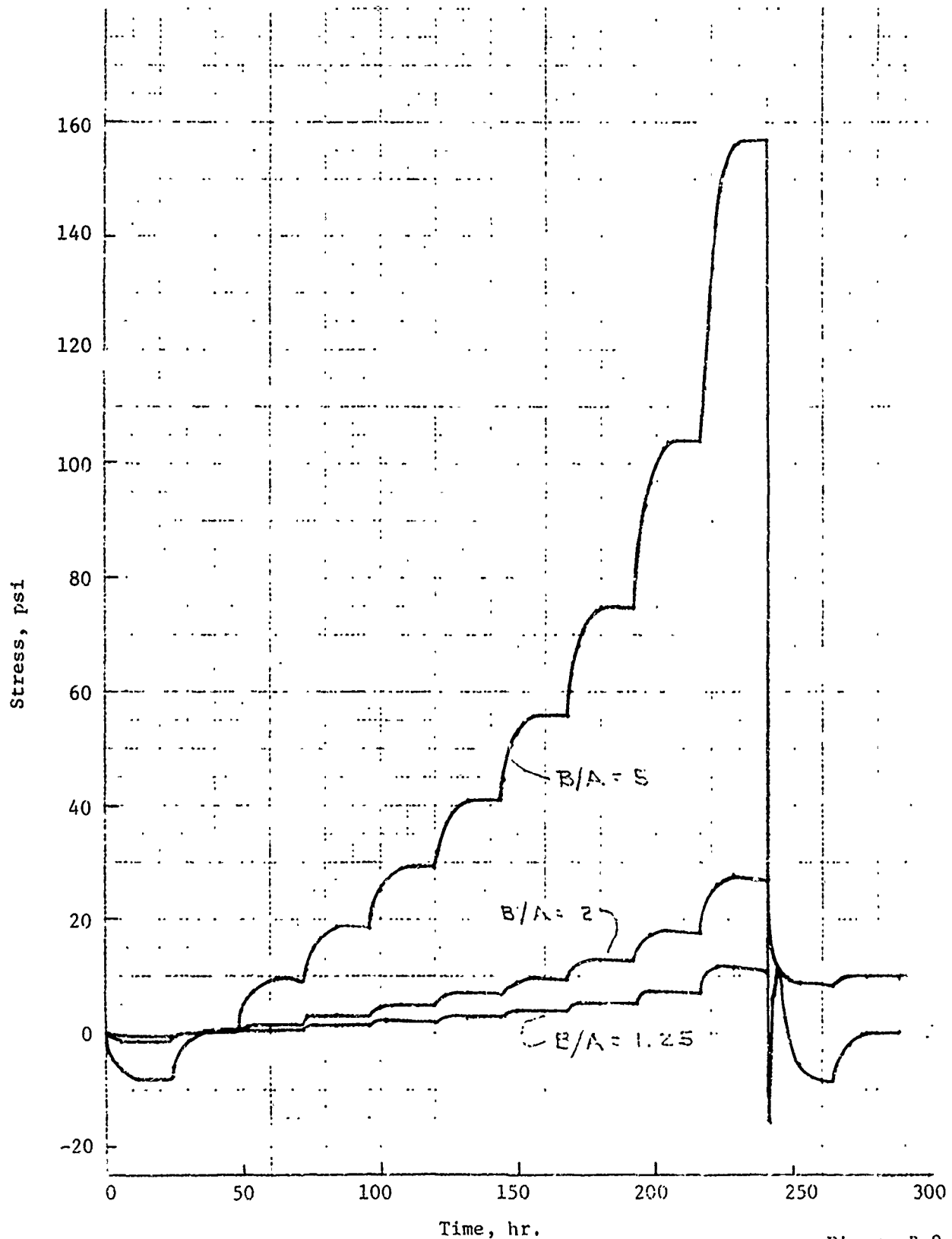
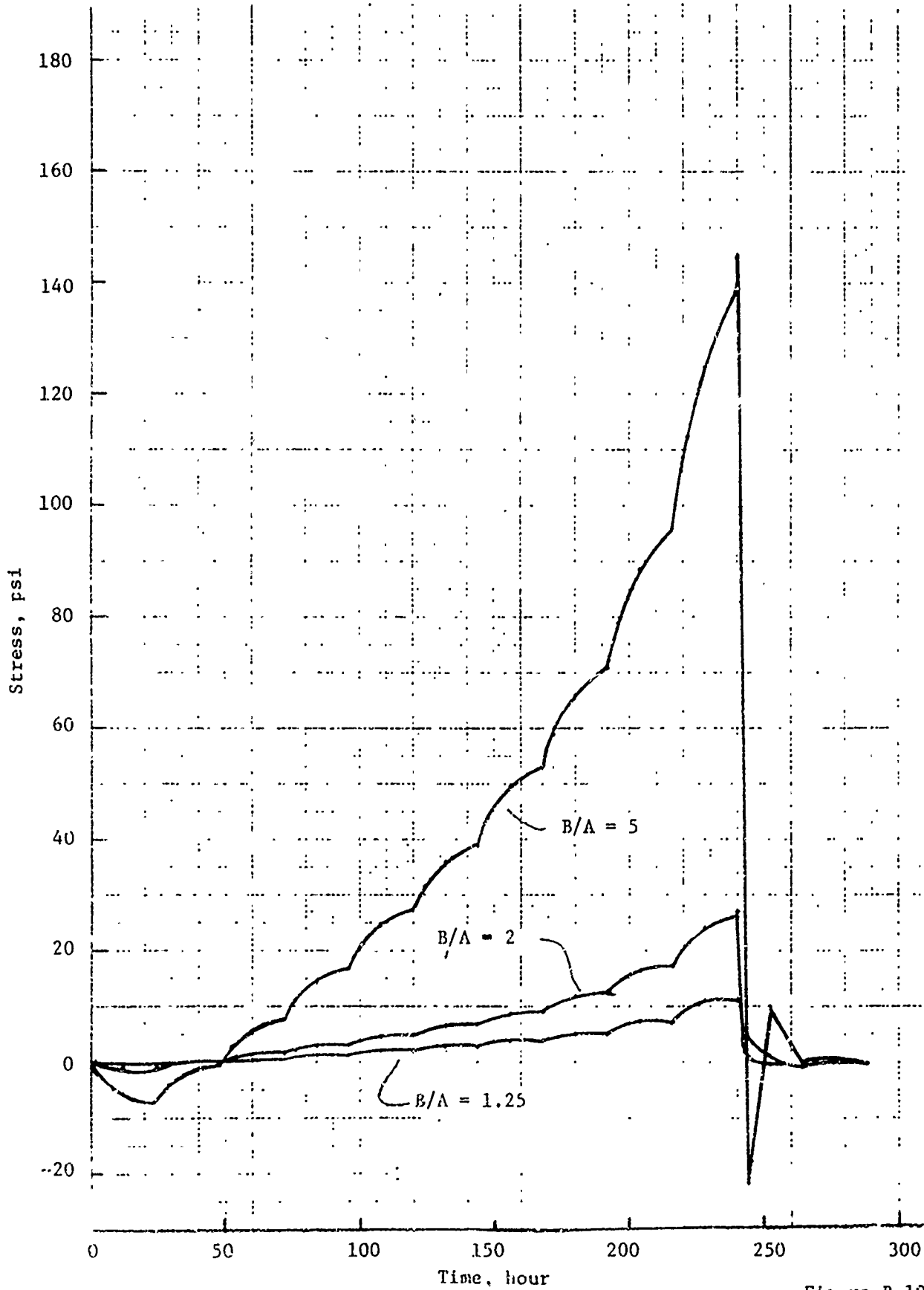
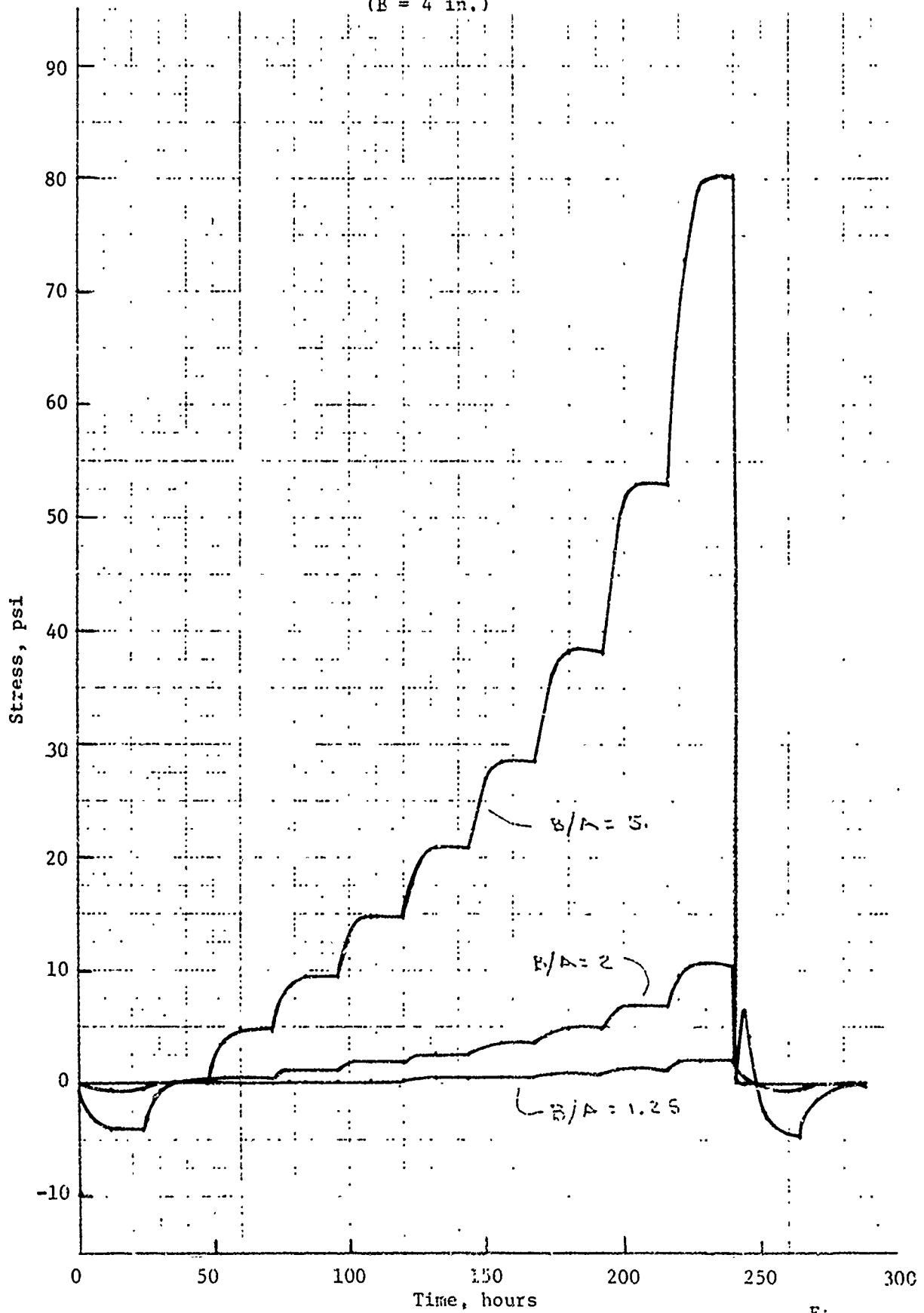


Figure B-9

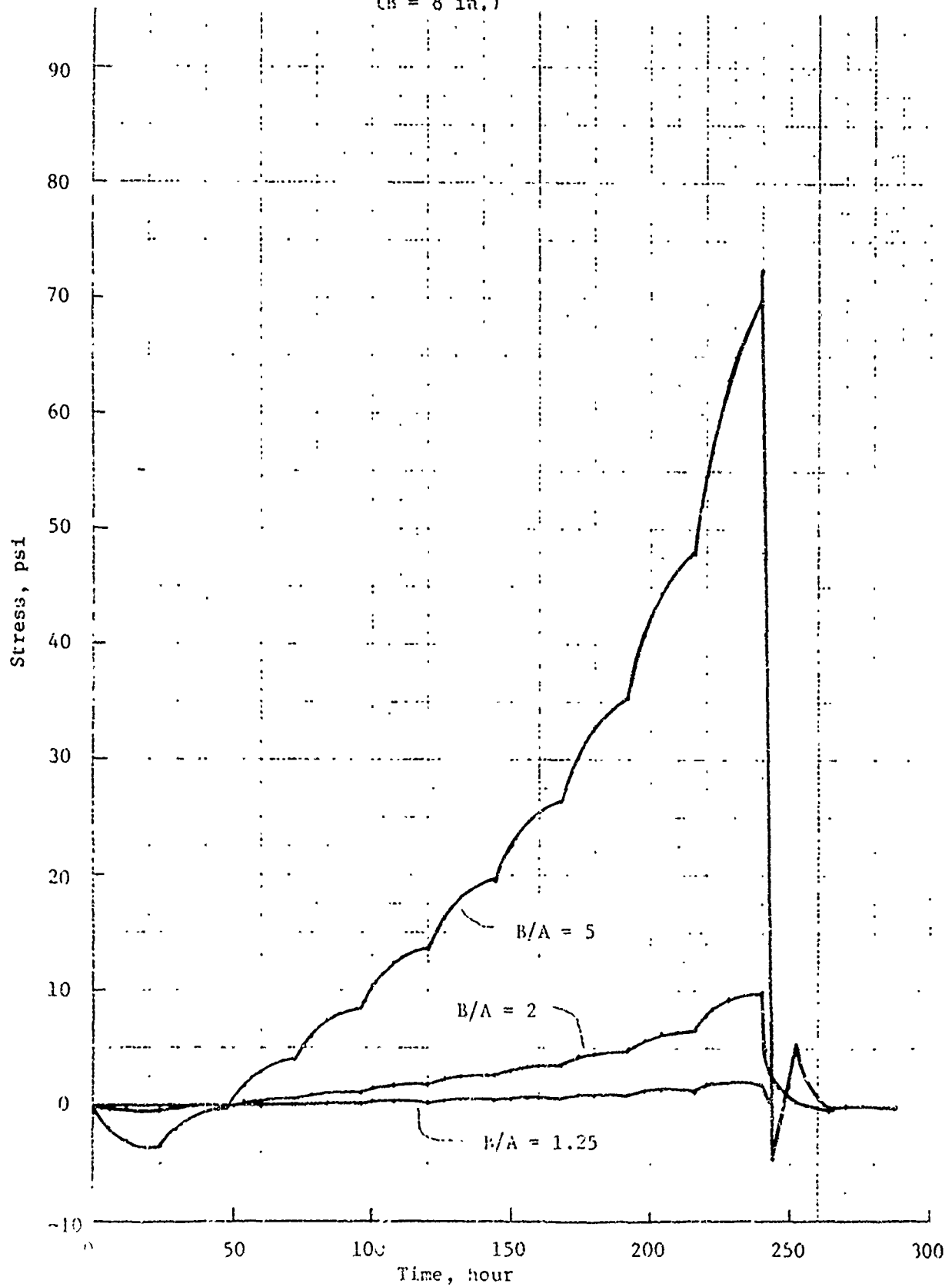
PARAMETER STUDY OF INNER-BORE HOOP STRESS SOLUTIONS
HTPB PROPELLANT - HISTORY 1
(B = 8 in.)



PARAMETER STUDY OF RADIAL BOND STRESS SOLUTIONS
HTPB PROPELLANT - HISTORY 1
(B = 4 in.)



PARAMETER STUDY OF RADIAL BOND STRESS SOLUTIONS
HTPB PROPELLANT - .. STORY 1
(R = 8 in.)



APPENDIX C

PARAMETER STUDY FOR HISTORY 2

Aerojet Solid Propulsion Company

Report 1341-26F

APPENDIX C

PARAMETER STUDY FOR HISTORY 2

The results of a series of one-dimensional, thermoviscoelastic analyses are presented graphically in this appendix. All of the results were based upon the environmental temperature history described in the e text and shown separately in each figure. The data for the CTPB and HTPB propellants are presented separately.

No analyses of the results are made here.

A. CTPB PROPELLANT

The following graphs give the thermoviscoelastic solutions for these grain designs.

Aerojet Solid Propulsion Company

Report 1341-26F

Appendix C

PARAMETER STUDY OF INNER-BORE HOOP STRAINS
CTPB PROPELLANT - HISTORY 2

(B = 4 in.)

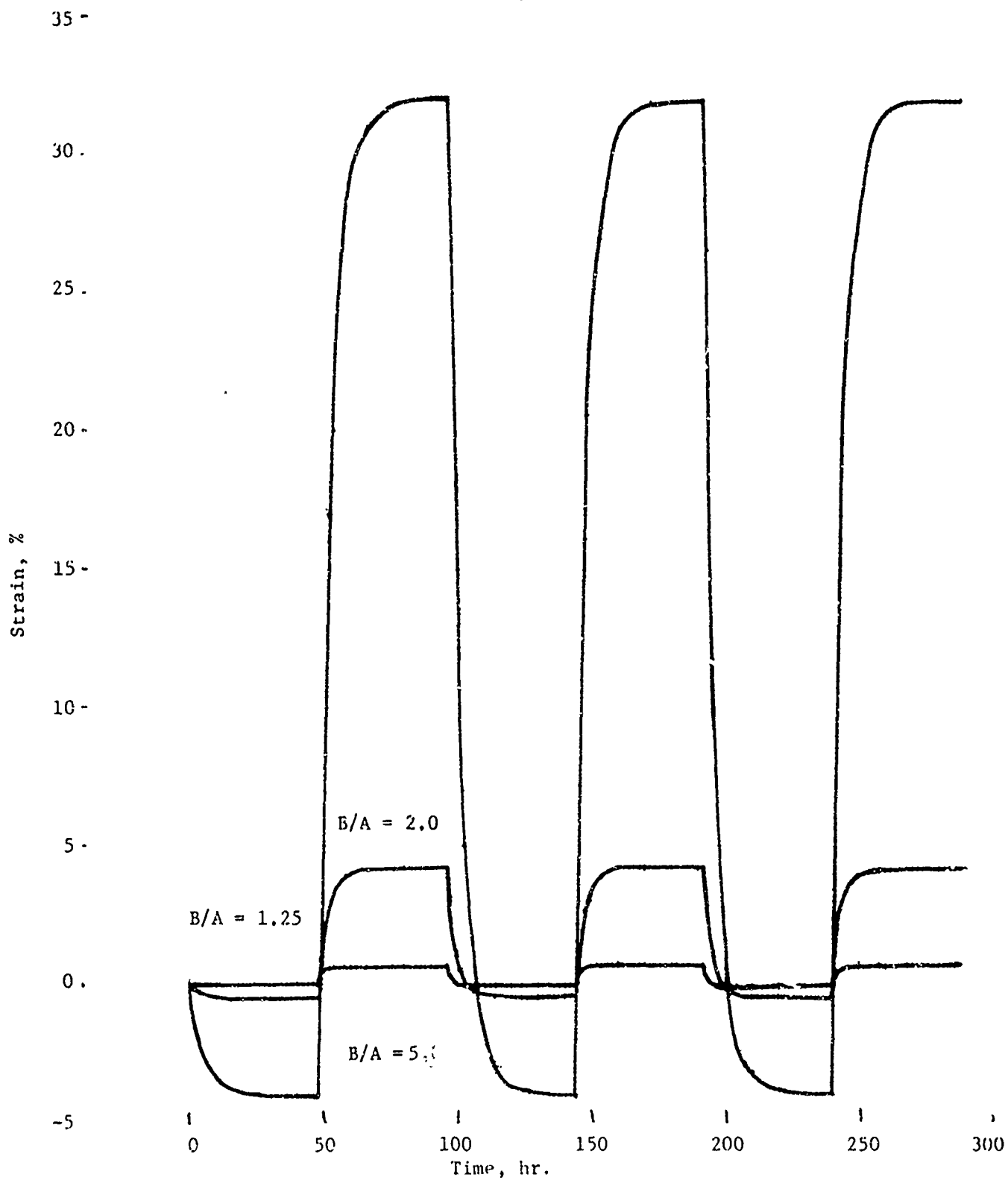


Figure C-1

Aerojet Solid Propulsion Company

Report 1341-26F

Appendix C

PARAMETER STUDY OF INNER-BORE HOOP STRAINS
CTPB PROPELLANT - HISTORY 2

(B = 8 in.)

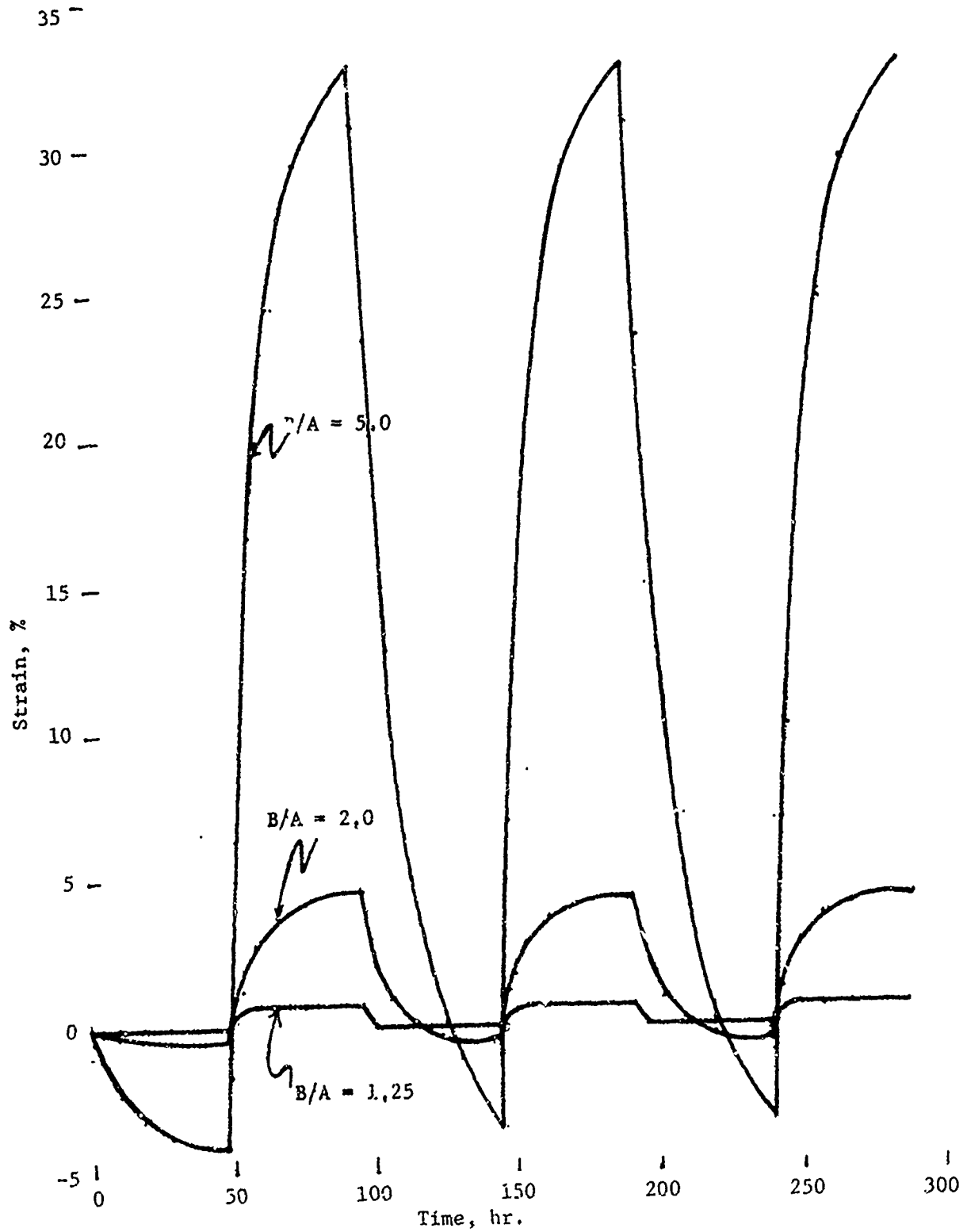


Figure C-2

Aerojet Solid Propulsion Company

Report 1341-26F

Appendix C

PARAMETER STUDY OF INNER-BORE HOOP STRESS
CTPB PROPELLANT - HISTORY 2

(B = 4 in.)

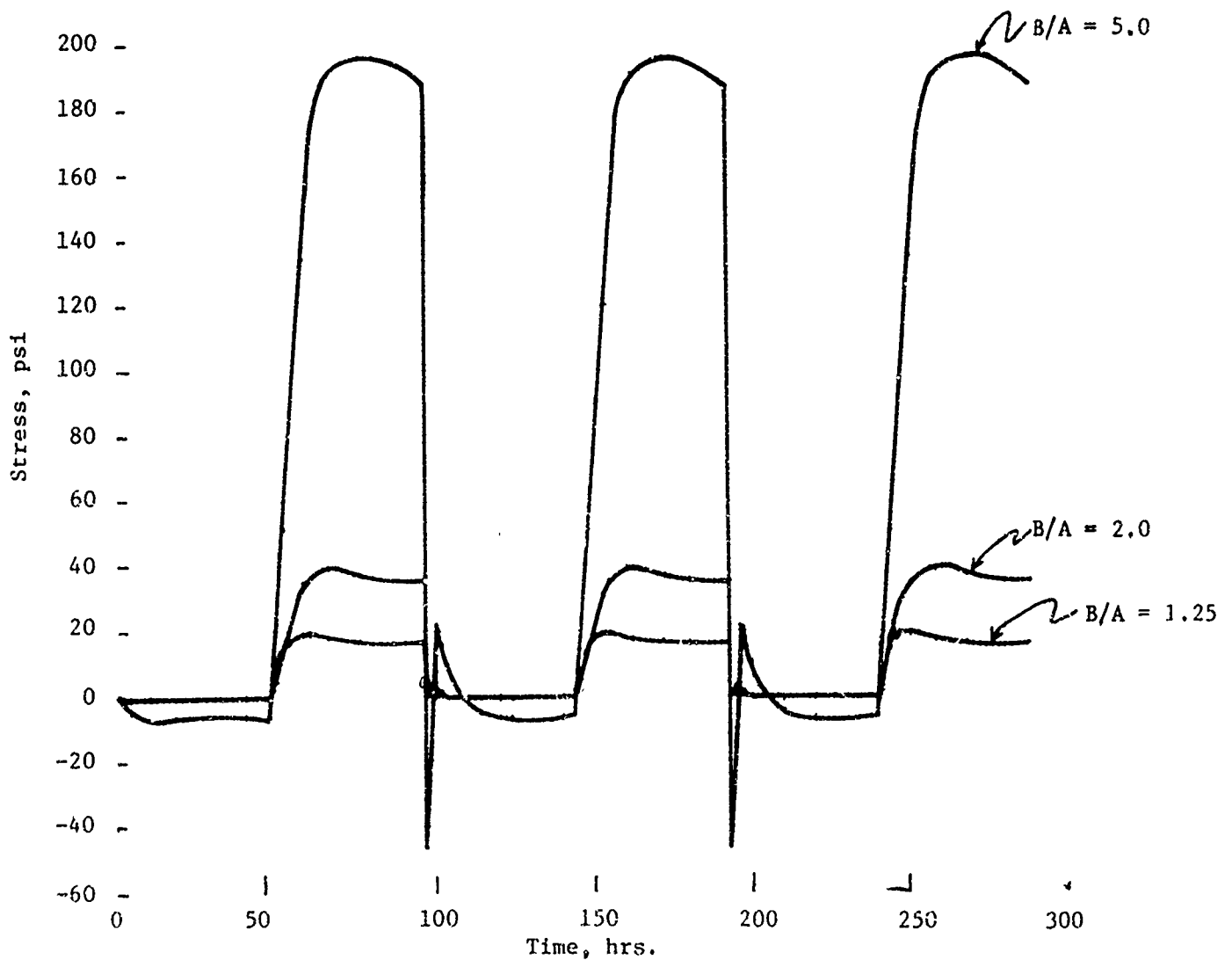


Figure C-3

Aerojet Solid Propulsion Company
Report 1341-26F

Appendix C

PARAMETER STUDY OF INNER-BORE HOOP STRESS
CTPB PROPELLANT - HISTORY 2

(B = 8 in.)

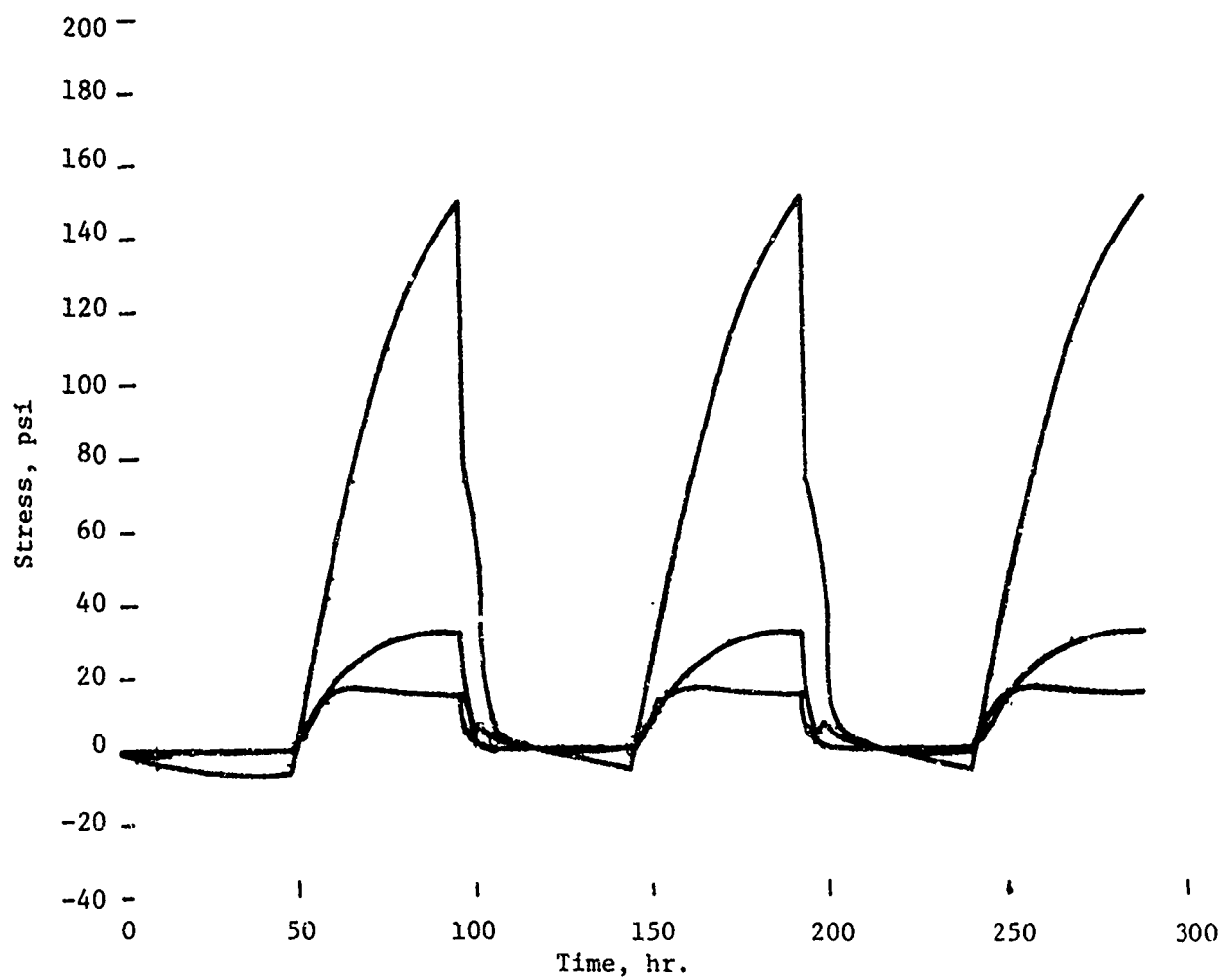


Figure C-4

Aerojet Solid Propulsion Company
Report 1341-26F

Appendix C

PARAMETER STUDY OF RADIAL BOND STRESS SOLUTIONS
CTPB PROPELLANT - HISTORY 2

(B = 4 in.)

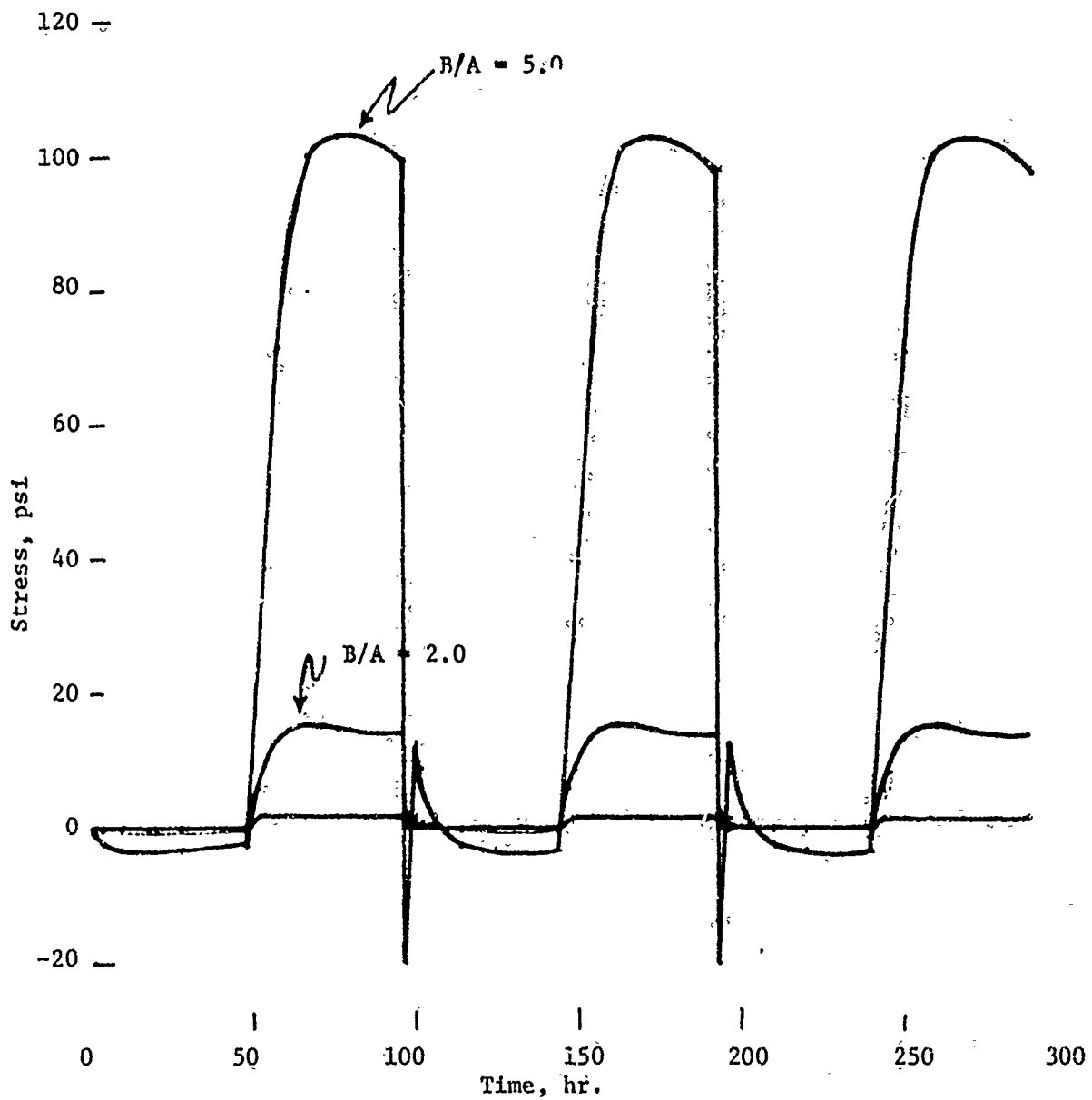


Figure C-5

Aerojet Solid Propulsion Company
Report 1341-26F

Appendix C

PARAMETER STUDY OF RADIAL BOND STRESS SOLUTIONS
CTPB PROPELLANT - HISTORY 2

(B = 8 in.)

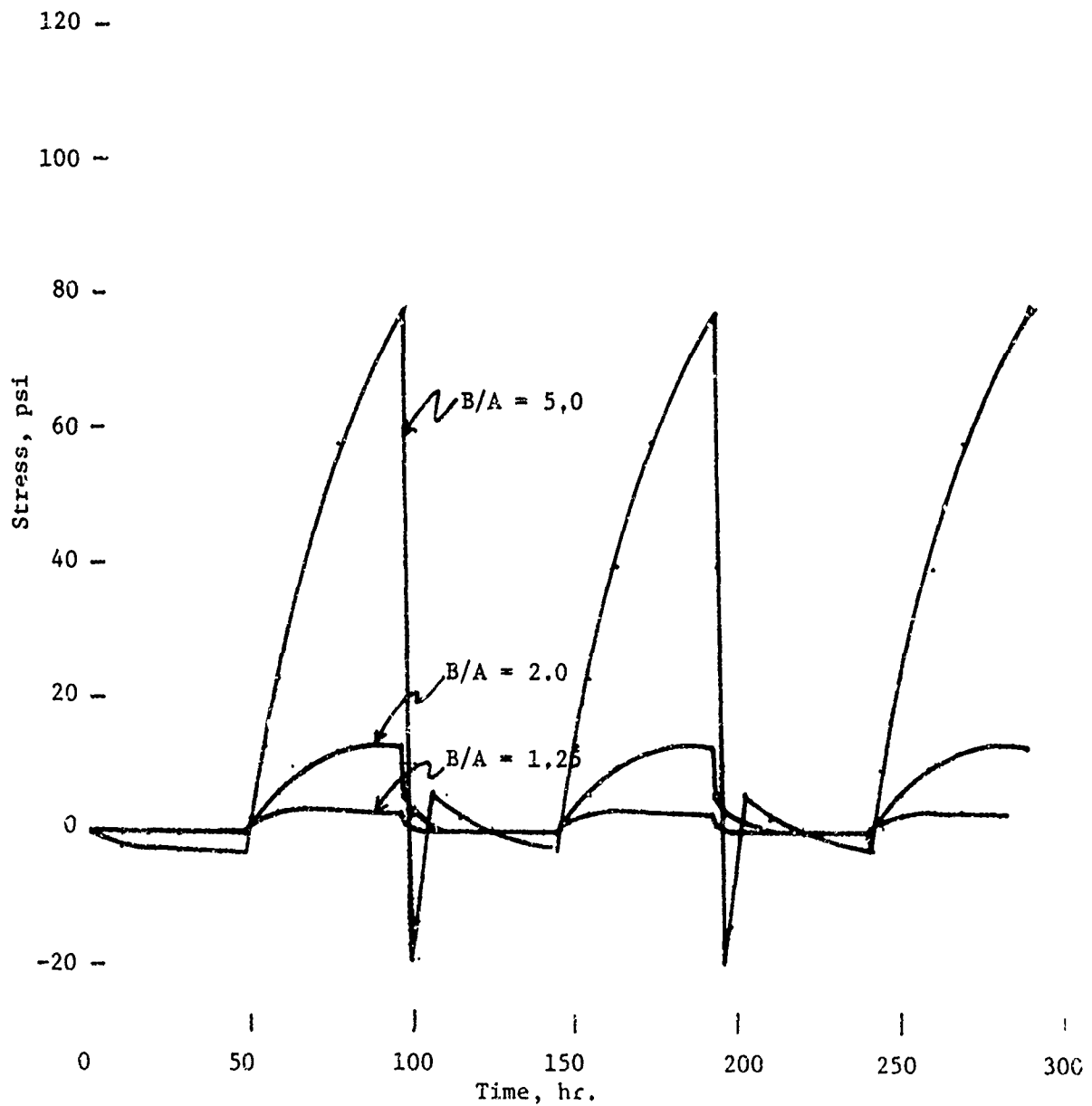


Figure C-6

Aerojet Solid Propulsion Company

Report 1341-26F

Appendix C

B. HTPB PROPELLANT

The following graphs give the thermoviscoelastic solutions for these grain designs.

PARAMETER STUDY OF INNER-BORE HOOP STRAINS
HTPB PROPELLANT - HISTORY 2

(B = 4 in.)

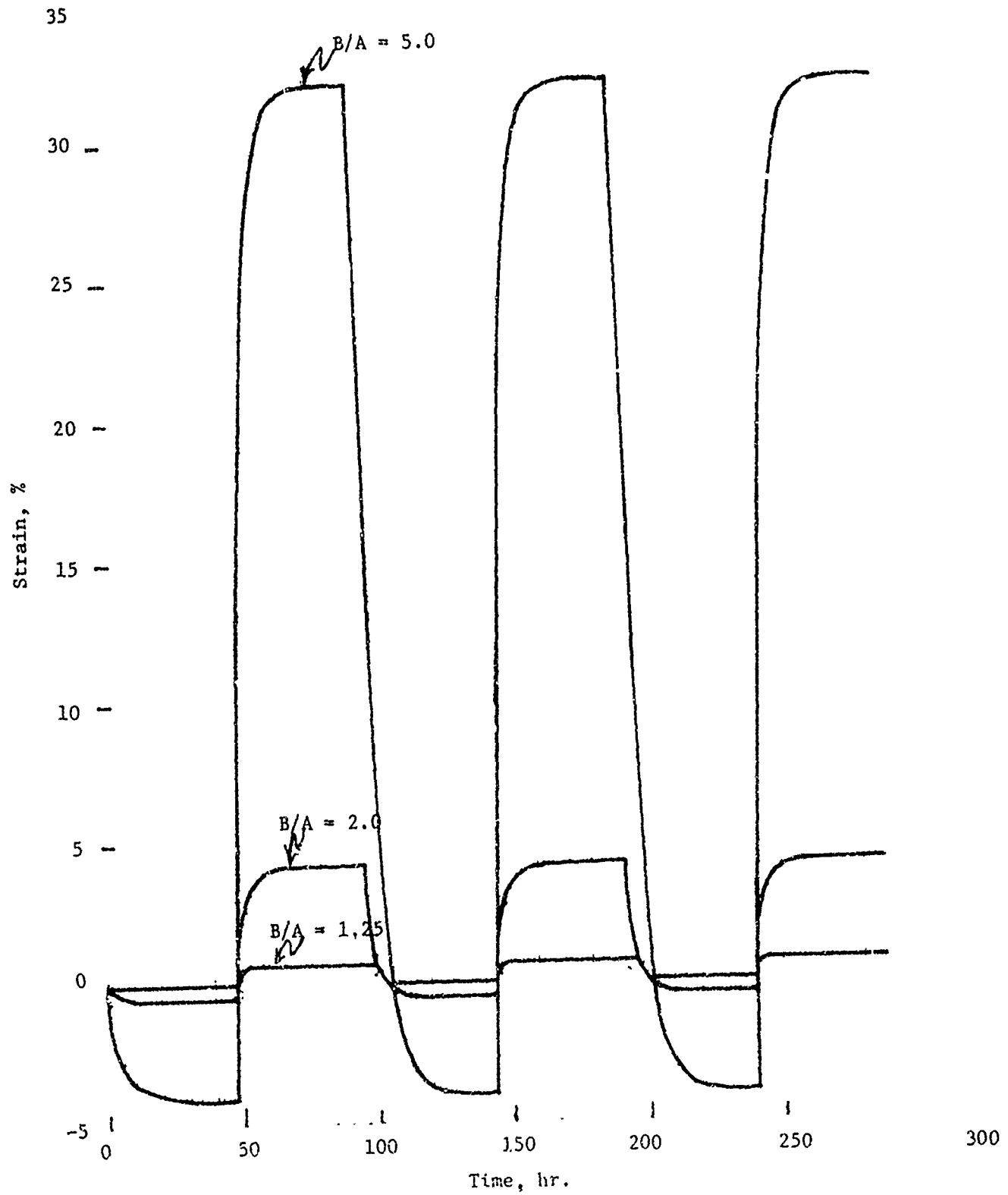


Figure C-7

Aerojet Solid Propulsion Company
Report 1341-26F

Appendix C

PARAMETER STUDY OF INNER-BORE HOOP STRAINS
HTPB PROPELLANT - HISTORY 2

(B = 8 in.)

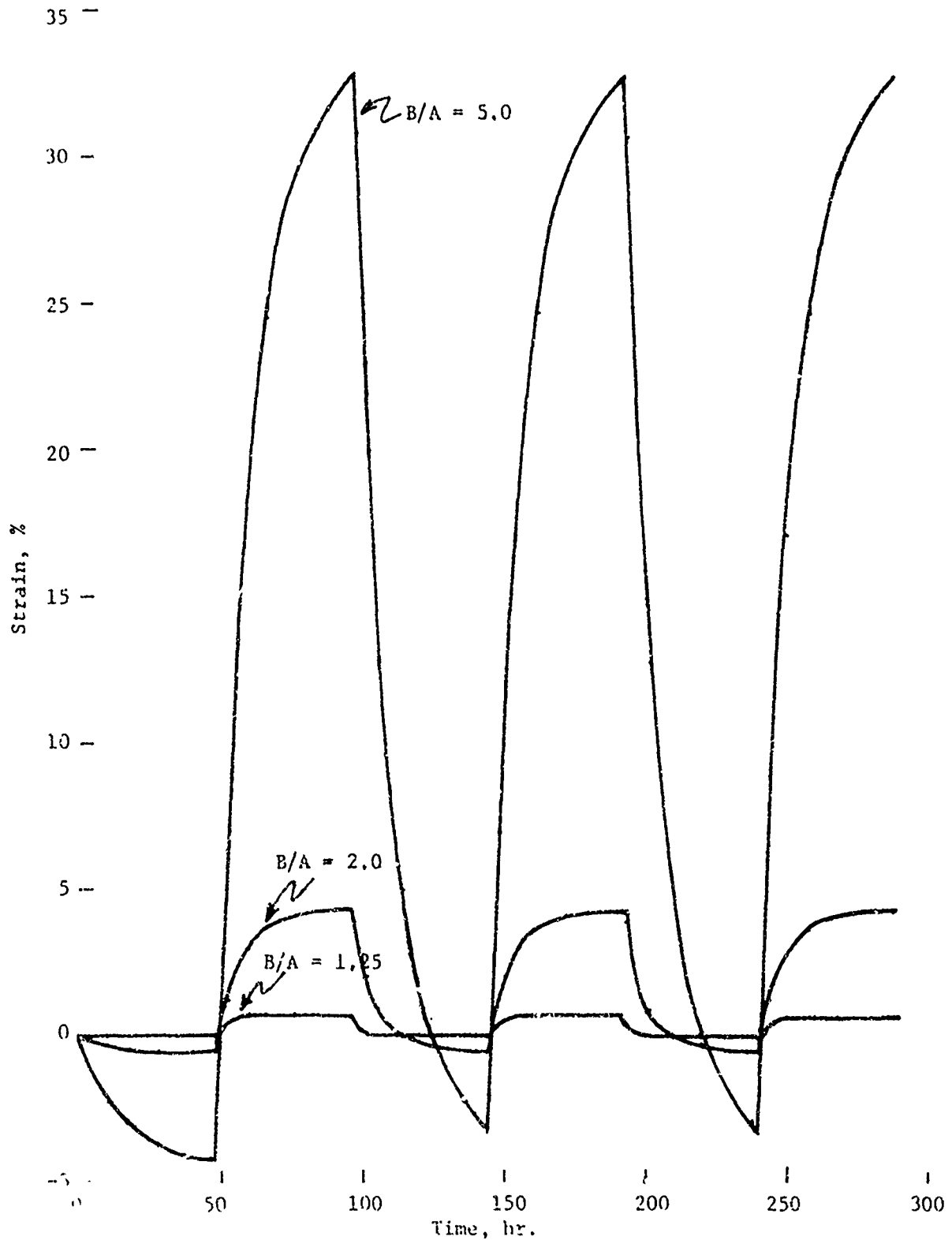


Figure C-8

Aerojet Solid Propulsion Company
Report 1341-26F

Appendix C

PARAMETER STUDY OF INNER-BORE HOOP STRESS SOLUTIONS
HTPB PROPELLANT - HISTORY 2

(B = 4 in.)

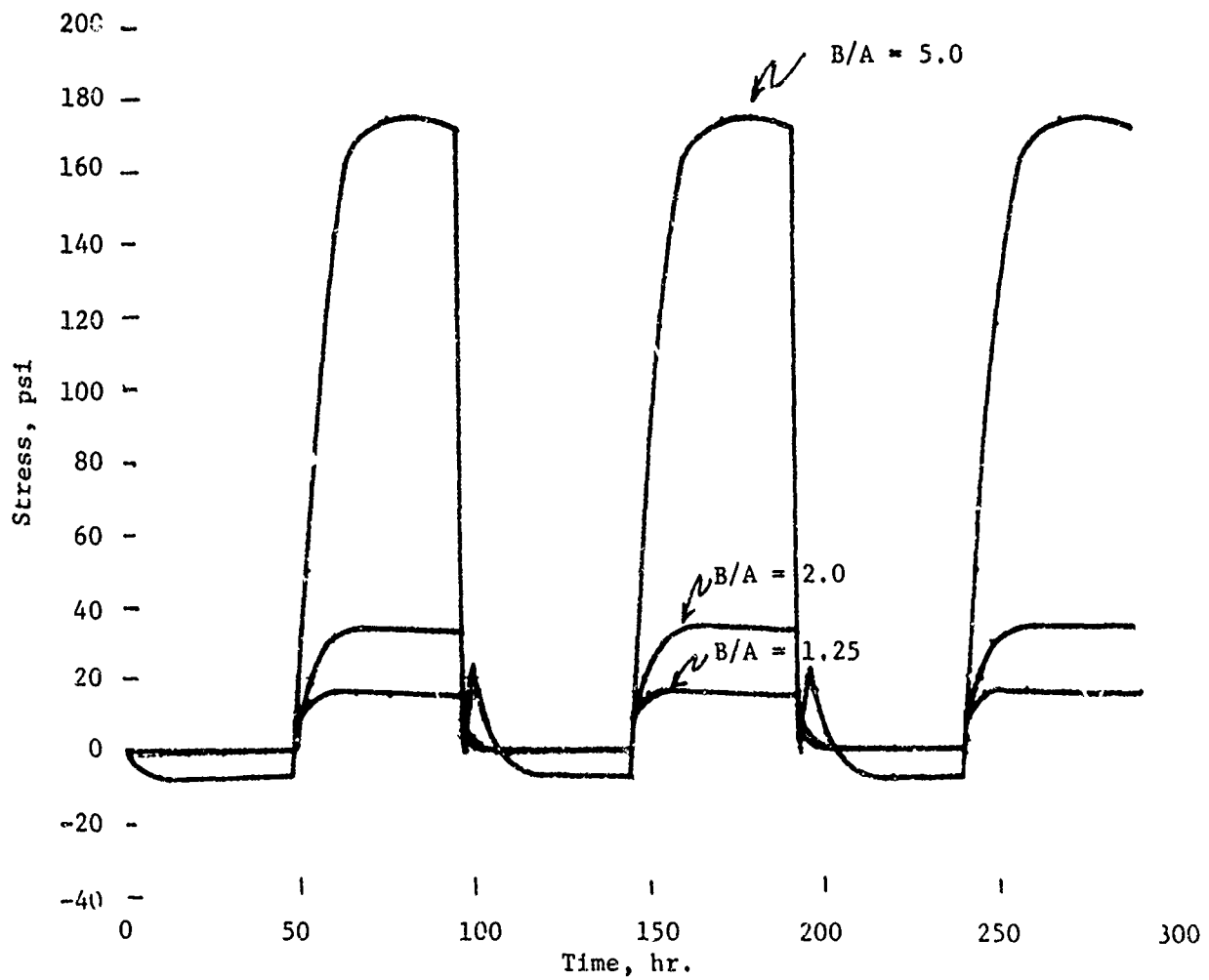


Figure C-9

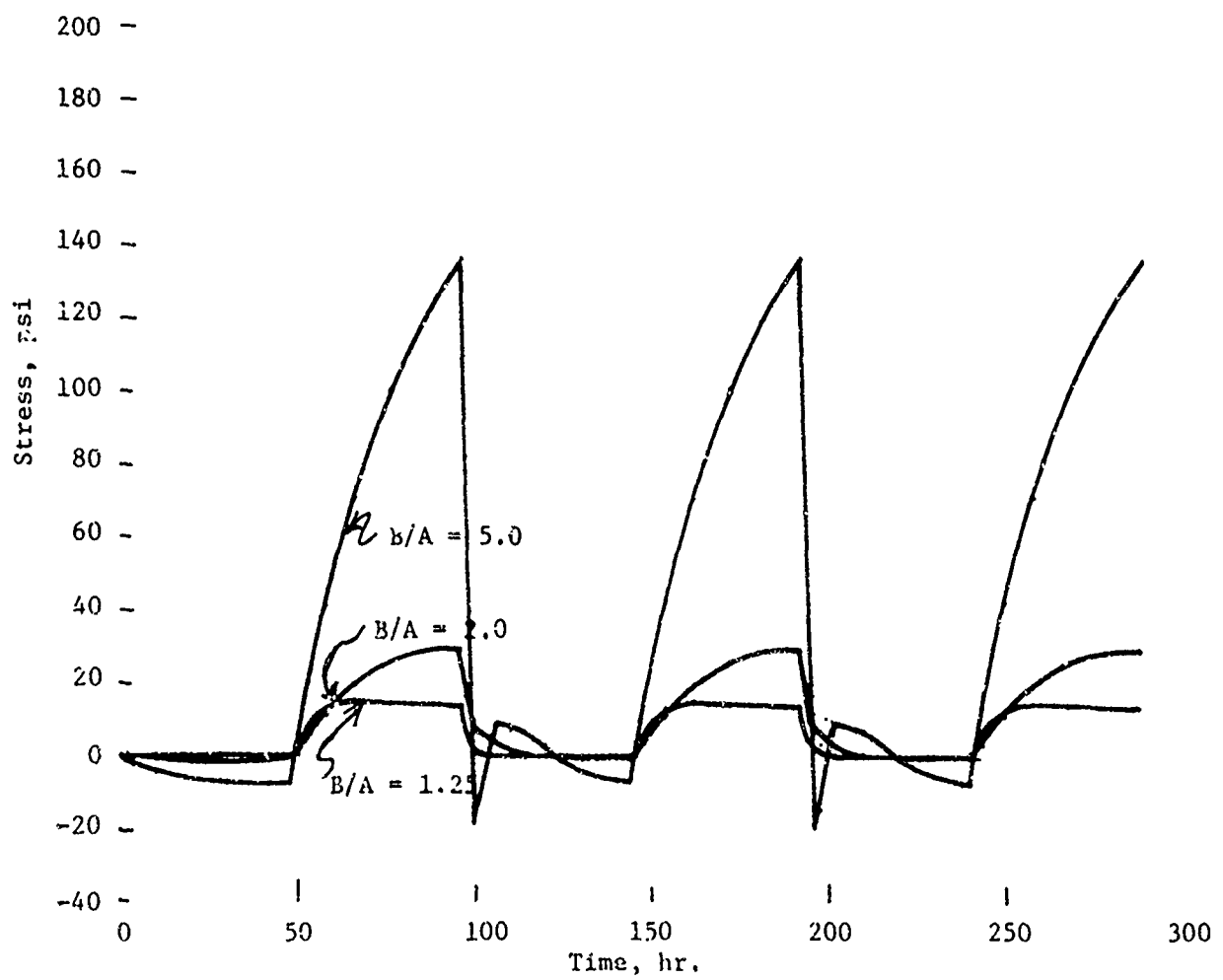
Aerojet Solid Propulsion Company

Report 1341-26F

Appendix C

PARAMETER STUDY OF INNER-BORE HOOP STRESS SOLUTIONS
HTPB PROPELLANT - HISTORY 2

(B = 8 in.)



PARAMETER STUDY OF RADIAL BOND STRESS SOLUTIONS
HTPB PROPELLANT - HISTORY 2

(B = 4 in.)

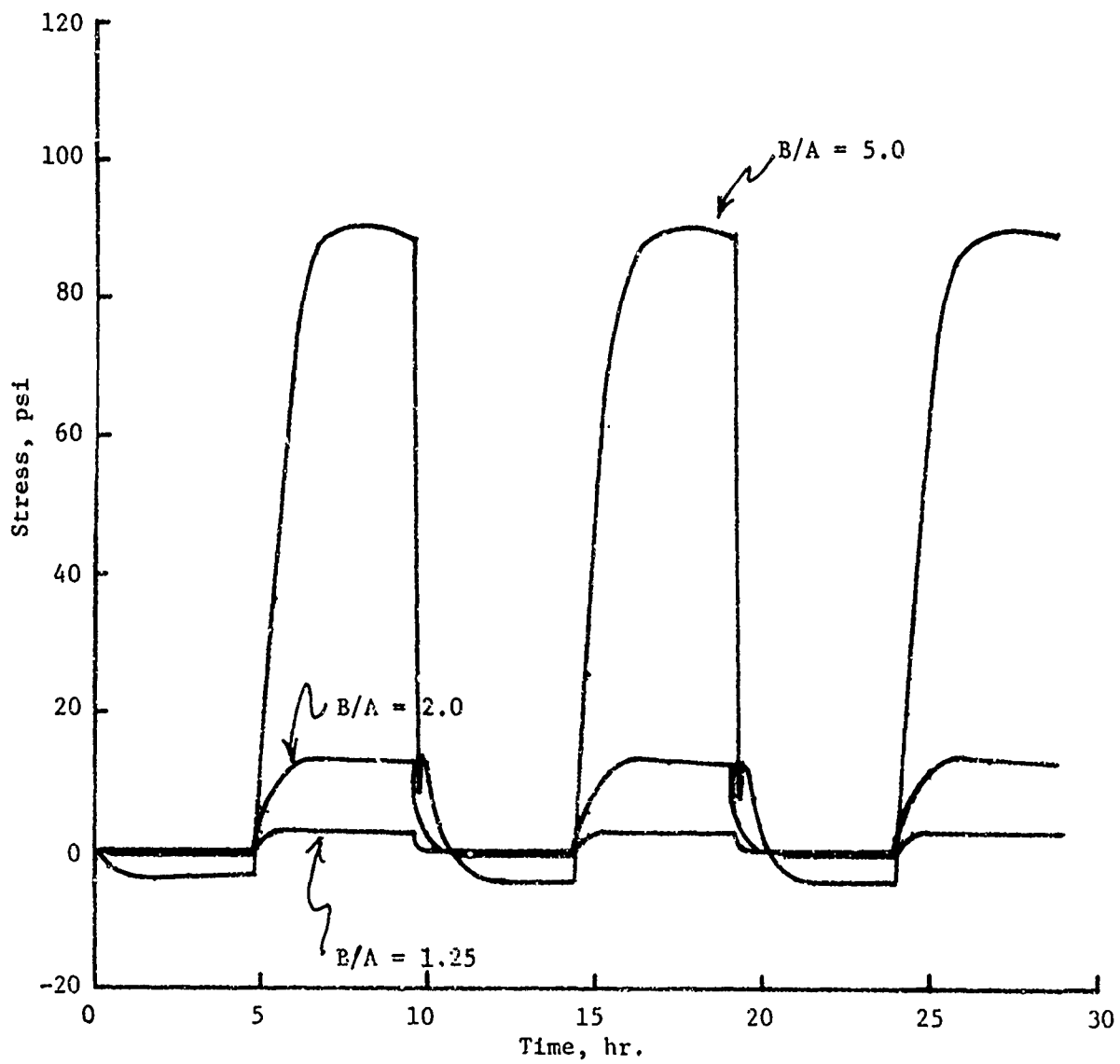


Figure C-11

Appendix C

PARAMETER STUDY OF RADIAL BOND STRESS SOLUTIONS
HTPB PROPELLANT - HISTORY 2
(B = 8 in.)

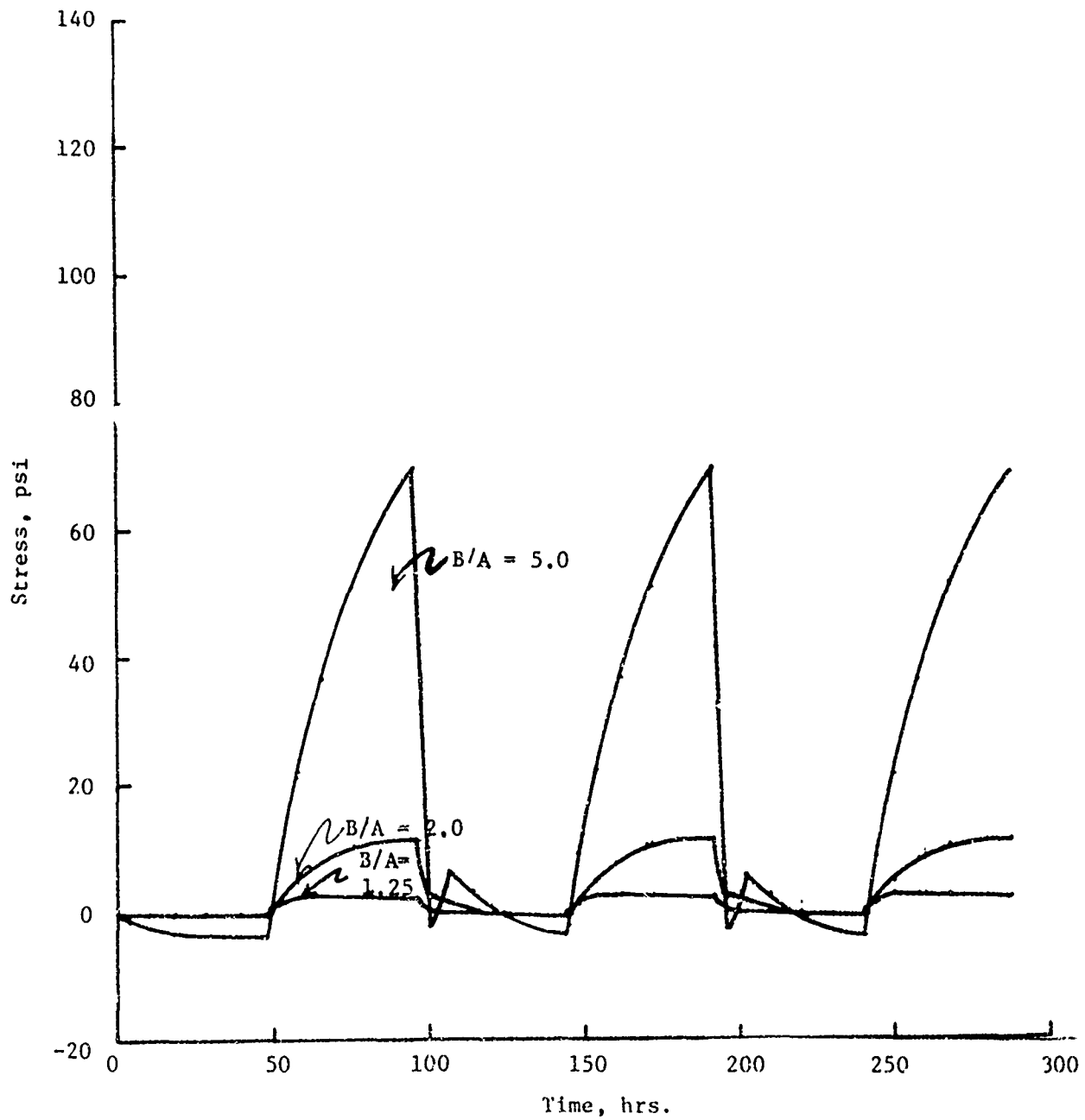


Figure C-12

APPENDIX D

A NEW NORMALIZED RELATION FOR THE RELAXATION MODULUS

Aerojet Solid Propulsion Company

APPENDIX D

A NEW NORMALIZED RELATION FOR THE RELAXATION MODULUS

A. NORMALIZATION OF THE SHEAR MODULUS

Conventional viscoelastic stress analyses involve the relaxation modulus in shear, $\mu(t)$. The basic relations for this modulus require difficult to perform experiments, the results of which are not always satisfactory. It was desirable, therefore, to devise a simpler to use expression for this modulus. This was done starting with the relation now used,

$$\mu(t) = \mu_e + (\mu_g - \mu_e) \int_{-\infty}^{\infty} h e^{-t/\tau} d\ln\tau \quad (D-1)$$

where μ_g is the glassy shear modulus

μ_e is the equilibrium shear modulus

h represents a continuous distribution of relaxation times (normalized)

t is the time of the test

τ is a relaxation time

Since μ_g is difficult to evaluate experimentally an attractive substitute was sought and found.

We solved for $\mu(t)$ at some specific time, like one minute, to obtain $\mu(1)$.

$$\mu(1) = \mu_e + (\mu_g - \mu_e) \int_{-\infty}^{\infty} h e^{-1/\tau} d\ln\tau \quad (D-2)$$

Letting

$$C = \int_{-\infty}^{\infty} h e^{-1/\tau} d\ln\tau \quad (D-3)$$

where C is a constant, we solve for $\mu_g - \mu_e$ in Equation (D-2) using Equation (D-3) and inserting the result into Equation (D-1) gives

$$\mu(t) = \mu_e + (\mu(1) - \mu_e) \int_{-\infty}^{\infty} \frac{h e^{-1/\tau}}{C} d\ln\tau \quad (D-4)$$

For practical experimental purposes the constant C can be combined with h to give h' , a quantity which is experimentally identified in the same manner as h .

Thus, the new relation becomes

$$\mu(t) = \mu_e + (\mu(1) - \mu_e) \int_{-\infty}^{\infty} h' e^{-t/\tau} d \ln \tau \quad (D-5)$$

In engineering practice it is unnecessary to evaluate h' . Instead, a graphical plot of $\mu(t)$ versus time is usually sufficient. When normalized results are required a plot of $\frac{\mu(t) - \mu_e}{\mu(1) - \mu_e}$ versus the time is equivalent

to a plot of $\int_{-\infty}^{\infty} h' e^{-t/\tau} d \ln \tau$ versus the time.

Obviously, a broad range of relaxation curves can be obtained for a given distribution of relaxation times, h' .

B. NORMALIZATION OF THE PRONY SERIES

The new relation permits a normalization of the Prony Series as well. This relation in its usual form is given as

$$\mu(t) = \alpha_0 + \sum_{m=1}^m \alpha_m e^{-\beta_m t} \quad (D-6)$$

where the α_m and β_m are constants

α_0 is the equilibrium relaxation modulus

We can normalize Equation (D-6) to give a form similar to that of Equation (D-5). First we replace α_0 by the equivalent term μ_e then normalize the constants α_m , as shown below, to give

$$\mu(t) = \mu_e + (\mu(1) - \mu_e) \sum_{m=1}^m \alpha'_m e^{-\beta_m t} \quad (D-7)$$

where

$$\alpha'_m = \alpha_m / (\mu(1) - \mu_e) \quad (D-8)$$

Aerojet Solid Propulsion Company
Report 1341-26F

Appendix D

Equation (D-7) forms the engineering basis of our normalization procedures. This normalization method defines the modulus in terms of two easily determined parameters, μ_e and $\mu(1) - \mu_e$. These same parameters can be used to normalize the stress and strain data from our engineering analyses.

APPENDIX E
INCREMENTAL ANALYSIS PROCEDURE

Aerojet Solid Propulsion Company

Report 1341-26F

APPENDIX E

INCREMENTAL ANALYSIS PROCEDURE

In an attempt to minimize accumulated numerical errors in our linear viscoelastic analyses, Dr. Herrmann developed this new approach. The "total stress analysis" was replaced by an "incremental analysis procedure"; i.e., instead of solving for the total stress and strain in the propellant for a given point in time, one could solve instead for the incremental changes in stress and strain. The incremental equations are very similar to those previously reported for the "total analysis" with the following exceptions (the equations referred to by number are reported in Reference (E-1)).

Consider first, Equation (13),

$$S_{ijN} = 2\mu_N e_{ijN} + L_{ijN} \quad (13)$$

The quantities S_{ijN} and e_{ijN} in Equation (13) need to be interpreted as the incremental changes in stress and strain during time step N (i.e., $S_{ijN} = 2\mu_N \Delta e_{ijN} + L_{ijN}$ where $S_{ijN} = S_{ijN-1} + \Delta S_{ijN}$, etc.). Equation (18)

$$L_{ijN} = 2 [\chi_{ijN} - (\mu_N - \alpha_0) e_{ijN-1}] \quad (18)$$

is replaced by

$$L_{ijN} = 2 \sum_{m=1}^M \alpha_m [e^{-\alpha_m \tau_N} - 1] C_{ijNm}$$

Equation (19)

$$X_{ijN} = \sum_{m=1}^M \alpha_m C_{ijNm} \quad (19)$$

is eliminated and Equation (24)

$$C_{ijNm} = e^{-\beta_m \Delta \xi_N} [C_{ijN-1,m} + (e_{ijN-1} - e_{ijN-2}) J_{N-1,m}] \quad (24)$$

becomes

$$C_{ijNm} = e^{-\beta_m \Delta \xi_{N-1}} C_{ijN-1,m} + \Delta e_{ijN-1} J_{N-1,m} \quad (24)$$

Finally, Equations (1), (2) and (3)

$$\tau_{ij} = S_{ij} + \delta_{ij} \sigma, \quad \sigma = \frac{1}{33} \tau_{ii} \quad (1)$$

$$\epsilon_{ij} = e_{ij} + \delta_{ij} \frac{\theta}{3}, \quad \theta = \epsilon_{ii} \quad (2)$$

$$\sigma = K (9 - 3\alpha\Delta T) \quad (3)$$

where

K = Bulk modulus
 α = Coefficient of linear thermal expansion
 $\Delta T = T(x, t) - T_0$
 T_0 = Initial stress free reference temperature

are replaced by their corresponding incremental forms (Note: $\Delta T_N = T_N - T_{N-1}$).

REFERENCES

- E-1 Herrmann, L. R., and Peterson, F. E., "A Numerical Procedure for Viscoelastic Stress Analysis", Bulletin of the 7th Meeting of the ICRPG Mechanical Behavior Working Group, CPIA Publication No. 177, p. 155 (October 1968).

APPENDIX F

PRONY SERIES CURVE FIT ANALYSIS

Aerojet Solid Propulsion Company
Report 1341-26F

APPENDIX F

PRONY SERIES CURVE FIT ANALYSIS

The shear relaxation modulus for most solid propellants has been found to fit the following series function with relatively few terms:

$$\phi(t) = A_0 + \sum_{i=1}^n A_i e^{-\beta_i t} \quad (F-1)$$

Equation (F-1) is a "Prony" series with two unknown coefficients A_i and β_i . The method of collocation is used to find these coefficients:

$$\text{Let } \beta_i = \frac{1}{2t_i} \quad (F-2)$$

Substitution of Equation (F-2) into Equation (F-1) gives

$$\phi = A_0 + \sum_{i=1}^n A_i e^{-\frac{t}{2t_i}} \quad (F-3)$$

Now, choose n points for the evaluation of ϕ

$$\phi_j = A_0 + \sum_{i=1}^n A_i e^{-\frac{t_j}{2t_i}} \quad (j = 1, n) \quad (F-4)$$

Equations (F-4) are sufficient to solve for the A_i . In matrix notation;

$$[\bar{E}] \{A_i\} = \{\phi_j - A_0\} \quad (F-5)$$

where,

$$E_{ji} = e^{-\frac{t_j}{2t_i}}$$

Equation (F-5) is readily solved for A_i ;

$$\{A_i\} = [E]^{-1} \{\phi_j - A_0\} \quad (F-6)$$

Aerojet Solid Propulsion Company
Report 1341-26F

Appendix F

Equation (F-6) has been programmed for computer solution from a times burning terminal in the BASIC language. A listing of the program is given on Page F-3. The order of data input is given below:

1. n
2. A_0
3. t_j ($j = 1, n$)
4. ϕ_j ($j = 1, n$)

Data statements 600 to 9000 may be used for data. Sample data statements are shown below:

600 Data 7,100

610 Data 1E-4, 1E-3, 1E-2, 1E-1, 1, 10, 100

620 Data 3000, 1800, 1000, 620, 410, 320, 280

A sample run with this data is shown on Page F-4.

Aerojet Solid Propulsion Company

Report 1341-26F

Appendix F

PROGRAM LISTING

```

100 REM "PRONY SERIES CURVE FIT"
110 DIM T(20,1),F(20,1),A(20,20),C(20,20)
120 DIM F(1,20),C(1,20)
130 READ N,E1
140 MAT REAL I(N,1)
150 MAT F = ZER(N,N)
160 MAT C = ZER(N,N)
170 MAT F = TRN(T)
180 PRINT "INPUT TIMES AND MODULI"
190 MAT PRINT F;
200 MAT A = ZER(N,N)
210 FOR J=2 TO N
220 LET E = -T(J,1)/T(1,1)
230 LET A(J,J) = 0.60653
240 IF E < -20.0 THEN 280
250 LET A(1,J) = EXP(0.5/E)
260 LET A(J,1) = EXP(0.5*E)
270 GOTO 300
280 LET A(1,J) = 1.0
290 LET A(J,1) = 0.0
300 NEXT J
310 LET A(1,1) = 0.60653
320 LET K1 = N - 1
330 FOR I=2 TO K1
340 LET L = 1
350 LET K2 = K1 - I + 2
360 FOR J=2 TO K2
370 LET L = L + 1
380 LET A(J,L) = A(1,1)
390 LET A(L,J) = A(1,1)
400 NEXT J
410 NEXT I
420 MAT C = ZER(N,N)
430 MAT C = INV(A)
440 MAT READ E(N,1)
450 MAT C = TRN(E)
460 MAT PRINT C;
470 FOR J=1 TO N
480 LET E(J,1) = F(J,1) - F1
490 NEXT J
500 MAT T = C*F
510 PRINT "SOLUTION"
520 MAT F = TRN(T)
530 MAT PRINT F;
540 GOTO 500
550 END

```

Aerojet Solid Propulsion Company
Report 1341-26F

Appendix F

SAMPLE RUN

PRON 9:57 SF FRI 02/13/70

INPUT TIMES AND MODULI

.0001 .001 .01 .1 1 10 100

3000 1800 1000 620 410 320 230

SOLUTION

1370.27 1031.23 464.66 247.646 184.314 -106.615 297.955

OUT OF DATA IN 440

APPENDIX G

INCLUSION OF NON-ZERO THICKNESS STRESSES IN PLANE STRESS ANALYSES

Aerojet Solid Propulsion Company

Report 1341-26F

APPENDIX G

INCLUSION OF NON-ZERO THICKNESS STRESSES
IN PLANE STRESS ANALYSES

The generalized plane stress option was modified so that the stress throughout the thickness of the body, may be specified as a constant rather than zero. The values of the thickness stress constitutes one of the input parameters. The inclusion of a non-zero thickness stress required the modification of the governing variational equation.

It was determined that the appropriate form of the variational function, for a nearly incompressible material ^(G-1) is (for $T = T_N$):

$$\begin{aligned}
 F_N = \iint \{ & \frac{2\mu_N}{3} [(\Delta\epsilon_{x_N})^2 + (\Delta\epsilon_{y_N})^2 - (\Delta\epsilon_{x_N})(\Delta\epsilon_{y_N})] + \frac{1}{2} \mu_N (\Delta\gamma_{x_N})^2 \\
 & + (\mu_N \Delta\bar{H}_N - \Delta\beta_N/3)(\Delta\epsilon_{x_N} + \Delta\epsilon_{y_N}) + L_{xx_N} \Delta\epsilon_{x_N} + L_{yy_N} \Delta\epsilon_{y_N} \\
 & + L_{xy_N} \Delta\gamma_{xy_N} - \frac{(\mu_N)^2}{2\bar{K}_N} (\Delta\bar{H}_N)^2 + \Delta\bar{H}_N \left(\frac{\Delta\beta_N}{2} - 3\mu_N \alpha \Delta T_N \right) \\
 & - \Delta F_{x_N} \Delta u_{x_N} - \Delta F_{y_N} \Delta u_{y_N} \} dx dy - \int \Delta u_N \cdot \Delta(\text{applied boundary load}) ds
 \end{aligned}$$

where

$$\Delta \epsilon_{xx_N} = \frac{2\mu_N}{3} (2\Delta \epsilon_{x_N} - \Delta \epsilon_{y_N}) + \mu_N \Delta \bar{H}_N + L_{xx_N} - \frac{\Delta \beta_N}{3}$$

$$\Delta \epsilon_{zz_N} = \frac{1}{3} (\Delta \epsilon_{x_N} + \Delta \epsilon_{y_N}) - \frac{\Delta \bar{H}_N}{2} + \frac{2}{3\mu_N} (\Delta \sigma_N - L_{zz_N}) + \frac{1}{3} \alpha \Delta T_N$$

$$\Delta \beta_N = 2\mu_N \alpha \Delta T_N + (\Delta \sigma_N - L_{zz_N})$$

$$\bar{K}_N = \frac{8\mu_N(1 - \frac{\mu_N}{6K})}{3(1 + \frac{4\mu_N}{3K})}$$

The symbol $\Delta \sigma_N$ denotes the incremental change in the specified thickness stress, L_{zz_N} denotes the history term associated with ϵ_z , the other symbols have their usual meanings.

REFERENCES

- G-1 Herrmann, L. R., "Elasticity Equations for Incompressible and Nearly Incompressible Materials by a Variational Theorem", AIAA J., Vol. 3, No. 10, pp. 1896-1901, October 1965.

APPENDIX H

A COMPUTER PROGRAM FOR VISCOELASTIC SOLIDS
OF REVOLUTION SUBJECTED TO TIME - VARYING THERMAL
AND MECHANICAL LOAD ENVIRONMENTS

VERSION 2.1

Aerojet Solid Propulsion Company

Report 1341-26F

Appendix H

A COMPUTER PROGRAM FOR VISCOELASTIC SOLIDS OF REVOLUTION
SUBJECTED TO TIME-VARYING THERMAL AND MECHANICAL LOAD ENVIRONMENTS

- VERSION 2.1 -

I. INTRODUCTION

The purpose of the computer code described in this section is to perform viscoelastic stress analyses. The analyses is applicable to arbitrary revolved solids and plane structures subjected to loads of mechanical or thermal origin. The program is segmented into two (2) phases: (1) Transient Heat Transfer Analysis; and (2) Viscoelastic Stress Analysis. The purpose of the heat transfer phase is to generate temperature distributions in the body as a function of time which are used subsequently in performing the stress analysis. The two phases of the program can be used in sequence within a given job or each phase can be used separately.

The method of solution employs the finite element procedure for solving the spatial problems (heat conduction and stress analysis) and time marching techniques to evaluate temperatures/stresses at successive points in time. The transient heat transfer problem is solved using the procedure developed by Wilson and Nickell*. Knowing thermal and mechanical loads as a function of time and having available the viscoelastic properties of the material(s), a set of equivalent elastic parameters is defined for a particular point in time; the equivalent elastic problem is posed using the procedure given by Herrmann and Peterson**. An elastic stress analysis must be performed at each point in time for which the viscoelastic response of the body is required. The stress analysis problem is solved using a finite element method given by Herrmann***.

II. APPLICATIONS

The principal application of the program is to stress analysis of solid propellant grains maintained in time varying temperature environments. A typical application might be the grain stress analysis of a motor system subjected to thermal cycling. Mechanical loads may also be applied to the body either isothermally or with simultaneous time varying temperature changes. The kinds of mechanical loading considered in the analysis include surface pressures, body forces (spin and/or axial accelerations), concentrated nodal forces, and specified nodal displacements; all mechanical loads can vary with time in accordance with user-supplied table.

* Wilson, E. L., and Nickell, R. E., "Application of the Finite Element Method to Heat Conduction Analysis", Nuclear Engineering and Design 4 (1966), p. 276-286. North Holland Publishing Company, Amsterdam.

** Herrmann, L. R., and Peterson, F. E., "A Numerical Procedure for Viscoelastic Stress Analysis", CPIA - 7th Meeting, Working Group on Mechanical Behavior (ICRPG), November 1968.

*** Herrmann, L. R., "Elasticity Equations for Incompressible Materials by A Variational Theorem", Journal of the AIAA, p. 1896-1900, October 1965.

Aerojet Solid Propulsion Company
Report 1341-26F

Appendix H

A. PHYSICAL PROPERTIES

The program can be used to perform simple elastic solutions, time-dependent elastic or thermoelastic analyses, or thermoviscoelastic analyses. A viscoelastic analysis requires a complete material property characterization including the master relaxation curve and shift function for each time dependent material, bulk modulus, expansion coefficient, density, etc. Table H-1 illustrates the thermal and mechanical properties data required to perform the thermoviscoelastic stress analysis of a bipropellant grain with a separate viscoelastic liner and an elastic case.

Shift function data is accepted by the program in the form of a table of $\log a_T$ versus T , ($^{\circ}\text{F}$); shift factors at temperatures other than those supplied in the input table are determined using linear interpolation between given points.

Relaxation data must be input as the coefficients (A_i, β_i) in a Prony Series fit to the experimental data. The relaxation behavior in shear must be expressed as an exponential series.

$$\phi(t) = A_0 + \sum_{i=1}^n A_i e^{-\beta_i t} \quad (\text{H-1})$$

where A_0 is the shear equilibrium modulus and (A_i, β_i) are found from curve fitting* calculations based on experimental data. Each viscoelastic material must have its relaxation behavior expressed in a separate series expansion. Elastic materials have no terms in the series other than A_0 . If there are no terms in the series expansion ($M = 0$) the program will not read a shift function table.

The special problem of bulk rapid pressurization of a propellant grain where a pressure shift function a_P is required is handled in a different manner. This type of problem^P can only be run isothermally with no superimposed thermal loads. In this case the shift function input values are interpreted as the product $a_P a_T$ as a function pressure where a_T is a constant for the temperature under consideration.

* One recommended curve fitting procedure is a "collocation method" originated by Schapery and summarized in the ICRPG Solid Propellant Mechanical Behavior Manual starting at Section 2.2-4 (June 1963). The method involves assuming values for the constants β_i and solving a set of linear simultaneous equations for the constants A_i . A time-share routine called "PRONY" has been programmed to perform the calculations at Aerojet.

Aerojet Solid Propulsion Company
Report 1341-26F

Appendix H

PHYSICAL PROPERTY INFORMATION REQUIRED
FOR A THERMOVISCOELASTIC STRESS ANALYSIS

PROBLEM IDENTIFICATION:

Propellant No. 1 -
Propellant No. 2 -
Liner -
Case -

Physical Property	Propellant No. 1	Propellant No. 2	Liner	Case
Coefficient of Linear Thermal Expansion ($^{\circ}\text{F}^{-1}$)				
Density (lb-in.^{-3})				
Specific Heat Capacity ($\text{btu-lb}^{-1} \text{ } ^{\circ}\text{F}^{-1}$)				
Thermal Conductivity, ($\text{Btu-in.}^{-1} \text{ hr}^{-1} \text{ } ^{\circ}\text{F}^{-1}$)				
Bulk Modulus (lb-in.^{-2})				
Shear Relaxation Modulus ($\text{lb.-in.}^{-2} \text{ vs. hr}$)	(Table or curve as a function of time)			
Shift Factor ($a_T \text{ vs. } ^{\circ}\text{F}$)	(Table or curve as a function of temperature)			
Elastic Shear Modulus (lb-in.^{-2})				

Table H-1

III. DATA INPUT DESCRIPTION

This section supplies information necessary for the preparation of data input cards. The input sequence is separated into four major groups:

1. Grid Definition
2. Solution Time and Temperature Information
3. Transient Heat Transfer Solution Data
4. Stress Analysis Information

A. NOMENCLATURE

The abbreviation "cc" used below stands for "card columns". The variable names assigned to the various parameters used by the program are given below in upper case letters; for example, "NMF" stands for the total number of nodes in the finite element mesh. All variables starting with any of the letters I, J, K, L, M, N are to be input to the program as integers (i.e., without a decimal point). All integers are to be packed to the right of the field specified by the "cc" numbers. Any variable whose first letter is not an I, J, ..., N is a real number requiring a decimal; "R(N)", for example, is the radius of the 'N-th' nodal point (entered in cc 6-15). If $R(N) = 13.45$, then the number "13.45" can be placed anywhere in the field: cc 6-15. Real numbers can also be input in "E" format; 13.45 could be entered as 1.345E1, .1345E2, 1345.E-2, etc., providing the set of characters is packed to the right of the cc field.

Whenever applicable, units of the variables are stated in symbolic notations. The symbols used below are defined as follows:

Aerojet Solid Propulsion Company
Report 1341-26F

Appendix H

(F) = Force units
(L) = Length units
(T) = Time units
(°F) = Temperature units
(R) = Radian
(Btu) = Thermal Heat Flow Units

Thus, the quantity $(F) (L)^{-2}$ written after the shear modulus means "psi" if pounds and inches are the units chosen by the user. There are no units, conversion factors, etc., built into the program; thus, once a set of units is chosen it must be used consistently throughout the analysis.

B. SEQUENCE OF OPERATIONS

The flow of program execution is controlled by three (3) user-supplied variables:

IPF = Plot Control Flag
NTEM = Temperature Information Flag
JOB = Job Control Flag

Table H-2 contains values which can be assigned to these variables showing what operation results from a particular specification. Certain combinations are not possible. For example, if $IPF < 0$, the program reads mesh data, prepares a plot and returns control to that portion of the program which looks for the next job; thus, the variables "NTEM" and "JOB" cannot be specified. "JOB" has no meaning unless $IPF \geq 0$ and $NTEM = 0$.

The option $NTEM = 1$ is impractical for real problems because of the amount of card data involved; this option is useful when solving "check cases" with temperature distributions generated from an analytical expression or formula. The $NTEM = 2$ option saves re-running the temperature problem if only the mechanical properties or mechanical loads change. $NTEM = 3$ is used for the isothermal problem in which the loading is mechanical in origin. Viscoelastic materials exhibit temperature dependence, so material temperatures must be defined even though there are no driving thermal strains in the body to be analyzed.

The variable "JOB" (which is only defined if $NTEM = 0$) controls what the program does with the results of the heat transfer solution and where the program goes after the heat transfer calculations. If $JOB = 0$, element temperatures are saved temporarily for use in the stress analysis to follow. $JOB = 1$ results in the same operation as $JOB = 0$, but in addition the element temperatures are saved for use in a later analysis (or series of analyses). If $JOB = 2$, the temperatures are saved (and printed at user specified time intervals) on a tape for use at some other time; at this point the program is through with this job and looks for another. $JOB = 3$ allows the user to run the program solely as a heat transfer analysis.

Aerojet Solid Propulsion Company
Report 1341-26F

Appendix H

EXECUTION CONTROL VARIABLES

FLAG	VALUE	OPERATION PERFORMED
IPF	< 0	Read grid data only, plot grid and <u>stop</u> .
	= 0	Read all data, <u>execute</u> the job <u>without</u> a plot.
	> 0	Read all data, <u>execute</u> the job <u>with</u> a plot.
NTEM	= 0	Calculate the element temperatures using the heat transfer analysis.
	= 1	Read the element temperatures from card input.
	= 2	Read the element temperatures from a tape created during a previous run.
	= 3	Read the element temperatures from card input and use the same distribution for all solution time points (isothermal response).
JOB	= 0	Run the heat transfer problem and use the results to perform the stress analysis.
	= 1	Run the heat transfer problem, save the element temperatures on a permanent file (which can be used as input to subsequent jobs) and use the results to perform the stress analysis.
	= 2	Run the heat transfer problem, save the element temperatures on a permanent file, and <u>stop</u> .
	= 3	Run the heat transfer problem and <u>stop</u> .

Table H-2

Aerojet Solid Propulsion Company
Report 1341-26F

Appendix H

C. DATA CARD INPUT

1. Grid Definition

a. Start Cards

(1) First Card (A3)

cc

1-3 Enter the characters "TVA"

(2) Title Card (12A6)

cc

1-72 HED Title information for job and plot (center about cc 36
for plot)

b. Control Card (One card, 3I5)

cc

1-5 NNP Number of nodal points \leq 273

6-10 NEL Number of quadrilateral elements \leq 240

11-15 IPF Plot flag
< 0, plot only
= 0, run only
> 0, plot and run

c. Node Coordinate Cards (I5, 2F10.3, I5, 2F10.3, I5)

cc

1-5 N Node Number

6-15 R(N) Radial Coordinate (L)

16-25 Z(N) Axial Coordinate (L)

26-30 NE Ending Node Point Number

31-40 R(NE) Radial Coordinate (L)

41-50 Z(NE) Axial Coordinate (L)

51-55 NI Node Number Increment

Aerojet Solid Propulsion Company
Report 1341-26F

Appendix H

If the ending node number NE is not zero (or blank), then nodes will be generated in equal distance increments along a line between node N and node NE. The first generated node is assigned the number $N + NI$; the second generated node number is $N + 2NI$, etc. Note that the node number difference $(NE - N)$ must be positive and divisible by NI.

If NI is omitted it will be assigned a value of "1" automatically.

d. Element Numbering Cards (815)

cc

1-5	N	Element Number
6-10	IX (N, 1)	{ Node numbers describing the corner points of the quadrilateral }
11-15	IX (N, 2)	
16-20	IX (N, 3)	
21-25	IX (N, 4)	
26-30	MN(N)	Material Number
31-35	NIG	Number of elements to be generated
36-40	NNI	Node Number Increment

If the number of elements to be generated (NIG) is not zero, then NIG elements will be generated. The first generated element is assigned the number $N + 1$; the second generated element is numbered $N + 2$, etc. The node numbers of the second generated element are found by adding NNI to the node numbers of the first generated element, etc. If NNI is omitted it will be assigned a value of "1".

The material number assigned to generated elements is the same as that for element N. Material numbers are not necessary if the program is to plot the grid only ($IPF < 0$).

If $IPF < 0$; data input ends here.

Aerofet Solid Propulsion Company
Report 1341-26F

Appendix B

2. Solution Time and Temperature Information

a. Control Card (One card 2I5, F10.0, 2I5, F10.0).

cc

1-5	NDT	Total number of time increments to be used in the solution for element temperatures and/or stresses.
6-10	NTR	Number of regions on the time axis having the same value of time increment ratio. ≤ 50
11-20	TMF	Value of time at the end of the NDT th increment. (T)
21-25	NBCF	Number of functions describing time dependent boundary conditions. ≤ 10
26-30	NTEM	Temperature information flag: = 0 Element temperatures are to be calculated using the heat transfer analysis. = 1 Element temperatures are to be read from cards. = 2 Element temperatures are to be read from a tape created on a previous run. = 3 Element temperatures are to be read from cards, and this distribution is to be used for all solution time points.
31-40	TZ	Temperature of every element at time zero (°F) (stress free temperature).

Aerojet Solid Propulsion Company
Report 1341-26F

Appendix H

b. Solution Time Points

At least one card in this section

(1) First Card (3 (I5,2F10.0))

cc

1-5	NTI(1)	Number of increments for which the time increment ratio C(1) remains constant in region 1.
6-15	DT (1)	Value of time after NTI(1) time increments in region 1.
16-25	C (1)	Time increment ratio in region 1.
26-30	NTI (2)	Same as cc 1-5 for region 2.
31-40	DT (2)	Value of time after NTI (1) HNTI (2) time increments (T)
41-50	C (2)	Same as cc 16-25 for region 2
51-55	NTI (3)	
56-65	DT (3)	Region 3
66-75	C (3)	

(2) Second Card (3 (I5, 2 F10.0)) (If required)

cc

1-5	NTI (4)	
6-15	DT (4)	Region 4
16-25	C (4)	

... Etc.

Use as many cards in this section as are required to enter NTR groups of (NTI (I), DT (I), C (I)). Note that

NTR
 $\sum_{i=1} \text{NTI}_i = \text{NDT}$, otherwise an error message will be issued by the program.

The solution time points in region r are found using:

$$t_{i+1} = t_i + C_r * (t_i - t_{i-1})$$

Aerojet Solid Propulsion Company
Report 1341-26F

Appendix H

This method of solution time point input has the effect of automatically producing small time steps at the beginning of the region while continuously widening the time steps toward the end of the region. As an example, if 50 solution time points are specified over a 24 hour period with $C = 1.1$ the first solution time point will occur at .0206 hrs (1.24 minutes) and the last solution step ($t_{50} - t_0$) will be 2.19 hours (132 minutes).

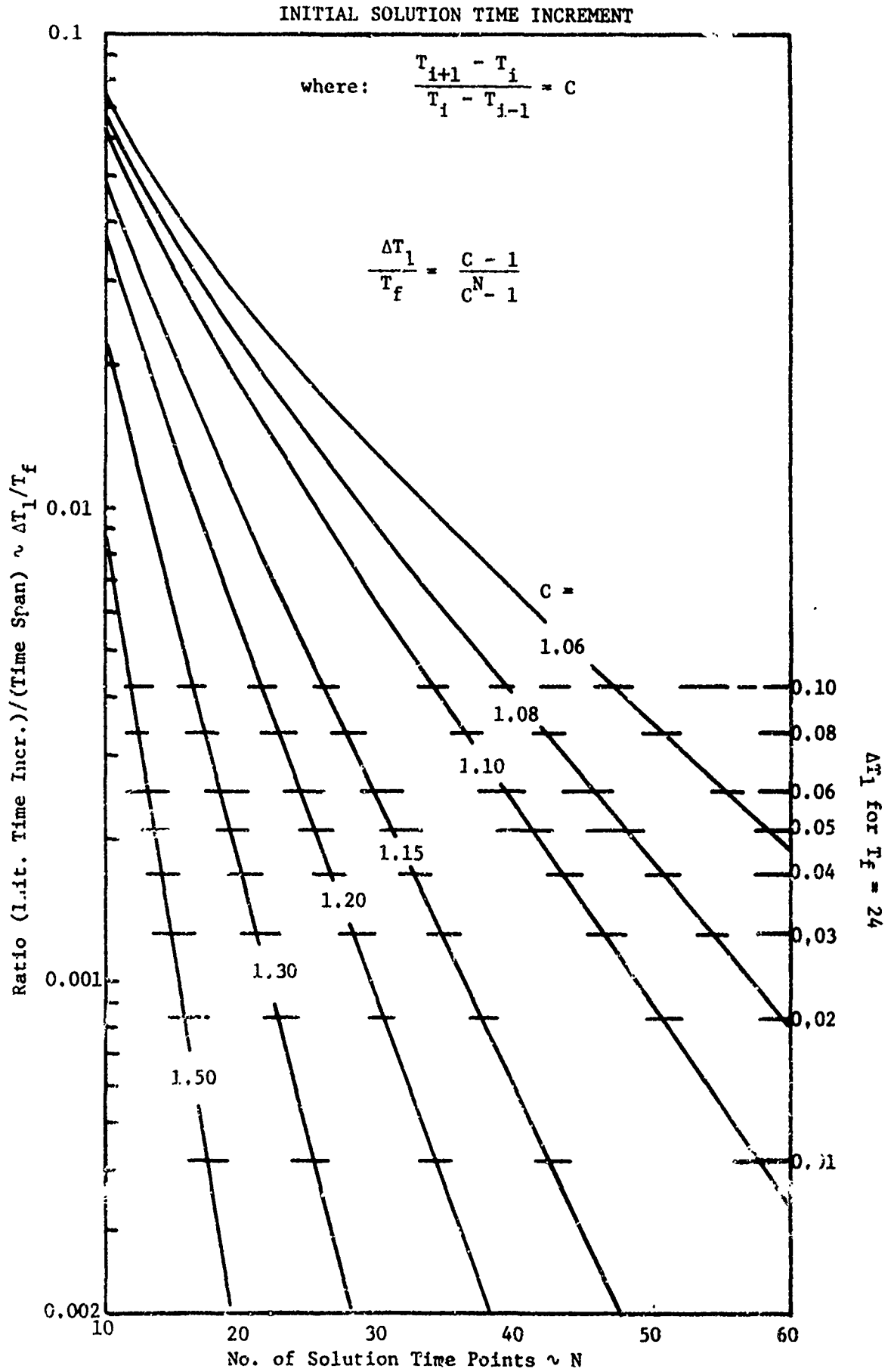
It is important to choose C such that the smallest time step will not be so small as to produce a reduced time falling off the mechanical properties table or the final time step too large. The following equations may be used to find these values:

$$\frac{\Delta T_i}{T_f} = \frac{C-1}{C^N-1} \quad \frac{\Delta T_N}{T_i} = \frac{C^{N-1}(C-1)}{C^N-1} \quad (H-2)$$

where

- C = time increment ratio
- ΔT_i = Initial solution time step
- ΔN = total number of solution time points
- ΔT_N = final time step
- T_f = final value of time ($T_0 = 0$)

These two equations are plotted for various values of C in Figures H-1 and H-2 respectively.



Aerojet Solid Propulsion Company
Report 1341-26F

FINAL SOLUTION TIME INCREMENT

where: $\frac{T_{i+1} - T_i}{T_i - T_{i-1}} = C$

$$\frac{\Delta T_N}{T_f} = \frac{C^{N-1} (C - 1)}{C^N - 1}$$

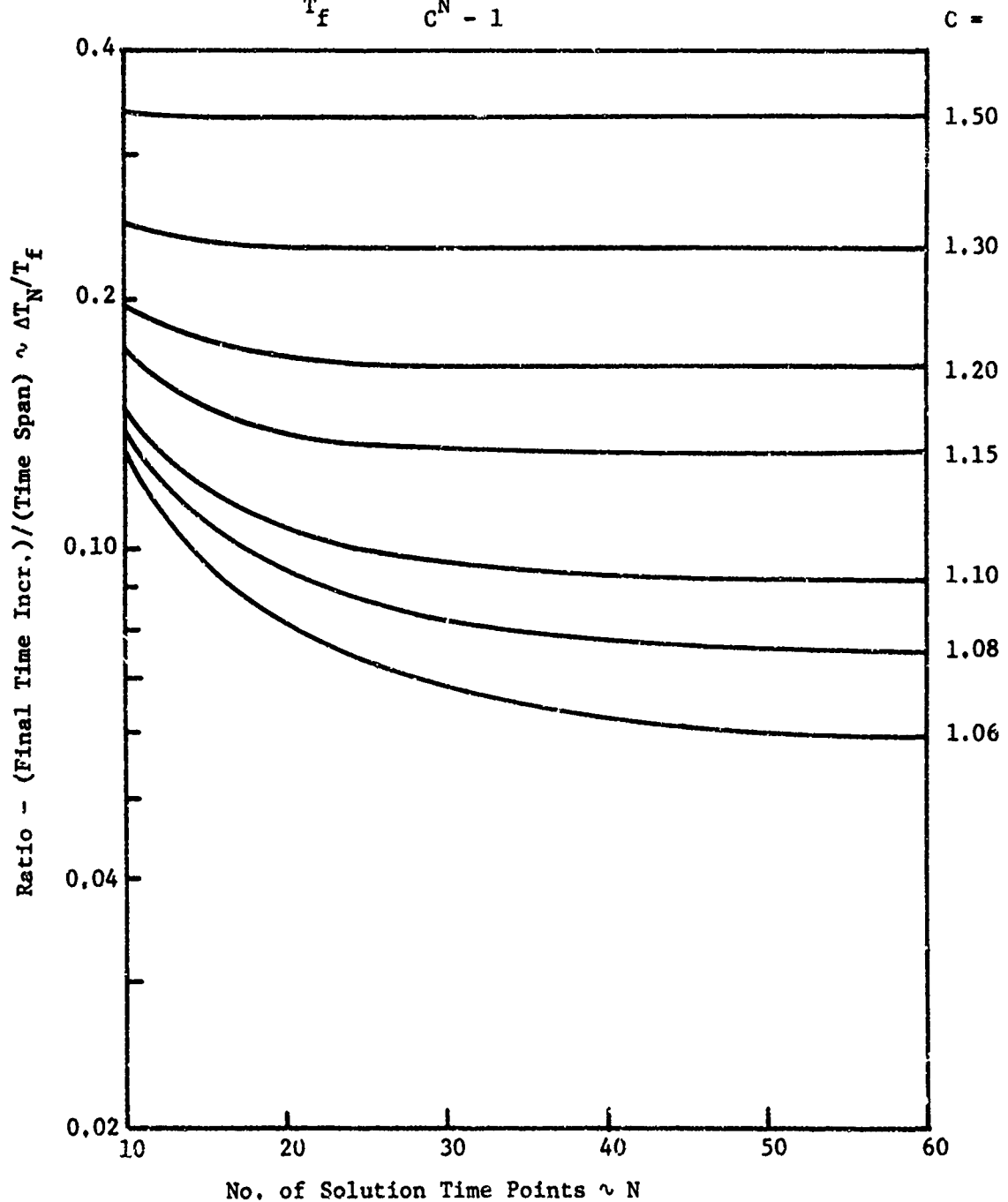


Figure H-2

Aerojet Solid Propulsion Company
Report 1341-26F

Appendix H

c. Boundary Condition Function Cards

Skip this section if NBCF = 0

(1) Card One (2I5)

cc

1-5	N	Number assigned to this function
6-10	NPTS(N)	Number of points in the table describing this function. ≤ 30

(2) Card Two (8F10.0)

cc

1-10	TFN (N, 1)	Time at point 1, t_1 (T)
11-20	FN (N, 1)	Value of the function at time t_1 , f_1
21-30	TFN(N, 2)	Time at point 2, t_2 (T)
31-40	FN (N, 2)	Value of the function at time t_2 , f_2
41-50	TFN (N, 3)	} Point 3
51-60	FN (N, 3)	
61-70	TFN(N, 4)	} Point 4
71-80	FN (N, 4)	

(3) Card Three (8F10.0) (If required)

cc

1-10	TFN (N, 5)	} Point 5
11-20	FN (N, 5)	

... etc.

Use as many cards 2, 3, etc., in this section as are required to enter NPTS(N) pairs of (TFN(N, I), FN(N, I)) which define this function (Number N). There are NBCF sets of cards 1, 2, 3, etc. in this section. Data for a new function begins on a new card 1.

Figure H-3 represents a function which might be used to describe the pressure transient in a motor. The last point in the table must have a value of time which is greater than or equal to the length of solution period (TMF); for this case $16.0 > 14.0 = \text{TMF}$ (Figure 3.1).

Aerojet Solid Propulsion Company
Report 1341-26F

Appendix H

EXAMPLE BOUNDARY CONDITION FUNCTION

I	TFN (3, I)	FN (3, I)
1	0.0	0.0
2	2.0	0.8
3	4.0	1.0
4	5.0	0.7
5	16.0	0.7

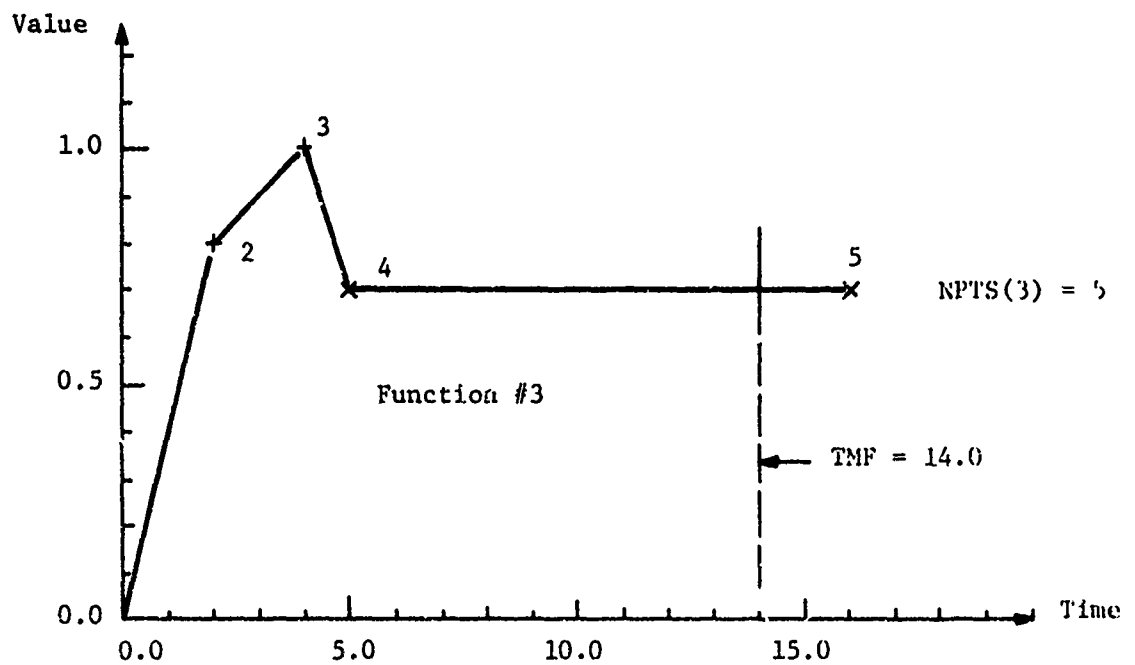


Figure H-3

Appendix H

If no data are input in this section ($NBCF = 0$), then all boundary specifications are independent of time and boundary values are assumed to be imposed as step function at $t = 0^+$.

At least one card in this section

• • • •

1-5	NO(9)	Output Interval
6-10	NPR(9)	Number of print operations at this interval
11-15	NO (10)	Output Interval
16-20	NPR (10)	Number of print operations at this interval

H-16

Aerojet Solid Propulsion Company
Report 1341-26F

Appendix H

Suppose that temperature output is required at time points 2, 4, 7 and 8 of Figure 2.1, then one card would be input in this section:

Card 1: 2,2,3,1,1,1 ; [2 (2) + 3 (1) + 1 (1) = 8].

If temperatures at all 8 points is requested, then

Card 1: 1, 8 ; [1 (8) = 8].

e. Average Element Temperature Cards (3I5, F10.0)

(Card 2-a is the reference for values of NDT, NTEM and TZ).

Skip this section if NTEM = 0, or NTEM = 2
--

cc

1-5	NELS	Starting element number for this group.
6-10	NELG	Number of elements with the same average temperature as element number NELS.
11-15	NELI	Element number increment.
16-25	TAVG	Average element temperature for this group of elements. (°F)

If NTEM = 1, there are NDT sets of element temperatures that must be defined in this section (one set for each of the NDT time points contained in the solution period). All element temperatures must be prescribed at a given time point before proceeding to the next point. If every element has a different temperature, then NEL cards (with cc 6-15 blank) must be prepared for that time point. It is possible to generate element temperatures at a time point if several elements are at the same temperature. NELG elements are assigned average temperatures TAVG. The number assigned to the first generated element is NELS + NELI; the second is NELS + 2 (NELI), etc.

Suppose that a body described using 50 elements (NEL = 50) is at a uniform 77°F, when $t \leq 0$ (TZ = 77.0), and at the end of the first time increment elements 1-25 drop to 60°F while elements 26-50 reach 45°F. Two cards are required to define the element temperature distribution at the end of time increment one ($t = t_1$):

Card 1: 1, 24, 1, 60.0

Card 2: 26, 24, 1, 45.0

If NTEM = 3, then there is only one set of element temperatures which must be input in this section. This temperature distribution applied to all solution time points; the body starts at $t = 0^-$ at a uniform temperature TZ (at which the body is assumed to be "stress free"), and at $t = 0^+$ the element temperatures assume the values prescribed in this section of the data input and remain constant for all time, $t > 0$.

3. Transient Heat Transfer Solution Data

Skip this section if NTEM = 1, 2, or 3

a. Control Card (One card; 4I5)

cc

1-5 NMAT Number of materials with different thermal properties. ≤ 10

6-10 NNBC Number of nodal point boundary conditions (temperatures or heat fluxes)

11-15 NCBC Number of convection boundary conditions ≤ 65

16-20 JOB Job Control Flag

= 0 : run heat transfer and use the results to perform the stress analysis.

= 1 : run heat transfer, save element temperatures on a permanent file, and use the results to perform the stress analysis.

= 2 : run heat transfer, save the results on a permanent file, and stop.

= 3 : run heat transfer and stop.

21-25 KAT KAT = 0 Axisymmetric Analysis
 KAT \neq 0 Planar Analysis

b. Material Cards (1I0, 6F10.0)

cc

1-10 N Material number

11-20 XCOND(N) Conductivity: K_{rr} , (Btu)(T) $^{-1}$ (L) $^{-2}$ ($^{\circ}$ F/L)

21-30 YCOND(N) Conductivity: K_{zz}

Aerojet Solid Propulsion Company
Report 1341-26F

Appendix H

31-40 XYCOND(N)	Conductivity: K_{rz}
41-50 SPHT (N)	Specific Heat, $(\text{Btu})(\text{F})^{-1}(\text{°F})^{-1}$
51-60 DENS(N)	Weight density, $(\text{F})(\text{L})^{-3}$
61-70 QX(N)	Heat generated per unit volume, $(\text{Btu})(\text{T})^{-1}(\text{L})$

Use one card for each different material number assigned in the element array (cards 1-d); NMAT cards must be prepared in this section - order is unimportant.

If the thermal conductivity of a material is independent of direction, then

$$K_{rr} = K_{zz} = k$$

$$k_{rz} = 0$$

The heat generated per unit volume is assumed to be constant with time.

c. Nodal Point Boundary Conditions (215, F10.0, 15)

Skip this section if NNBC = 0

cc

1-5	N	Node Number
6-10	KODE(N)	Boundary condition type $\left\{ \begin{array}{l} = 0, \text{ externally supplied heat flux} \\ = 1, \text{ prescribed node temperature} \end{array} \right.$
11-20	T(N)	Boundary value amplitude $\left\{ \begin{array}{l} = \text{Heat flux (KODE(N) = 0), } (\text{Btu})(\text{T})^{-1} (\text{R}) \\ = \text{Temperature (KODE(N) = 1), } (\text{°F}) \end{array} \right.$
21-25	NFN(N)	Function number

All nodal points not specified in this section are assumed to have externally supplied heat flux of zero for all values of time.

A function number equal to zero (or blank) means that the prescribed boundary condition is applied at time zero and remains constant for all time, $t > 0$.

Aerojet Solid Propulsion Company
Report 1341-26F

Appendix H

The functions assigned in this section must have been defined previously in Section 2-c. For time varying boundary conditions, the magnitude of the boundary value at some time t is found by selecting the value of the function at t and then multiplying this value times the boundary value amplitude (cc 11-20). A given function can be used to describe any number of boundary conditions.

d. Convection Boundary Conditions

Skip this section if NCBC = 0

(NCBC Cards, 215, 2F10.0, 15)

cc

1-5	I(N)	Node number i
6-10	J(N)	Node number j
11-20	H(N)	Heat transfer coefficient, h : $(\text{BTU})(T)^{-1}(L)^{-2} (^{\circ}\text{F})^{-1}$ $q = h (T - T_0)$
21-30	TE(N)	Environmental temperature amplitude, \bar{T}_0
31-35	NFCV(N)	Function number

If the environmental temperature T is time dependent, then a non-zero function number must be specified in cc 31-35. \bar{T}_0 will be multiplied by the appropriate value of the function of time t in order to establish the value of environmental temperature, T_0 .

If the environment does not change temperature with time, then $\text{NFCV}(N) = 0$ and $T_0 = T_0$, constant for $t > 0$.

If JOB = 2 or 3 (Card 3-a), then data ends here

Aerojet Solid Propulsion Company
Report 1341-26F

Appendix H

4. Stress Analysis Information

The program will not read data in this section if
NTEM = 0 (card 2a) and JOB = 2 or 3 (card 3a)

a. Title card (20A4)

cc

1-8 HED Any alpha numeric information (printed with
the solution)

b. Control Card (5I5, 2(F10.0, I5), 3I5, F10.0)

cc

1-5	NMAT	Number of materials	≤ 4
6-10	NCMN	Number of elements with material identification numbers which are to be redefined.	
11-15	NBCN	Number of node points for which boundary cards are used	≤ 60
16-20	NPC	Number of pressure cards	≤ 55
21-25	NDMG	Number of elements for damage evaluation	≤ 20
26-35	ANGV	Angular velocity amplitude, (R) (T) ⁻¹	
36-40	NFAV	Function number for ANGV	
41-50	AZZ	Axial acceleration amplitude, (L) (T) ⁻²	
51-55	NFAZ	Function number for AZZ	
56-60	IDSF	Pressure boundary condition function no. for use of pressurization shift function data	
61-65	IPSC	Geometry type flag	
		IPSC = 0 Axisymmetric analysis	
		= 1 Plane strain analysis	
		= 2 Generalized plane strain analysis	
		= 3 Generalized plane stress analysis	
66-70	NSM	Material No. (if IPSC = 2) of case material	
71-80	SZV	Value of normal stress (if IPSC = 3) (F) (L) ⁻²	

Aerojet Solid Propulsion Company
Report 1341-26F

Appendix H

NMAT is the total number of materials (viscoelastic and elastic).

If the material I.D. numbers assigned to the elements in Section 1-d are appropriate for both the heat transfer and stress analyses, then NCMN is set to zero (or blank). NBCN is a count of nodes at which force and/or displacement boundary values are specified. NPC is the total number of element sides subjected to pressure loads.

IDSP is the boundary condition function number which describes the bulk pressure as a function of time when an isothermal pressurization case is being run. For a thermal analysis leave this field blank. This function will be used to find the pressurization shift function values in the properties determination and also will be used in the damage calculations. When IPSC - 2 a special generalized plane strain analysis will be run. The normal strain will be set equal to the average thermal strain ($\alpha_c \Delta T_c$) in the case which is found by the material number NSM specified in cc 66-70.

c. Material Properties

(1) Control Card (3I5, 4F10.0)

cc

1-5 K Material number

6-10 NON(K) Number of terms in the Prony series representation of the shear relaxation function. ≤ 16

11-15 NSFP(K) Number of points in the shift function table. ≤ 16

16-25 APO(K) Equilibrium shear modulus, (F) (L)⁻²

26-35 XK(K) Bulk modulus, (F)(L)⁻²

36-45 AIP(K) Linear coefficient of thermal expansion, (L)(L)⁻¹(°F)⁻¹

46-55 DENS(K) Mass density, (F)(L)⁻⁴(T)²

The shear relaxation function is written in the form:

$$\phi(t) = A_0 + \sum_{i=1}^M A_i e^{-\beta_i t}$$

where

NON(K) = M for the Kth material
APO(K) = A₀ for the Kth material

An elastic material is input by leaving cc 6-15 blank and entering the shear and bulk moduli in cc 16-25 and cc 26-35, respectively. A non-zero value of density is required for the calculation of body forces arising from specified values of spin velocity and/or axial acceleration.

(2) Prony Series Coefficients Card(s) (8F10.0)

Skip this section if NON(K) = 0

cc

1-10	AP(K, 1)	A ₁ for material K	(F)(L) ⁻²
11-20	BP(K, 1)	β_1	(T) ⁻¹
21-30	AP(K, 2)	A ₂	(F)(L) ⁻²
31-40	BP(K, 2)	β_2	(T) ⁻¹
41-50	AP(K, 3)	A ₃	(F)(L) ⁻²

etc.

Aerojet Solid Propulsion Company
Report 1341-26F

Appendix H

Use as many cards in this section as are required to specify
NON(K) pairs of (A_1, B_1) ; four pairs per card.

(3) Shift Function Table (3F10.0)

Skip this section if NSFP(K) = 0

cc

1-10	FST(K,1)	Temperature at 1st point, T_1 (°F)
11-20	FS(K,1)	$\log_{10} a_{T_1}$
21-30	FST(K,2)	Temperature at 2nd point, T_2 (°F)
31-40	FS(K,2)	$\log_{10} a_{T_2}$
41-50	FST(K,3)	etc.

Use as many cards in this section as are required to specify
NSFP(K) pairs of $(T_1, \log_{10} a_T)$; four pairs per card. If IDSP > 0 (card

4b) FST (K, 1) will be interpreted as pressures and FS (K, 1) are $\log_{10} a_p$.

d. Element Material Numbers

Skip this section if NCMN = 0

cc

1-5	N1 (1)	Element number
6-10	N2 (1)	Material number assigned to element N1 (1)
11-15	N3 (1)	Number of elements with the same material number as element N1 (1)
16-20	N4 (1)	Element number increment
21-25	N1 (2)	Element number
26-30	N2 (3)	Material number assigned to element N1 (2)
31-35	N3 (2)	Number of elements with the same material number as element N1 (2)
etc.		

Aerojet Solid Propulsion Company
Report 1341-26F

Appendix H

Use as many cards in this section as are required to re-define the material numbers of NCMN elements; 16 entries per card are possible.

Suppose that a 50 element problem is to have all its material numbers changed (NCMN = 50), and all even numbered elements are material 1 while all odd elements are material 2; one card describing these changes would read:

[1, 2, 24, 2, 2, 1, 24, 2]

e. Node Point Boundary Specification(s)

At least one card in this section

(I5, 2(I5, F10.0, I5))

cc

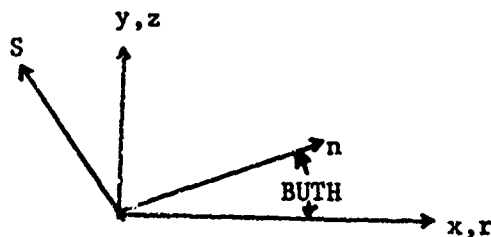
1-5	K	Node point number (NB(N) = K)	
6-10	NFLR(N)	Radial boundary condition type	
		$\begin{cases} = 0; \text{externally applied } \underline{\text{force}} \\ = 1; \text{specified } \underline{\text{displacement}} \end{cases}$	$\begin{matrix} (F) (R)^{-1} \\ (L) \end{matrix}$
11-20	BVR(N)	Radial boundary value amplitude	
21-25	NFNR(N)	Function Number	
26-30	NFLZ(N)	Axial boundary condition type	
		$\begin{cases} = 0; \text{externally applied } \underline{\text{force}} \\ = 1; \text{specified } \underline{\text{displacement}} \end{cases}$	$\begin{matrix} (F) (R)^{-1} \\ (L) \end{matrix}$
31-40	BVZ(N)	Axial boundary value amplitude	
41-45	NFNZ(N)	Function number	
46-55	BUTH(N)	Skew boundary angle (degrees)	

A total of NBCN cards must be prepared in this section. The axial displacement at one node must be specified as a minimum requirement.

Positive boundary values are in the direction of the positive coordinate axes.

Zero (or blank) function numbers assigned to boundary value components implies time independence (constant for $t > 0$). The variation of a boundary value with time is determined by multiplying amplitude times the appropriate value of the corresponding function. All nodes not specified in this section are assumed to have no externally applied loads and are free to displace as the solution dictates.

The shew boundary is shown in the figure below. If $BUTH(N) \neq 0$ the boundary conditions are expressed in the n - s system.



f. Pressure Loads

Skip this section if NPC = 0

cc

1-5	IPC(N)	Node number i
6-10	JPC(N)	Node number j
11-20	PR(N)	Pressure amplitude (F) (L) ⁻²
21-25	NFNP(N)	Function

There are NPC cards in this section. $NFNP(N) = 0$ means that pressure is applied as a step function at $t = 0^+$.

Positive pressure acts in the direction shown in Figure 4.1.

Aerojet Solid Propulsion Company
Report 1341-26F

Appendix H

g. Damage Parameters

Skip this section if NDMG = 0

cc

1-5	LDMG(N)	Element no.	whose damage is to be evaluated	
6-15	STZR(N)	σ_{to}		
16-25	TZR(N)	t_o	See below	
26-35	SCR(N)	σ_{cr}		

There are NDMG cards in this section. LDMG(N) may be positive or negative. If positive, the hoop stress will be used in damage calculations; if negative the maximum principal r-z stress will be used. The damage is evaluated using

$$PED_t = \frac{1}{a_T} \int_0^t \frac{(\sigma(t') - \sigma_{cr} + P(t'))^B}{(\sigma_{to} - \sigma_{cr})^B a_p (P(t'))} dt$$

If IDSP = 0 (card 4b) then $P(t') = 0$ for all times. If IDSP > 0 the $P(t')$ will be found from the boundary condition function indicated by IDSP.

Data input ends at this point

Aerojet Solid Propulsion Company
Report 1341-26F

Appendix H

IV. PROGRAM OUTPUT DESCRIPTION

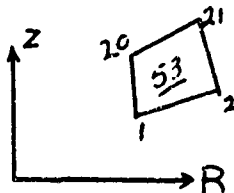
Output from the program includes:

1. Input geometry, material properties and solution time information in a self-explanatory format.
2. Nodal point temperatures at the specified time-point interval.
3. The radial, tangential, axial and shear stresses and strains and the average element temperature at the specified time-print interval.
4. The damage rate and accumulated damage for specific elements at each time-print interval.

The printed program output consists of (1) "echo" reproduction of the data input cards identified in self-explanatory format, and (2) results of the analysis which might include nodal point temperatures, element stresses/strains, node displacements, etc.

A. ELEMENT NODE NUMBERING

It should be noted that element node number data may not be listed in the same order as these data appear on the input card. The program logic permutes the order of the element node numbers so that the largest node number is always last (4th) in the printed list for each element. For example, if element number 53 (shown below)



is input as (1, 2, 21, 20), the program will print the data as (20, 1, 2, 21) so that "21" is last while the original counter clockwise order is preserved. Efficiency is gained if the user specifies the 4th node as the largest for every element.

The reason for having the largest node as last one in the sequence for a given element is that three (3) equations are assigned to this node as opposed to only two (2) equations per node for the others. A node number that is not the largest one in any element has the R and Z displacement components as its unknowns (2 total). All other nodes have R, Z displacement components plus the "mean pressure variable" H as unknowns at that point (3 total). Thus, node "21" of element "53" above has assigned to it U_{R21} , U_{Z21} , and H_{53} as unknowns.

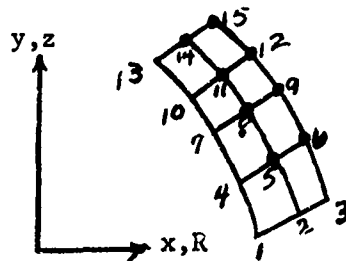
Aerojet Solid Propulsion Company
Report 1341-26F

Appendix H

In order to assign equations uniquely to the unknown values of "H" for every element, the program has the following restriction:

The finite element quadrilateral mesh must be numbered so that any node number is maximum in only one (1) element.

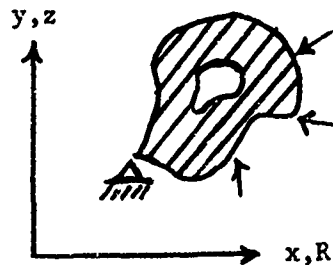
With a "layered" numbering scheme (across the "narrow" direction of the grid) the restriction is complied with automatically:



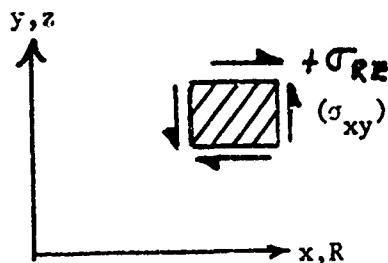
The "heavy" nodes (●) shown above have three (3) unknowns associated with them.

B. SIGN CONVENTION

All positive vector quantities (forces/displacements) are in the directions of the positive coordinate axes providing the grid is positioned in the "positive" R-Z quadrant:



Normal stress (strains) are tensile when positive and the shear stress (strain) sign convention is shown below:



Aerojet Solid Propulsion Company
Report 1341-26F

Appendix H

$$PED_t = \frac{1}{a_t} \int_0^t \frac{(\sigma(t') - \sigma_{cr} + P(t'))^B}{(\sigma_{to} - \sigma_{cr})^B a_p (P(t'))} dt'$$

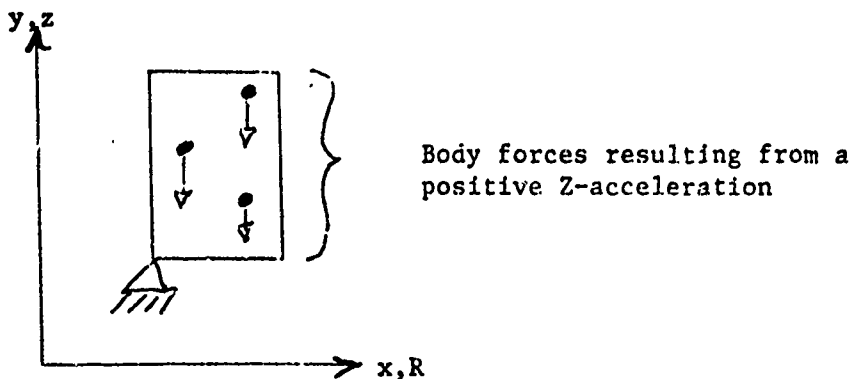
If IDSP = 0 (Card 4b) then $P(t') = 0$ for all times. If IDSP > 0 the $P(t')$ will be found from the boundary condition function indicated by IDSP.

The value of $P(t')$ is that portion of the inner-bore firing pressure, $P_i(t)$, which is transmitted to the point in the grain where the principal stress, $\sigma(t')$, is evaluated. The relation of $P(t')$ to $P_i(t')$ in infinite-length cylinders is well known () (See Section IV of this report). For finite length cylinders the ratio of $P(t')$ to $P_i(t)$ must be obtained from the stress analysis.

For metal cases $P(t')$ seldom differs from $P_i(t')$ by more than 5%. For most firing problems this difference is not significant and $P(t')$ can be approximated by $P_i(t')$.

Data input ends at this point

A positive spin velocity produces hoop tension, and positive axial acceleration causes body forces to be applied on the body acting in the $(-Z)$ direction:



V. EXAMPLE PROBLEMS

A. TRANSIENT HEAT CONDUCTION IN A LONG CYLINDER

The purpose of this example is to illustrate the use of the program in solving heat conduction problems. A long, hollow cylinder constructed from a single material is initially at a uniform temperature of 0°F ; then, at $t = 0^+$ the outer surface of the cylinder is instantaneously heated to 1°F along its entire length. The ends of the cylinder are insulated against axial heat flow so that at any axial station the heat flow is purely radial.

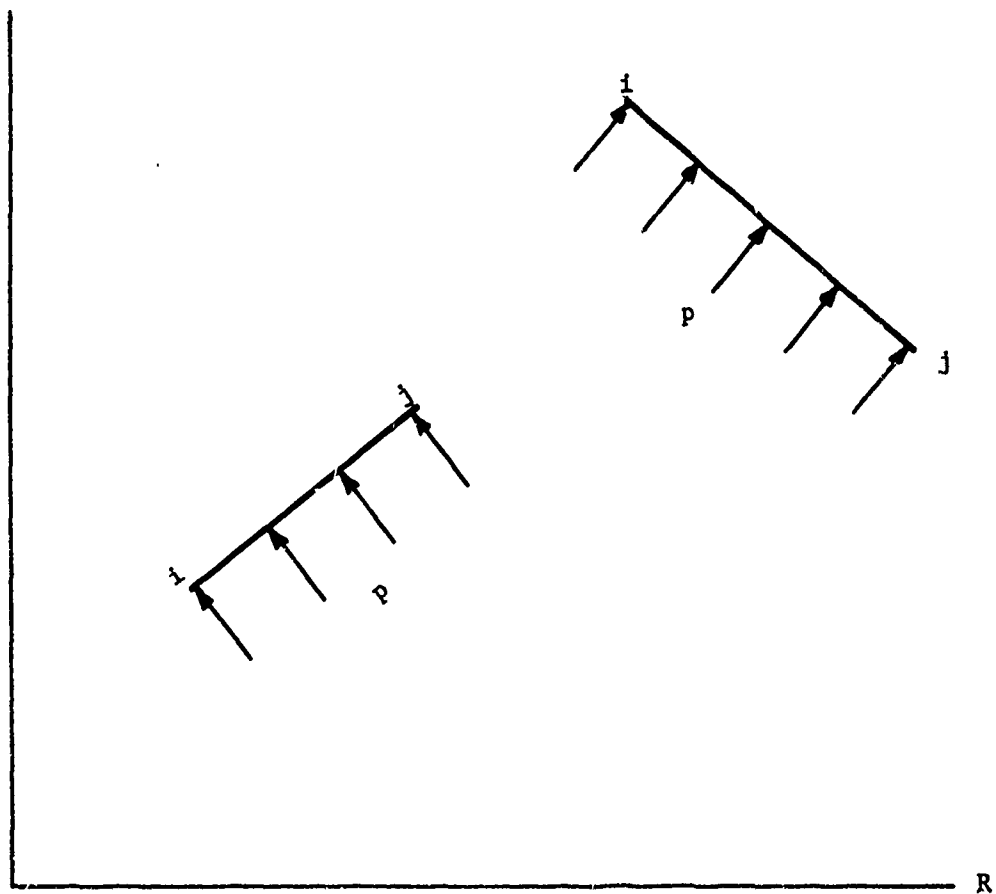
Figure H-4 shows a one (1) inch slice of the cylinder whose inner and outer radii are 1.00" and 2.00", respectively. The slice has been modeled with a mesh composed of ten (10) equal sized elements; the "Z" axis is the center-line of the cylinder. At time zero the temperature of nodes 11 and 22 is changed from 0°F ($TZ = 0.0$) to 1°F , and as time proceeds the interior of the cylinder begins to warm up; thermal equilibrium is reached when the entire cylinder is at a uniform 1°F . Nodes 1-10 and 12-21 are insulated in the sense that no externally supplied heat enters the body at these points. The program assumes that all nodes not specifically included as boundary condition nodes are insulated against externally supplied heat flow; i.e., for all non-boundary nodes, the amount of heat entering a node must balance the amount of heat leaving that node in a unit of time.

The solution span is sub-divided into fifty (50) equal time increments of 0.01 hours each so that the time at the end of solution is 0.050 hours ($TMF = 0.05$), Figure H-5.

Aerojet Solid Propulsion Company
Report 1341-26F

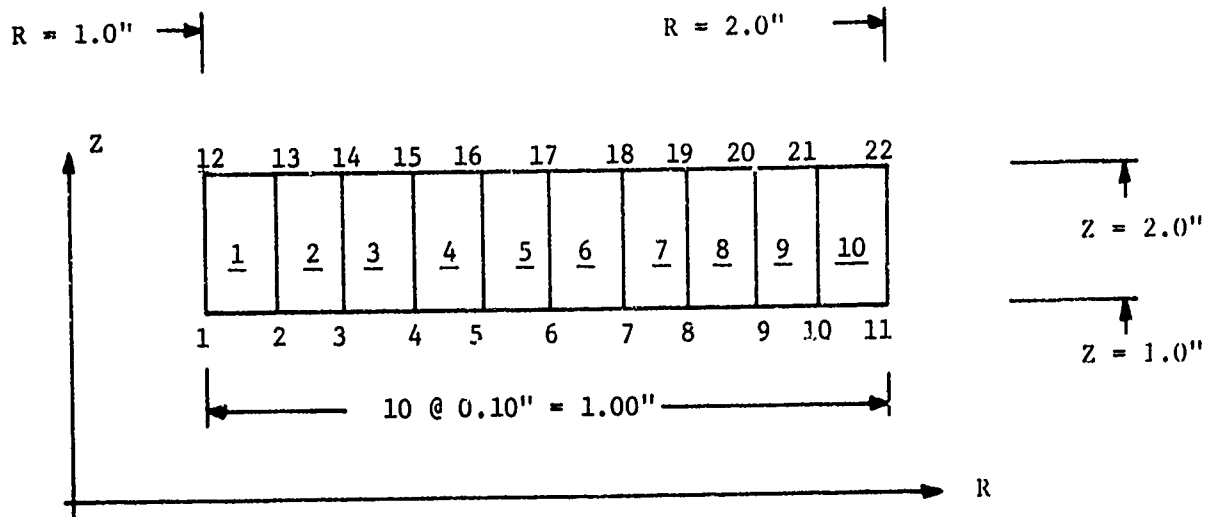
Appendix H

SIGN CONVENTION FOR PRESSURE LOADS

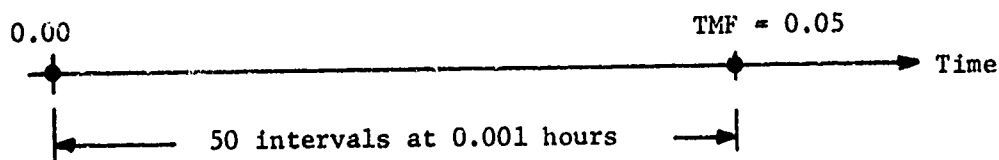


Aerojet Solid Propulsion Company
Report 1341-26F

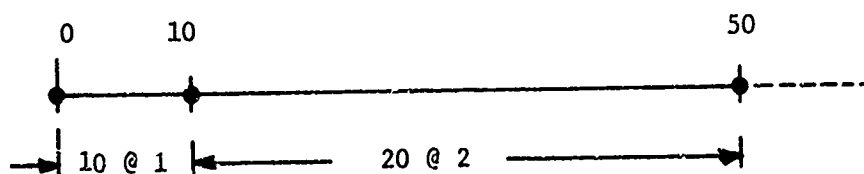
Appendix H



a. Mesh For Example Problem A



a. Solution Time Point Array



b. Solution Output Intervals

Figure H-5: Solution Time Point and Output Schedules

Aerojet Solid Propulsion Company
Report 1341-26F

Appendix H

The output printing schedule is set up so that results are printed at every solution time point for the first ten (10) increments and then at every other solution for the remaining forty (40) increments, Figure H-5.

10 print operations at an interval of 1 = 10
20 print operations at an interval of 2 = 40
50 increments

The thermal properties of the material are summarized as follows:

$$K_{rr} = 0.20 \text{ (Btu)(hr.)}^{-1} \text{ (in.)}^{-2} \text{ (}^{\circ}\text{F/in.)}^{-1}$$

$$K_{zz} = 0.20$$

$$K_{rz} = 0.$$

$$\text{Specific Heat} = 0.20 \text{ (Btu) (lb.)}^{-1} \text{ (}^{\circ}\text{F)}^{-1}$$

$$\text{Weight Density} = 0.20 \text{ (lb.) (in.)}^{-3}$$

$$\text{Heat generated per unit volume per unit time} = 0.*$$

The data cards for this job are shown in Table H-3.

Figure H-6 is a plot of temperature versus time for three (3) points in the cylinder: (1) outer surface (nodes 11 or 22); (2) mid-radius (nodes 6 or 17); and, (3) inner-radius (nodes 1 or 12). For long times, all nodes approach 1°F in the limit.

A value of 3 was assigned to the control variable "JOB" causing a termination of execution after the heat transfer solution. If the results were to be saved**, then the node temperatures would be averaged for each element before saving the results.

B. ELASTIC RING SUBJECTED TO AXIAL TENSION

The purpose of this example is to illustrate the use of the program in solving elastic problems. A hollow, short cylinder is subjected to an axial tension of 6000 psi on one surface and restrained (without radial shear) against axial displacement on the opposite end (Figure H-7). The problem has been modeled with four (4) quadrilateral elements as shown in Figure H-8. The applied stress has been converted to equivalent concentrated loads of 4000, 12000, and 8000 lbs./radian applied at nodes 7, 8 and 9, respectively.

Output from the computer program is shown in Figure H-9 a, b and c.

For purposes of data preparation, unit heat generation is treated as a physical property which can vary from material to material.

**JOB = 1 or 2

360 FIREARM CODING FORM

CODER _____ DATE _____

JOB: _____ DECK _____ SEQ _____
COL 73. 73 .76. 77. 78

FORTRAN STATEMENT		72	73	74	75	76	77	78	79	80	81	82	83	84	85	86	87	88	89	90	91	92	93	94	95	96	97	98	99	100
1	517																													
2																														
3																														
4																														
5																														
6																														
7																														
8																														
9																														
10																														
11																														
12																														
13																														
14																														
15																														
16																														
17																														
18																														
19																														
20																														
21																														
22																														
23																														
24																														

Table H-

TRANSIENT TEMPERATURES IN THE CYLINDER OF EXAMPLE A

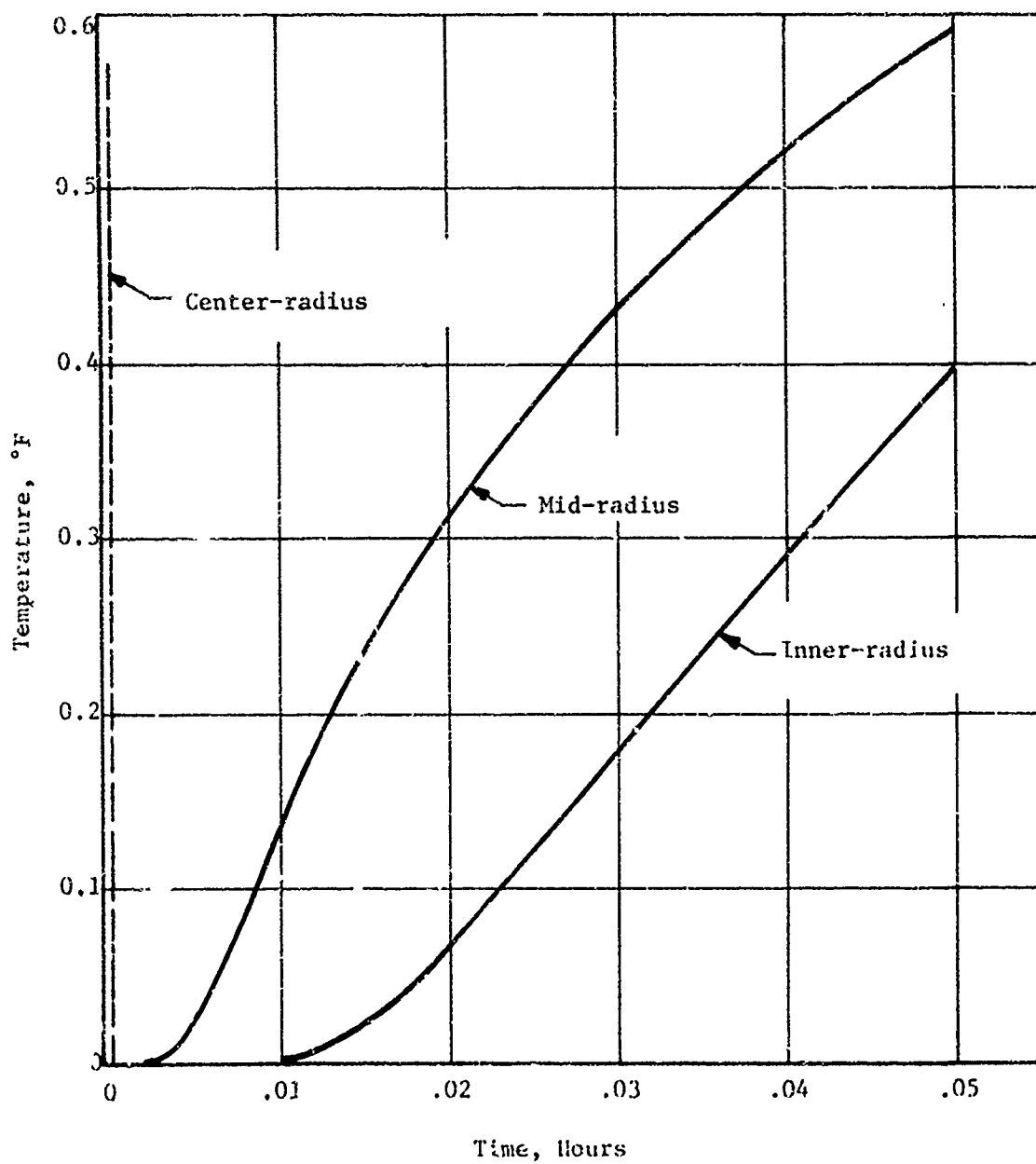
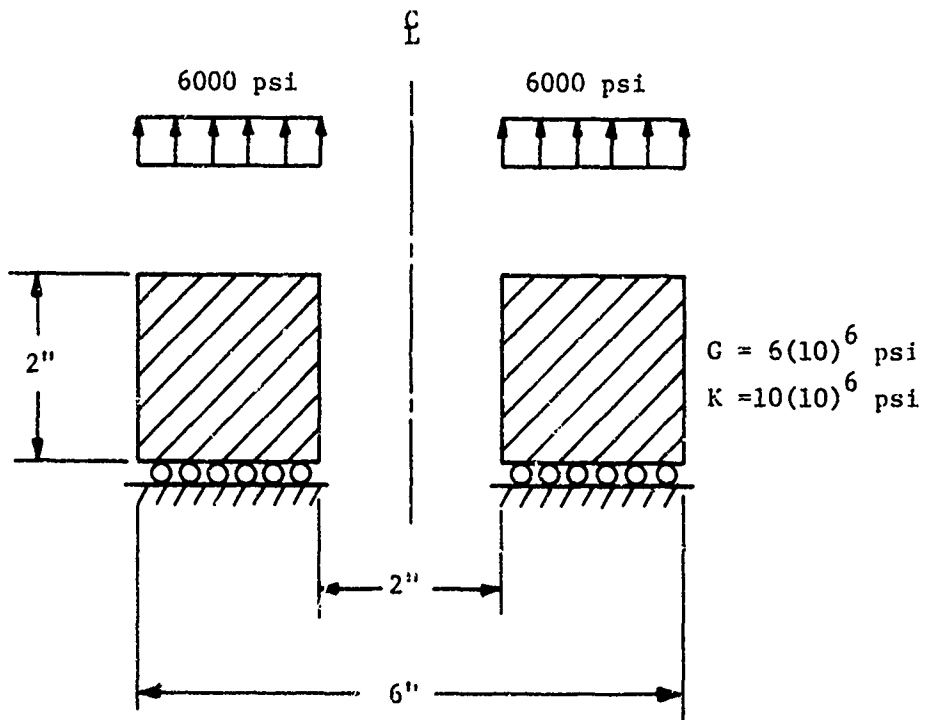


Figure H-6

Aerojet Solid Propulsion Company
Report 1341-26F

Appendix H

EXAMPLE B: AXIAL LOADING OF AN ELASTIC CYLINDER



Aerojet Solid Propulsion Company
Report 1341-26F

Appendix H

GRID FOR EXAMPLE B

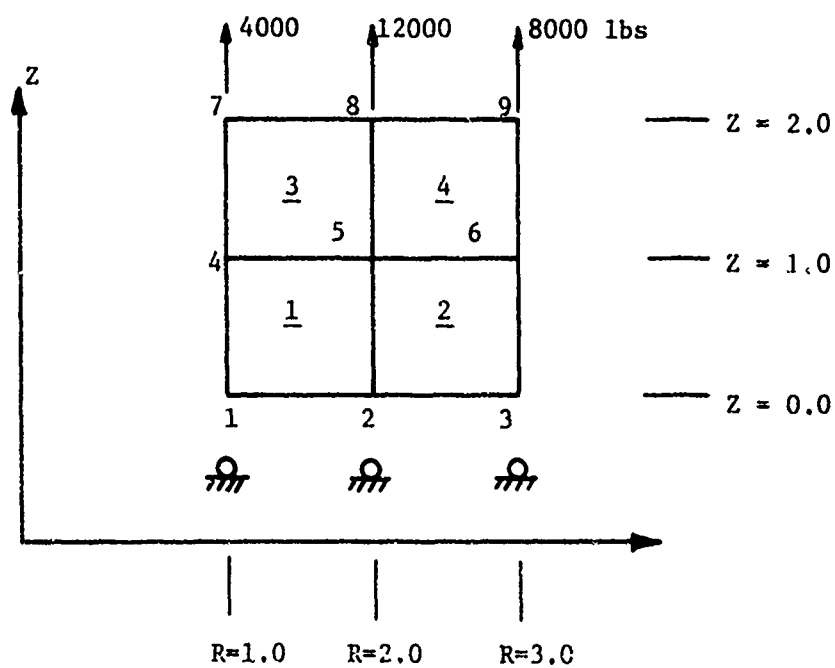


Figure H-8

TWO-DIMENSIONAL THERMOVISCOELASTIC ANALYSIS

P/A. DIRECT-AXIAL-LOADING (LRH SAMPLE) (HOLLOW CYLINDER)

LRH-1.1

CONTROL PARAMETERS

NUMBER OF NODES 5
NUMBER OF ELEMENTS 4

NODE COORDINATE DATA

NODE	R-COORDINATE	Z-COORDINATE
1	1.00000	0.0
2	2.00000	0.0
3	3.00000	0.0
4	1.00000	1.00000
5	2.00000	1.00000
6	3.00000	1.00000
7	1.00000	2.00000
8	2.00000	2.00000
9	3.00000	2.00000

ELEMENT DATA

ELEMENT	NODE 1	NODE 2	NODE 3	NODE 4	MATERIAL
1	4	1	2	5	1
2	5	2	3	6	1
3	7	4	5	8	1
4	8	5	6	9	1

TIME - TEMPERATURE CONTROL INFORMATION

TOTAL NUMBER OF TIME INCREMENTS.....	1
NUMBER OF REGIONS WITH EQUAL TIME INCREMENTS.....	1
TIME AT END OF LAST INCREMENT.....	60.000
NUMBER OF TIME DEPENDENT BOUNDARY CONDITION FUNCTIONS..	0
ELEMENT TEMPERATURE FLAG.....	3
STRESS-FREE TEMPERATURE.....	0.0

SOLUTION TIME POINTS

REGION	NUMBER OF INCREMENTS	INCREMENT VALUE
1	1	60.0000

ELEMENT TEMPERATURE PRINT CONTROL

OUTPUT INTERVAL PRINT OPERATIONS

1 1

AVERAGE ELEMENT TEMPERATURES

(ELEMENT TEMPERATURE DISTRIBUTION CONSTANT)

SOLUTION TIME VALUE = 0.60000E 02

ELEMENT	AVERAGE TEMPERATURE
---------	---------------------

1	0.0
2	0.0
3	0.0
4	0.0

Figure H-9a

APPENDIX H

MECHANICAL PROPERTIES INFORMATION

P/A = 6000.0 PSI, AXIAL

NUMBER OF MATERIALS.....	1
NUMBER OF ELEMENTS WITH REDEFINED MATERIALS.....	0
NUMBER OF NODES WITH SPECIFIED BOUNDARY VALUES.....	8
NUMBER OF PRESSURE CARDS.....	0
ANGULAR VELOCITY AMPLITUDE.....	0.0
ANGULAR VELOCITY FUNCTION.....	0
AXIAL ACCELERATION AMPLITUDE.....	0.0
AXIAL ACCELERATION FUNCTION.....	0
OUTPUT INTERVAL FLAG.....	0
DISPLACEMENT PRINT CONTROL FLAG.....	0

MATERIALS DATA

MATERIAL NUMBER	TERMS IN PRONY SERIES	POINTS IN SHIFT FUNCTION	EQUILIBRIUM MODULUS	BULK MODULUS	EXPANSION COEFFICIENT
1	0	0	6000000.000	10000000.000	0.0

SERIES REPRESENTATION OF THE SHEAR RELAXATION FUNCTIONS

MATERIAL NUMBER	TERM IN THE SERIES	COEFFICIENT ALPHA(I)	EXPONENT BETA(I)
1	ELASTIC MATERIAL (NO SERIES EXPANSION)		

TABULATION OF TIME-TEMPERATURE SHIFT FUNCTIONS

MATERIAL NUMBER	POINT NUMBER	TEMPERATURE T(I)	SHIFT FACTOR LOG-10 A(T(I))
1	TEMPERATURE INDEPENDENT MATERIAL		

NOT REPRODUCIBLE

NODAL POINT BOUNDARY CONDITIONS

NODE NUMBER	TYPE CODE	P A D I A L BOUNDARY VALUE	FUNCTION NUMBER	TYPE CODE	A X I A L BOUNDARY VALUE	FUNCTION NUMBER
1	0	C.C	0	1	0.0	0
2	0	C.C	0	1	0.0	0
3	0	C.C	0	1	0.0	0
4	0	C.C	0	0	0.0	0
5	0	C.C	0	0	0.0	0
6	0	C.C	0	0	0.0	0
7	0	C.C	0	0	0.400000E 04	0
8	0	C.C	0	0	0.120000E 05	0
9	0	C.C	0	0	0.900000E 04	0

NODE	DISPLACEMENT	TIME =
1	-1.00000E-04 0.0	6.00000E 01
2	-2.00000E-04 0.0	
3	-3.00001E-04 0.0	
4	-1.00001E-04 4.00000E-04	
5	-2.00001E-04 4.00001E-04	
6	-1.00002E-04 4.00001E-04	
7	-1.00003E-04 3.00001E-04	
8	-2.00003E-04 8.00003E-04	
9	-3.00003E-04 9.00003E-04	

Figure H-9b

APPENDIX H

	SIGW	SIGTH	SIGZ	SIGRZ
1	-1.22070E-03	-7.41250E-03	6.00000E 03	-4.14729E-03
2	-4.39453E-03	1.22070E-03	6.00002E 03	-2.48838E-03
3	-9.76562E-03	-2.73437E-02	6.00001E 03	-4.36557E-05
4	-4.15039E-03	-9.76562E-03	6.00001E 03	-3.97267E-03

	EPR	FPT	FPZ	EPRZ	TEM
	-9.39799E-05	-1.00000E-04	4.00000E-04	-6.91216E-10	0.0
	-1.00001E-04	-1.00000E-04	4.00002E-04	-4.14730E-10	0.0
	-9.99799E-05	-1.00001E-04	4.00002E-04	-7.27596E-12	0.0
	-1.00000E-04	-1.00001E-04	4.00001E-04	-6.62112E-10	0.0

Figure H-9c

Aerojet Solid Propulsion Company
Report 1341-26F

Appendix II

The solution time span which has no meaning when constant loads are applied to elastic media consists of one (1) time increment arbitrarily selected as being 60 seconds long; one print operation is performed at the end of the first (and only) time increment. The average temperature of all elements is read in as 0°F. The pertinent mechanical properties are the shear ($G = 6(10)^6$ psi) and bulk ($K = 10(10)^6$ psi) moduli of the material. There were eight (8) of the nine (9) nodes designated as boundary nodes; nodes 4 and 6 are unloaded and unrestrained and do not have to appear in the statement of boundary conditions. Nodes 4 and 6 were inadvertently retained from a previous data deck.

The results consist of R and Z displacements of each node, average element stresses and strains and the average element temperatures all quoted at $t_1 = 60$ seconds. The applied axial stress is recovered exactly as 6000 psi (SIGZ) constant in each element.

C. PLANE-STRAIN VISCOELASTIC CYLINDER, EXAMPLE PROBLEM

The problem is a long cylindrical bore propellant grain (1.50 I.D., 8.0 O.D.) in a .060 steel case. The element geometry is shown in Figure H-10. The propellant relaxation and shift function curves are shown in Figures H-11 and H-12. Sixteen decade reduced time points were used to perform a prony series curve fit to the relaxation function and the coefficients are shown in Table H-4.

The motor, initially stress free at 135°F, was subjected to the thermal environment, through a heat transfer coefficient at the case, shown in Figure H-13. All nodes in the system were fixed in the axial direction to simulate a plane strain condition and the linear cumulative damage was calculated for two elements in the system, one at bore and one next to the case - grain bond.

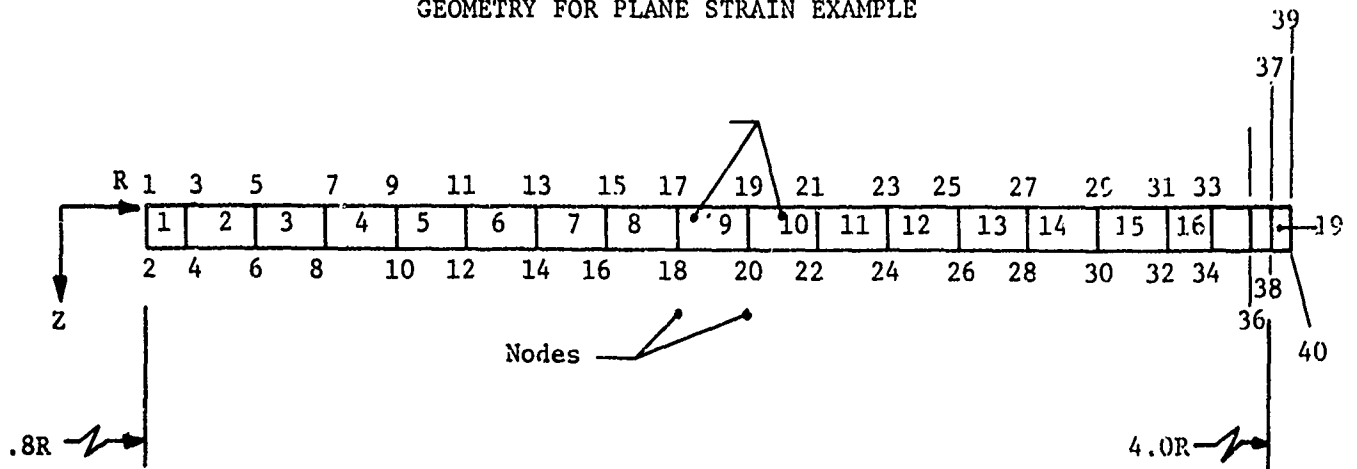
A listing of the data input cards required to describe this problem is shown in Table H-5. Line 2 is the title; line 3 is the control card; lines 4-9 describe the node point coordinates; lines 10, 11 establish the element I.D.; line 12 is the solution time point and reference temperature control and lines 13-29 describe the solution time points. Lines 31-36 describe the free stream temperature function. Line 37 describes the output print interval. Lines 39 and 40 are the thermal properties for the grain and case. Line 41 describes the convection boundary condition. Line 42 is the stress analysis title card and 43 is the stress control card. Lines 45-48 are the relaxation series coefficients. Lines 49-51 are the shift function points. Line 52 describes the case properties. Lines 53-92 are the displacement boundary conditions. The last two lines give the damage parameters.

Selected portions of the output from this analysis are shown in Table H-6.

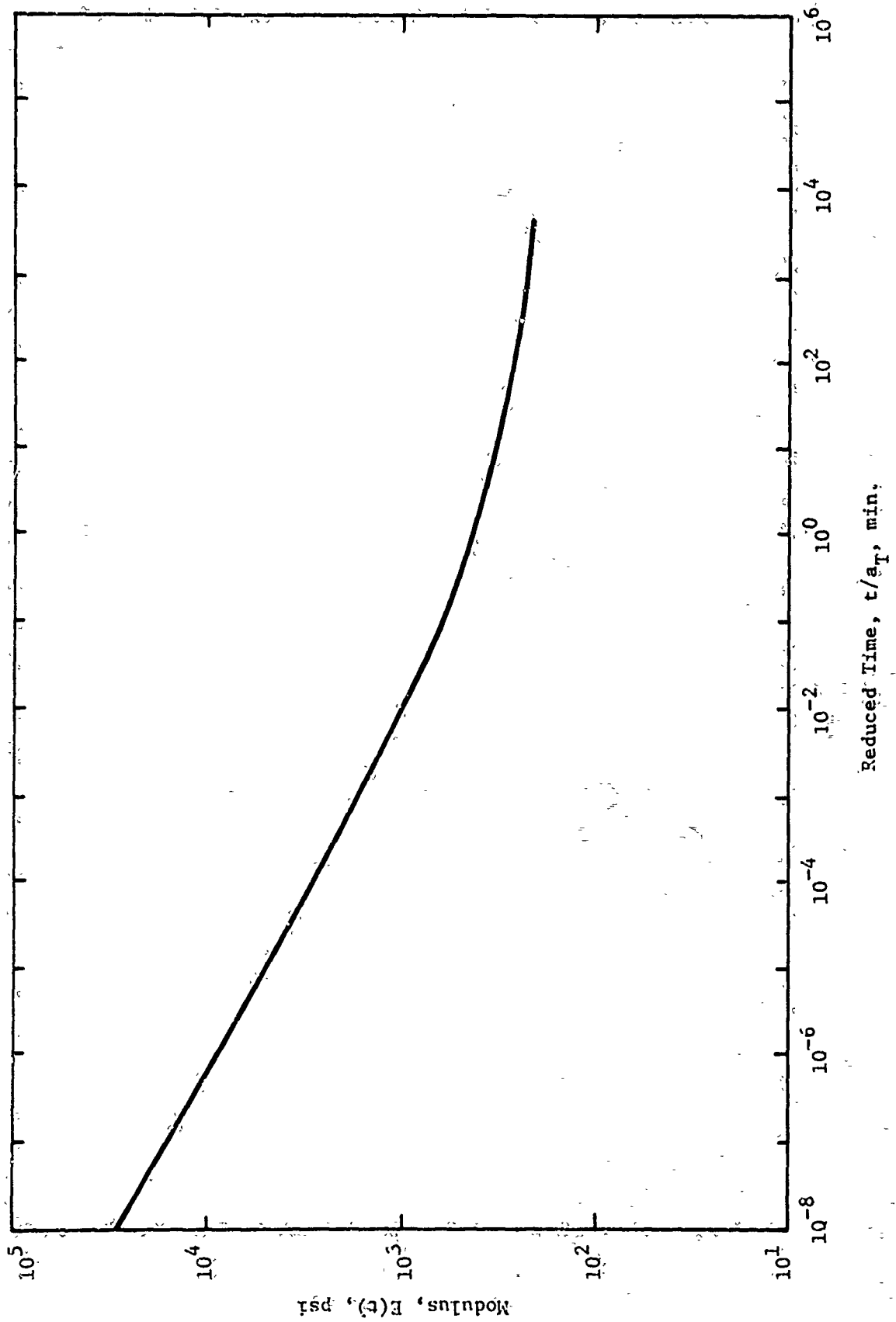
Aerojet Solid Propulsion Company
Report 1341-26F

Appendix II

GEOMETRY FOR PLANE STRAIN EXAMPLE



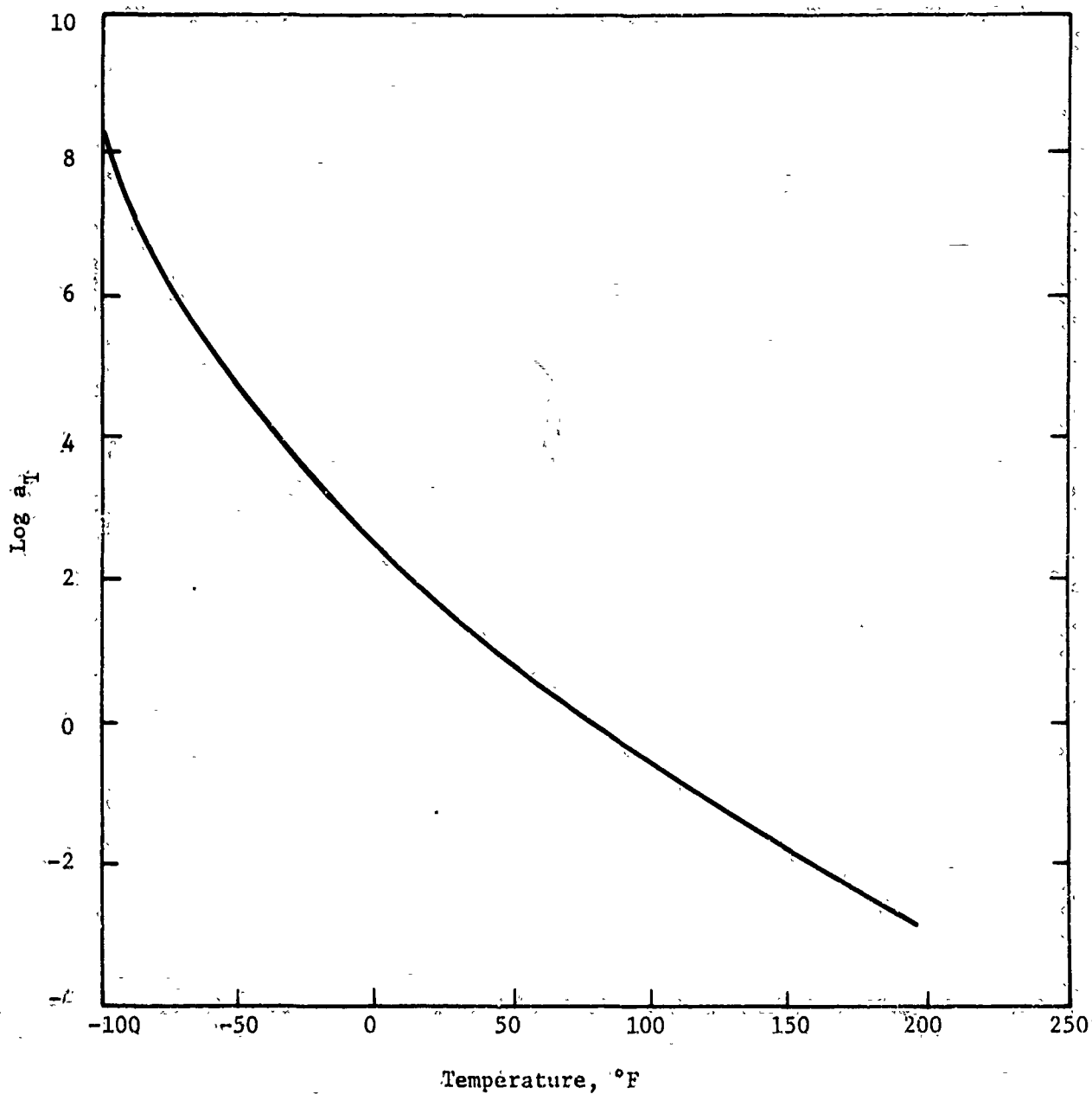
RELAXATION MODULUS OF A CTPB PROPELLANT



Aerojet Solid Propulsion Company
Report 1341-26F

Appendix H

TIME TEMPERATURE SHIFT FACTORS FOR A CTPB PROPELLANT



Aerojet Solid Propulsion Company
Report 1341-26F

Appendix H

Propellant Relaxation Function

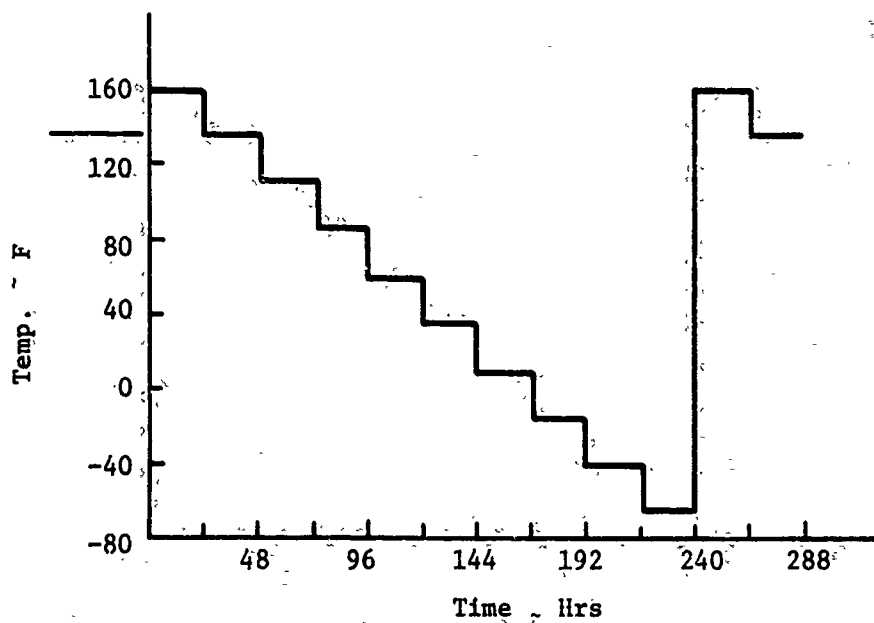
$\log(t/a_T)$ (min)	E_r (psi)	B_i (hr ⁻¹)	A_i	$A_i/3$	i
			100	33.333	0
-9	44000	3×10^{10}	25836	8612	1
-8	29000	3×10^9	12087	4029	2
-7	14000	3×10^8	6919.2	2306.4	3
-6	8300	3×10^7	3915.5	1305.2	4
-5	5000	3×10^6	2435.2	811.40	5
-4	3000	3×10^5	1341.9	447.3	6
-3	1800	3×10^4	1033.9	344.63	7
-2	1000	3×10^3	457.98	152.66	8
-1	620	3×10^2	265.80	88.60	9
0	410	3×10^1	137.74	45.91	10
1	320	3×10^0	.16481	.0546	11
2	280	3×10^{-1}	113.47	37.82	12
3	210	3×10^{-2}	-2.9029	-.9676	13
4	190	3×10^{-3}	60.2506	20.0835	14
5	150	3×10^{-4}	4.26975	1.42325	15
6	130	3×10^{-5}	49.4143	1.64714	16

$$E_r = A_0 + \sum_{i=1}^{16} A_i e^{-B_i t}$$

Aerojet Solid Propulsion Company
Report 1341-26F

Appendix H

FREE-STREAM TEMPERATURE
($H = .0125 \text{ BTU/HR/IN.}^2/\text{F}$)



APPENDIX H

Data Input for Example Problem 3

[illegible]**Table H-6**

Table 5.4
Computer Output for Example Problem C

TWO-DIMENSIONAL TIME/INVISCOELASTIC ANALYSIS
VISCOELASTIC PARAMETER STUDY B/A=9.00 B=4 EQUIVALENT PLANE STRAIN MIP=1

CONTROL PARAMETERS

NUMBER OF NODES 40
NUMBER OF ELEMENTS 19

NODE COORDINATE DATA

NODE	R-COORDINATE	Z-COORDINATE
1	0.00000	0.00000
2	0.50000	0.00000
3	0.50000	0.00000
4	0.50000	0.00000
5	1.00000	0.00000
6	1.00000	0.00000
7	1.00000	0.00000
8	1.00000	0.00000
9	1.00000	0.00000
10	1.00000	0.00000
11	1.00000	0.00000
12	1.00000	0.00000
13	1.00000	0.00000
14	1.00000	0.00000
15	1.00000	0.00000
16	1.00000	0.00000
17	1.00000	0.00000
18	1.00000	0.00000
19	1.00000	0.00000
20	1.00000	0.00000
21	1.00000	0.00000
22	1.00000	0.00000
23	1.00000	0.00000
24	1.00000	0.00000
25	1.00000	0.00000
26	1.00000	0.00000
27	1.00000	0.00000
28	1.00000	0.00000
29	1.00000	0.00000
30	1.00000	0.00000
31	1.00000	0.00000
32	1.00000	0.00000
33	1.00000	0.00000
34	1.00000	0.00000
35	1.00000	0.00000
36	1.00000	0.00000
37	1.00000	0.00000
38	1.00000	0.00000
39	1.00000	0.00000
40	1.00000	0.00000

APPENDIX H

APPENDIX H

Table 5.6 (cont.)

ELEMENT DATA	ELEMENT	MODE 1	MODE 2	MODE 3	MODE 4	MATERIAL
	1	2	1	3	4	1
	2	3	2	4	1	2
	3	4	3	1	2	3
	4	1	4	2	3	4
	5	2	1	3	4	1
	6	3	2	4	1	2
	7	4	3	1	2	3
	8	1	4	2	3	4
	9	2	1	3	4	1
	10	3	2	4	1	2
	11	4	3	1	2	3
	12	1	4	2	3	4
	13	2	1	3	4	1
	14	3	2	4	1	2
	15	4	3	1	2	3
	16	1	4	2	3	4
	17	2	1	3	4	1
	18	3	2	4	1	2
	19	4	3	1	2	3
	20	1	4	2	3	4
	21	2	1	3	4	1
	22	3	2	4	1	2
	23	4	3	1	2	3
	24	1	4	2	3	4
	25	2	1	3	4	1
	26	3	2	4	1	2
	27	4	3	1	2	3
	28	1	4	2	3	4
	29	2	1	3	4	1
	30	3	2	4	1	2
	31	4	3	1	2	3
	32	1	4	2	3	4
	33	2	1	3	4	1
	34	3	2	4	1	2
	35	4	3	1	2	3
	36	1	4	2	3	4
	37	2	1	3	4	1
	38	3	2	4	1	2
	39	4	3	1	2	3
	40	1	4	2	3	4

TIME-TEMPERATURE CONTROL INFORMATION

TOTAL NUMBER OF TIME INCREMENTS..... 336
 NUMBER OF REGIONS WITH EQUAL TIME INCREMENTS..... 84
 TIME AT END OF LAST TIME INCREMENT..... 288.000
 NUMBER OF TIME DEPENDENT BOUNDARY CONDITION FUNCTIONS..... 1
 ELEMENT TEMPERATURE FLAG..... 0
 STRESS-FREE TEMPERATURE..... 135.000

APPENDIX H

Table 5.4. (cont.)

SOLUTION TIME POINTS	REGION	NUMBER OF INCREMENTS	INCREMENT VALUE
1	1	1	0.0250
2	1	1	0.0550
3	1	1	0.1700
4	1	1	0.4500
5	1	1	0.8000
6	1	1	1.5000
7	1	1	3.0000
8	1	1	0.0250
9	1	1	0.0550
10	1	1	0.1700
11	1	1	0.4500
12	1	1	0.8000
13	1	1	1.5000
14	1	1	3.0000
15	1	1	0.0250
16	1	1	0.0550
17	1	1	0.1700
18	1	1	0.4500
19	1	1	0.8000
20	1	1	1.5000
21	1	1	3.0000
22	1	1	0.0250
23	1	1	0.0550
24	1	1	0.1700
25	1	1	0.4500
26	1	1	0.8000
27	1	1	1.5000
28	1	1	3.0000
29	1	1	0.0250
30	1	1	0.0550
31	1	1	0.1700
32	1	1	0.4500
33	1	1	0.8000
34	1	1	1.5000
35	1	1	3.0000
36	1	1	0.0250
37	1	1	0.0550
38	1	1	0.1700
39	1	1	0.4500
40	1	1	0.8000
41	1	1	1.5000
42	1	1	3.0000
43	1	1	0.0250
44	1	1	0.0550
45	1	1	0.1700
46	1	1	0.4500
47	1	1	0.8000
48	1	1	1.5000
49	1	1	3.0000
50	1	1	0.0250
51	1	1	0.0550
52	1	1	0.1700
53	1	1	0.4500
54	1	1	0.8000
55	1	1	1.5000
56	1	1	3.0000
57	1	1	0.0250
58	1	1	0.0550
59	1	1	0.1700
60	1	1	0.4500
61	1	1	0.8000
62	1	1	1.5000
63	1	1	3.0000
64	1	1	0.0250
65	1	1	0.0550
66	1	1	0.1700
67	1	1	0.4500
68	1	1	0.8000
69	1	1	1.5000
70	1	1	3.0000
71	1	1	0.0250
72	1	1	0.0550
73	1	1	0.1700
74	1	1	0.4500
75	1	1	0.8000
76	1	1	1.5000
77	1	1	3.0000
78	1	1	0.0250
79	1	1	0.0550
80	1	1	0.1700
81	1	1	0.4500
82	1	1	0.8000
83	1	1	1.5000
84	1	1	3.0000
85	1	1	0.0250
86	1	1	0.0550
87	1	1	0.1700
88	1	1	0.4500
89	1	1	0.8000
90	1	1	1.5000
91	1	1	3.0000
92	1	1	0.0250
93	1	1	0.0550
94	1	1	0.1700
95	1	1	0.4500
96	1	1	0.8000
97	1	1	1.5000
98	1	1	3.0000
99	1	1	0.0250
100	1	1	0.0550

Table H-6. Cont'd

Table 3.4 (cont.)

SOLUTION TO THE TRANSIENT HEAT CONDUCTION PROBLEM

[illegible]

APPENDIX H.

Table 5.4 (cont.)

MECHANICAL PROPERTIES INFORMATION

VISCOELASTIC PARAMETER STUDY 8/A/3.00 8% EQUIVALENT PLANE STRAIN

NUMBER OF MATERIALS..... 2
 NUMBER OF ELEMENTS WITH PREDESIGNED MATERIALS..... 2
 NUMBER OF NODES WITH SPECIFIED BOUNDARY VALUES..... 40
 NUMBER OF ELEMENTS WITH SPECIFIED BOUNDARY VALUES..... 2
 NUMBER OF PRESSURE CARDS..... 0
 NUMBER OF ELEMENTS FOR DAMAGE EVALUATION..... 0
 ANGULAR VELOCITY AMPLITUDE..... 0.0
 ANGULAR VELOCITY FUNCTION..... 0.0
 AXIAL ACCELERATION AMPLITUDE..... 0.0
 AXIAL ACCELERATION FUNCTION..... 0.0
 DISPLACEMENT PRINT CONTROL FLAG..... 0

MATERIALS DATA

MATERIAL NUMBER	TERMS IN PRONY SERIES	POINTS IN SHIFT FUNCTION	EQUILIBRIUM MODULUS	BULK MODULUS	EXPANSION COEFFICIENT	HEIGHT DENSITY
1	16	12	33.300	500000.000	0.56700E-04	0.0
2	16	0	11500000.000	25000000.000	0.59000E-03	0.0

SERIES REPRESENTATION OF THE SHEAR RELAXATION FUNCTIONS

MATERIAL NUMBER	TERM IN THE SERIES	COEFFICIENT ALPHA(I)	EXPONENT BETA(I)
1	1	0.86120E 04	0.30000E 11
1	2	0.4290E 04	0.30000E 10
1	3	0.23064E 04	0.30000E 09
1	4	0.13052E 04	0.30000E 08
1	5	0.81140E 03	0.30000E 07
1	6	0.44730E 03	0.30000E 06
1	7	0.34664E 03	0.30000E 05
1	8	0.13260E 03	0.30000E 04
1	9	0.8600E 02	0.30000E 03
1	10	0.45910E 02	0.30000E 02
1	11	0.5600E 01	0.30000E 01
1	12	0.37820E 02	0.30000E 00
1	13	0.96760E 00	0.30000E -01
1	14	0.20083E 02	0.30000E -02
1	15	0.14232E 01	0.30000E -03
1	16	0.18471E 01	0.30000E -04

2 ELASTIC MATERIAL (NO SERIES EXPANSION)

TABULATION OF TIME-TEMPERATURE SHIFT FUNCTIONS

MATERIAL NUMBER	POINT NUMBER	TEMPERATURE T(I)	SHIFT FACTOR LOG-10 ALT(I)
1	1	-100.000	8.2800
1	2	-75.000	6.0000
1	3	-50.000	4.6000
1	4	-25.000	3.5400
1	5	0.0	2.5200
1	6	25.000	1.6000
1	7	50.000	0.8000
1	8	75.000	0.0
1	9	100.000	-0.5600
1	10	125.000	-1.2200
1	11	150.000	-1.8200
1	12	200.000	-2.9400

2 TEMPERATURE INDEPENDENT MATERIAL

Table H-6 Cont'd

APPENDIX H

Table 5.4 (cont.)

NODAL POINT BOUNDARY CONDITIONS

NODE NUMBER	TYPE CODE	1 A D I A L BOUNDARY VALUE	FUNCTION NUMBER	TYPE CODE	A X I A L BOUNDARY VALUE	FUNCTION NUMBER
1	0	0.00	0	1	0.00	0
2	0	0.00	0	1	0.00	0
3	0	0.00	0	1	0.00	0
4	0	0.00	0	1	0.00	0
5	0	0.00	0	1	0.00	0
6	0	0.00	0	1	0.00	0
7	0	0.00	0	1	0.00	0
8	0	0.00	0	1	0.00	0
9	0	0.00	0	1	0.00	0
10	0	0.00	0	1	0.00	0
11	0	0.00	0	1	0.00	0
12	0	0.00	0	1	0.00	0
13	0	0.00	0	1	0.00	0
14	0	0.00	0	1	0.00	0
15	0	0.00	0	1	0.00	0
16	0	0.00	0	1	0.00	0
17	0	0.00	0	1	0.00	0
18	0	0.00	0	1	0.00	0
19	0	0.00	0	1	0.00	0
20	0	0.00	0	1	0.00	0
21	0	0.00	0	1	0.00	0
22	0	0.00	0	1	0.00	0
23	0	0.00	0	1	0.00	0
24	0	0.00	0	1	0.00	0
25	0	0.00	0	1	0.00	0
26	0	0.00	0	1	0.00	0
27	0	0.00	0	1	0.00	0
28	0	0.00	0	1	0.00	0
29	0	0.00	0	1	0.00	0
30	0	0.00	0	1	0.00	0
31	0	0.00	0	1	0.00	0
32	0	0.00	0	1	0.00	0
33	0	0.00	0	1	0.00	0
34	0	0.00	0	1	0.00	0
35	0	0.00	0	1	0.00	0
36	0	0.00	0	1	0.00	0
37	0	0.00	0	1	0.00	0
38	0	0.00	0	1	0.00	0
39	0	0.00	0	1	0.00	0
40	0	0.00	0	1	0.00	0

DAMAGE PARAMETERS ... MSG. EL. NO. = DAMAGE BASED ON MAX. PRINC. M-L STRESS
 MSG. EL. NO. = DAMAGE BASED ON HOOP STRESS

ELEMENT SIGNA(T-ZERO) T-ZERO SIGMA(CHIT-1)

1 1.00-00 0.02 0.0 0.43
 -10 1.00-00 0.02 0.0 0.43

Table H-6 Cont'd

Table 5.4 (cont.)

TIME = 1.000000000-01

[illegible]

TIME = 3.200000000D-01

[illegible]

Price = 1.00000000000000

STOR	SOUTH	SIGZ	SIGZ	SIGZ	EPH	EPTM	EPZ	EPZ	DEM
1	1.01E	00	00	00	00	00	00	00	1.02E
2	1.01E	00	00	00	00	00	00	00	1.02E
3	1.01E	00	00	00	00	00	00	00	1.02E
4	1.01E	00	00	00	00	00	00	00	1.02E
5	1.01E	00	00	00	00	00	00	00	1.02E
6	1.01E	00	00	00	00	00	00	00	1.02E
7	1.01E	00	00	00	00	00	00	00	1.02E
8	1.01E	00	00	00	00	00	00	00	1.02E
9	1.01E	00	00	00	00	00	00	00	1.02E
10	1.01E	00	00	00	00	00	00	00	1.02E
11	1.01E	00	00	00	00	00	00	00	1.02E
12	1.01E	00	00	00	00	00	00	00	1.02E
13	1.01E	00	00	00	00	00	00	00	1.02E
14	1.01E	00	00	00	00	00	00	00	1.02E
15	1.01E	00	00	00	00	00	00	00	1.02E
16	1.01E	00	00	00	00	00	00	00	1.02E
17	1.01E	00	00	00	00	00	00	00	1.02E
18	1.01E	00	00	00	00	00	00	00	1.02E
19	1.01E	00	00	00	00	00	00	00	1.02E
20	1.01E	00	00	00	00	00	00	00	1.02E
21	1.01E	00	00	00	00	00	00	00	1.02E
22	1.01E	00	00	00	00	00	00	00	1.02E
23	1.01E	00	00	00	00	00	00	00	1.02E
24	1.01E	00	00	00	00	00	00	00	1.02E
25	1.01E	00	00	00	00	00	00	00	1.02E
26	1.01E	00	00	00	00	00	00	00	1.02E
27	1.01E	00	00	00	00	00	00	00	1.02E
28	1.01E	00	00	00	00	00	00	00	1.02E
29	1.01E	00	00	00	00	00	00	00	1.02E
30	1.01E	00	00	00	00	00	00	00	1.02E
31	1.01E	00	00	00	00	00	00	00	1.02E
32	1.01E	00	00	00	00	00	00	00	1.02E
33	1.01E	00	00	00	00	00	00	00	1.02E
34	1.01E	00	00	00	00	00	00	00	1.02E
35	1.01E	00	00	00	00	00	00	00	1.02E
36	1.01E	00	00	00	00	00	00	00	1.02E
37	1.01E	00	00	00	00	00	00	00	1.02E
38	1.01E	00	00	00	00	00	00	00	1.02E
39	1.01E	00	00	00	00	00	00	00	1.02E
40	1.01E	00	00	00	00	00	00	00	1.02E
41	1.01E	00	00	00	00	00	00	00	1.02E
42	1.01E	00	00	00	00	00	00	00	1.02E
43	1.01E	00	00	00	00	00	00	00	1.02E

Table H-6 Cont'd

NOT REPRODUCIBLE

[illegible][illegible]

$\tau_{12} = 2.6000 \times 10^{-1}$

[illegible]

TOTAL = 7000000000

[illegible]

NOT REPRODUCIBLE

TI 4 = 7.2057700033 51

NO	DATE	TIME	NAME	ADDRESS	CITY	STATE	ZIP	PHONE	TELETYPE	TELEFAX	TELEVISION	RADIO	OTHER
1	1991	10:00	JOHN	1234	NEW YORK	NY	10001	212-1234					
2	1991	10:00	JANE	5678	LOS ANGELES	CA	90001	213-5678					
3	1991	10:00	BOB	9012	CHICAGO	IL	60601	312-9012					
4	1991	10:00	ALICE	3456	HONOLULU	HI	96801	808-3456					
5	1991	10:00	CHARLIE	7890	PHOENIX	AZ	85001	602-7890					
6	1991	10:00	DAN	1122	PORTLAND	OR	97201	503-1122					
7	1991	10:00	EVE	3344	SAN FRANCISCO	CA	94101	415-3344					
8	1991	10:00	FRANK	5566	SEATTLE	WA	98101	206-5566					
9	1991	10:00	GRACE	7788	MINNEAPOLIS	MN	55401	612-7788					
10	1991	10:00	HELEN	9900	DENVER	CO	80201	303-9900					
11	1991	10:00	IRVING	1133	KANSAS CITY	MO	64101	816-1133					
12	1991	10:00	JACK	3355	INDIANAPOLIS	IN	46201	317-3355					
13	1991	10:00	JILL	5577	COLUMBIA	SC	29201	803-5577					
14	1991	10:00	JOHN	7799	HOUSTON	TX	77001	713-7799					
15	1991	10:00	JANE	9911	MEMPHIS	TN	38101	901-9911					
16	1991	10:00	BOB	1144	MIAMI	FL	33101	305-1144					
17	1991	10:00	ALICE	3366	NEW ORLEANS	LA	70101	504-3366					
18	1991	10:00	CHARLIE	5588	PHILADELPHIA	PA	19101	215-5588					
19	1991	10:00	DAN	7700	RICHMOND	VA	23201	804-7700					
20	1991	10:00	EVE	9922	SAN JUAN	PR	00901	787-9922					
21	1991	10:00	FRANK	1155	WASHINGTON	DC	20001	202-1155					
22	1991	10:00	GRACE	3377	WICHITA	KS	67201	316-3377					
23	1991	10:00	HELEN	5599	YAKIMA	WA	98901	509-5599					
24	1991	10:00	IRVING	7711	ALBUQUERQUE	NM	87101	505-7711					
25	1991	10:00	JACK	9933	ANCHORAGE	AK	99501	907-9933					
26	1991	10:00	JILL	1166	BIRMINGHAM	AL	35201	205-1166					
27	1991	10:00	JOHN	3388	BOULDER	CO	80501	303-3388					
28	1991	10:00	JANE	5500	BOULDER	CO	80501	303-5500					
29	1991	10:00	BOB	7722	BOULDER	CO	80501	303-7722					
30	1991	10:00	ALICE	9944	BOULDER	CO	80501	303-9944					
31	1991	10:00	CHARLIE	1177	BOULDER	CO	80501	303-1177					
32	1991	10:00	DAN	3399	BOULDER	CO	80501	303-3399					
33	1991	10:00	EVE	5511	BOULDER	CO	80501	303-5511					
34	1991	10:00	FRANK	7733	BOULDER	CO	80501	303-7733					
35	1991	10:00	GRACE	9955	BOULDER	CO	80501	303-9955					
36	1991	10:00	HELEN	1188	BOULDER	CO	80501	303-1188					
37	1991	10:00	IRVING	3300	BOULDER	CO	80501	303-3300					
38	1991	10:00	JACK	5522	BOULDER	CO	80501	303-5522					
39	1991	10:00	JILL	7744	BOULDER	CO	80501	303-7744					
40	1991	10:00	JOHN	9966	BOULDER	CO	80501	303-9966					
41	1991	10:00	JANE	1199	BOULDER	CO	80501	303-1199					
42	1991	10:00	BOB	3311	BOULDER	CO	80501	303-3311					
43	1991	10:00	ALICE	5533	BOULDER	CO	80501	303-5533					
44	1991	10:00	CHARLIE	7755	BOULDER	CO	80501	303-7755					
45	1991	10:00	DAN	9977	BOULDER	CO	80501	303-9977					
46	1991	10:00	EVE	1200	BOULDER	CO	80501	303-1200					
47	1991	10:00	FRANK	3422	BOULDER	CO	80501	303-3422					
48	1991	10:00	GRACE	5644	BOULDER	CO	80501	303-5644					
49	1991	10:00	HELEN	7866	BOULDER	CO	80501	303-7866					
50	1991	10:00	IRVING	9088	BOULDER	CO	80501	303-9088					
51	1991	10:00	JACK	1211	BOULDER	CO	80501	303-1211					
52	1991	10:00	JILL	3433	BOULDER	CO	80501	303-3433					
53	1991	10:00	JOHN	5655	BOULDER	CO	80501	303-5655					
54	1991	10:00	JANE	7877	BOULDER	CO	80501	303-7877					
55	1991	10:00	BOB	9099	BOULDER	CO	80501	303-9099					
56	1991	10:00	ALICE	1322	BOULDER	CO	80501	303-1322					
57	1991	10:00	CHARLIE	3544	BOULDER	CO	80501	303-3544					
58	1991	10:00	DAN	5766	BOULDER	CO	80501	303-5766					
59	1991	10:00	EVE	7988	BOULDER	CO	80501	303-7988					
60	1991	10:00	FRANK	9100	BOULDER	CO	80501	303-9100					
61	1991	10:00	GRACE	1333	BOULDER	CO	80501	303-1333					
62	1991	10:00	HELEN	3555	BOULDER	CO	80501	303-3555					
63	1991	10:00	IRVING	5777	BOULDER	CO	80501	303-5777					
64	1991	10:00	JACK	7999	BOULDER	CO	80501	303-7999					
65	1991	10:00	JILL	9211	BOULDER	CO	80501	303-9211					
66	1991	10:00	JOHN	1444	BOULDER	CO	80501	303-1444					
67	1991	10:00	JANE	3666	BOULDER	CO	80501	303-3666					
68	1991	10:00	BOB	5888	BOULDER	CO	80501	303-5888					
69	1991	10:00	ALICE	8000	BOULDER	CO	80501	303-8000					
70	1991	10:00	CHARLIE	9222	BOULDER	CO	80501	303-9222					
71	1991	10:00	DAN	1455	BOULDER	CO	80501	303-1455					
72	1991	10:00	EVE	3677	BOULDER	CO	80501	303-3677					
73	1991	10:00	FRANK	5899	BOULDER	CO	80501	303-5899					
74	1991	10:00	GRACE	8122	BOULDER	CO	80501	303-8122					
75	1991	10:00	HELEN	9344	BOULDER	CO	80501	303-9344					
76	1991	10:00	IRVING	1566	BOULDER	CO	80501	303-1566					
77	1991	10:00	JACK	3788	BOULDER	CO	80501	303-3788					
78	1991	10:00	JILL	5900	BOULDER	CO	80501	303-5900					
79	1991	10:00	JOHN	8111	BOULDER	CO	80501	303-8111					
80	1991	10:00	JANE	9333	BOULDER	CO	80501	303-9333					
81	1991	10:00	BOB	1577	BOULDER	CO	80501	303-1577					
82	1991	10:00	ALICE	3799	BOULDER	CO	80501	303-3799					
83	1991	10:00	CHARLIE	6022	BOULDER	CO	80501	303-6022					
84	1991	10:00	DAN	8244	BOULDER	CO	80501	303-8244					
85	1991	10:00	EVE	9466	BOULDER	CO	80501	303-9466					
86	1991	10:00	FRANK	1688	BOULDER	CO	80501	303-1688					
87	1991	10:00	GRACE	3900	BOULDER	CO	80501	303-3900					
88	1991	10:00	HELEN	6122	BOULDER	CO	80501	303-6122					
89	1991	10:00	IRVING	8344	BOULDER	CO	80501	303-8344					
90	1991	10:00	JACK	9566	BOULDER	CO	80501	303-9566					
91	1991	10:00	JILL	1788	BOULDER	CO	80501	303-1788					
92	1991	10:00	JOHN	4000	BOULDER	CO	80501	303-4000					
93	1991	10:00	JANE	6222	BOULDER	CO	80501	303-6222					
94	1991	10:00	BOB	8444	BOULDER	CO	80501	303-8444					
95	1991	10:00	ALICE	9666	BOULDER	CO	80501	303-9666					
96	1991	10:00	CHARLIE	1888	BOULDER	CO	80501	303-1888					
97	1991	10:00	DAN	4100	BOULDER	CO	80501	303-4100					
98	1991	10:00	EVE	6322	BOULDER	CO	80501	303-6322					
99	1991	10:00	FRANK	8544	BOULDER	CO	80501	303-8544					
100	1991	10:00	GRACE	9766	BOULDER	CO	80501	303-9766					

10-600000000000

[illegible]

TIME = 1.270300000 32

[illegible]

H-57

NOT REPRODUCIBLE

Y141 = 1.4433300 12

Year	1954	1955	1956	1957	1958	1959	1960	1961	1962	1963	1964	1965	1966	1967	1968	1969	1970	1971	1972	1973	1974	1975	1976	1977	1978	1979	1980	1981	1982	1983	1984	1985	1986	1987	1988	1989	1990	1991	1992	1993	1994	1995	1996	1997	1998	1999	2000	2001	2002	2003	2004	2005	2006	2007	2008	2009	2010	2011	2012	2013	2014	2015	2016	2017	2018	2019	2020	2021	2022	2023	2024	2025	2026	2027	2028	2029	2030	2031	2032	2033	2034	2035	2036	2037	2038	2039	2040	2041	2042	2043	2044	2045	2046	2047	2048	2049	2050	2051	2052	2053	2054	2055	2056	2057	2058	2059	2060	2061	2062	2063	2064	2065	2066	2067	2068	2069	2070	2071	2072	2073	2074	2075	2076	2077	2078	2079	2080	2081	2082	2083	2084	2085	2086	2087	2088	2089	2090	2091	2092	2093	2094	2095	2096	2097	2098	2099	2100
1954	1955	1956	1957	1958	1959	1960	1961	1962	1963	1964	1965	1966	1967	1968	1969	1970	1971	1972	1973	1974	1975	1976	1977	1978	1979	1980	1981	1982	1983	1984	1985	1986	1987	1988	1989	1990	1991	1992	1993	1994	1995	1996	1997	1998	1999	2000	2001	2002	2003	2004	2005	2006	2007	2008	2009	2010	2011	2012	2013	2014	2015	2016	2017	2018	2019	2020	2021	2022	2023	2024	2025	2026	2027	2028	2029	2030	2031	2032	2033	2034	2035	2036	2037	2038	2039	2040	2041	2042	2043	2044	2045	2046	2047	2048	2049	2050	2051	2052	2053	2054	2055	2056	2057	2058	2059	2060	2061	2062	2063	2064	2065	2066	2067	2068	2069	2070	2071	2072	2073	2074	2075	2076	2077	2078	2079	2080	2081	2082	2083	2084	2085	2086	2087	2088	2089	2090	2091	2092	2093	2094	2095	2096	2097	2098	2099	2100	

TIME 3-1-540000000 02

[illegible]

$\log = 1.920000000 \times 72$

[illegible]

H-58

APPENDIX H

NOT REPRODUCIBLE

Table 3.4 (cont.)

TIME = 2.150000000 02

	SIGR	SIGM	SIGZ	SIGRZ	EPR	EPTH	EPZ	EPZ	TEM
1	0.90E	00	1.15E	02	0.35E	01	0.00	1.58E-00	-4.05E 01
2	2.24E	00	1.15E	02	0.35E	01	0.00	1.77E-00	-4.05E 01
3	4.16E	00	1.15E	02	0.35E	01	0.00	1.77E-00	-4.05E 01
4	4.16E	00	1.15E	02	0.35E	01	0.00	1.77E-00	-4.05E 01
5	4.16E	00	1.15E	02	0.35E	01	0.00	1.77E-00	-4.05E 01
6	4.16E	00	1.15E	02	0.35E	01	0.00	1.77E-00	-4.05E 01
7	4.16E	00	1.15E	02	0.35E	01	0.00	1.77E-00	-4.05E 01
8	4.16E	00	1.15E	02	0.35E	01	0.00	1.77E-00	-4.05E 01
9	4.16E	00	1.15E	02	0.35E	01	0.00	1.77E-00	-4.05E 01
10	4.16E	00	1.15E	02	0.35E	01	0.00	1.77E-00	-4.05E 01
11	4.16E	00	1.15E	02	0.35E	01	0.00	1.77E-00	-4.05E 01
12	4.16E	00	1.15E	02	0.35E	01	0.00	1.77E-00	-4.05E 01
13	4.16E	00	1.15E	02	0.35E	01	0.00	1.77E-00	-4.05E 01
14	4.16E	00	1.15E	02	0.35E	01	0.00	1.77E-00	-4.05E 01
15	4.16E	00	1.15E	02	0.35E	01	0.00	1.77E-00	-4.05E 01
16	4.16E	00	1.15E	02	0.35E	01	0.00	1.77E-00	-4.05E 01
17	4.16E	00	1.15E	02	0.35E	01	0.00	1.77E-00	-4.05E 01
18	4.16E	00	1.15E	02	0.35E	01	0.00	1.77E-00	-4.05E 01
19	4.16E	00	1.15E	02	0.35E	01	0.00	1.77E-00	-4.05E 01

TIME = 2.400000000 02

	SIGR	SIGM	SIGZ	SIGRZ	EPR	EPTH	EPZ	EPZ	TEM
1	1.06E	01	1.77E	02	0.35E	01	0.00	2.67E-00	-6.61E 01
2	3.42E	01	1.77E	02	0.35E	01	0.00	2.67E-00	-6.61E 01
3	6.74E	01	1.77E	02	0.35E	01	0.00	2.67E-00	-6.61E 01
4	7.00E	01	1.77E	02	0.35E	01	0.00	2.67E-00	-6.61E 01
5	7.00E	01	1.77E	02	0.35E	01	0.00	2.67E-00	-6.61E 01
6	7.00E	01	1.77E	02	0.35E	01	0.00	2.67E-00	-6.61E 01
7	7.00E	01	1.77E	02	0.35E	01	0.00	2.67E-00	-6.61E 01
8	7.00E	01	1.77E	02	0.35E	01	0.00	2.67E-00	-6.61E 01
9	7.00E	01	1.77E	02	0.35E	01	0.00	2.67E-00	-6.61E 01
10	7.00E	01	1.77E	02	0.35E	01	0.00	2.67E-00	-6.61E 01
11	7.00E	01	1.77E	02	0.35E	01	0.00	2.67E-00	-6.61E 01
12	7.00E	01	1.77E	02	0.35E	01	0.00	2.67E-00	-6.61E 01
13	7.00E	01	1.77E	02	0.35E	01	0.00	2.67E-00	-6.61E 01
14	7.00E	01	1.77E	02	0.35E	01	0.00	2.67E-00	-6.61E 01
15	7.00E	01	1.77E	02	0.35E	01	0.00	2.67E-00	-6.61E 01
16	7.00E	01	1.77E	02	0.35E	01	0.00	2.67E-00	-6.61E 01
17	7.00E	01	1.77E	02	0.35E	01	0.00	2.67E-00	-6.61E 01
18	7.00E	01	1.77E	02	0.35E	01	0.00	2.67E-00	-6.61E 01
19	7.00E	01	1.77E	02	0.35E	01	0.00	2.67E-00	-6.61E 01

TIME = 2.600000000 02

	SIGR	SIGM	SIGZ	SIGRZ	EPR	EPTH	EPZ	EPZ	TEM
1	7.04E	01	7.18E	00	4.41E	00	0.00	2.17E-00	1.58E 02
2	2.21E	00	4.41E	00	4.41E	00	0.00	2.17E-00	1.58E 02
3	2.21E	00	4.41E	00	4.41E	00	0.00	2.17E-00	1.58E 02
4	2.21E	00	4.41E	00	4.41E	00	0.00	2.17E-00	1.58E 02
5	2.21E	00	4.41E	00	4.41E	00	0.00	2.17E-00	1.58E 02
6	2.21E	00	4.41E	00	4.41E	00	0.00	2.17E-00	1.58E 02
7	2.21E	00	4.41E	00	4.41E	00	0.00	2.17E-00	1.58E 02
8	2.21E	00	4.41E	00	4.41E	00	0.00	2.17E-00	1.58E 02
9	2.21E	00	4.41E	00	4.41E	00	0.00	2.17E-00	1.58E 02
10	2.21E	00	4.41E	00	4.41E	00	0.00	2.17E-00	1.58E 02
11	2.21E	00	4.41E	00	4.41E	00	0.00	2.17E-00	1.58E 02
12	2.21E	00	4.41E	00	4.41E	00	0.00	2.17E-00	1.58E 02
13	2.21E	00	4.41E	00	4.41E	00	0.00	2.17E-00	1.58E 02
14	2.21E	00	4.41E	00	4.41E	00	0.00	2.17E-00	1.58E 02
15	2.21E	00	4.41E	00	4.41E	00	0.00	2.17E-00	1.58E 02
16	2.21E	00	4.41E	00	4.41E	00	0.00	2.17E-00	1.58E 02
17	2.21E	00	4.41E	00	4.41E	00	0.00	2.17E-00	1.58E 02
18	2.21E	00	4.41E	00	4.41E	00	0.00	2.17E-00	1.58E 02
19	2.21E	00	4.41E	00	4.41E	00	0.00	2.17E-00	1.58E 02

Table H-6 Cont'd

APPENDIX II

Table 5.6 (cont.)

TIME	2	3	4	5	6	7	8	9	10	11	12	13	14	15	16	17	18	19	20	21	22	23	24	25	26	27	28	29	30	31	32	33	34	35	36	37	38	39	40	41	42	43	44	45	46	47	48	49	50	51	52	53	54	55	56	57	58	59	60	61	62	63	64	65	66	67	68	69	70	71	72	73	74	75	76	77	78	79	80	81	82	83	84	85	86	87	88	89	90	91	92	93	94	95	96	97	98	99	100
TIME	2	3	4	5	6	7	8	9	10	11	12	13	14	15	16	17	18	19	20	21	22	23	24	25	26	27	28	29	30	31	32	33	34	35	36	37	38	39	40	41	42	43	44	45	46	47	48	49	50	51	52	53	54	55	56	57	58	59	60	61	62	63	64	65	66	67	68	69	70	71	72	73	74	75	76	77	78	79	80	81	82	83	84	85	86	87	88	89	90	91	92	93	94	95	96	97	98	99	100

Table H-6-Cont'd

APPENDIX I

NON-LINEAR ANALYSIS BASED ON PROPELLANT DILATATION

Aerojet Solid Propulsion Company
Report 1341-26F

Appendix I

NON-LINEAR ANALYSIS BASED ON PROPELLANT DILATATION

In general, the response of grains to various loading conditions is mainly determined by the dilatational behavior of the propellant, hence, it would appear that accounting for the non-linear dilatational response of propellant is of primary importance.

Although insufficient experimental data is available to permit a comprehensive characterization of the non-linear dilatational effects, it was felt that an evaluation could be obtained by utilizing a description which qualitatively accounts for the behavior reported for a limited class of stress states in References I-1 and I-2, and which predicts reasonable results for other stress states. Because of the tentative nature of the characterization, it was deemed desirable to approximate the non-linear behavior by an equation which could be incorporated into the existing analysis with a minimum amount of effort.

With the above objectives in mind the following approximations were made: (1) The thermo-rheologically simple linear viscoelastic distortional stress-strain law and the temperature induced volume change relationships would remain unchanged; (2) the stress induced dilatational response would be approximated as elastic. It was felt that the viscoelastic dilatation (compare Figures 11 and 12 of Reference I-2), is of secondary importance as compared to the basic non-linear effects. Additionally, the lack of experimental evidence concerning dilatation during unloading precludes its consideration at this time. (3) The stress-dilatation relationship would be considered to be temperature independent (it was felt that the actual temperature dependence was of secondary importance). (4) The characterization would be limited to relatively small strains. (5) The elastic relationship between the dilatation and the stress state could be expressed as:

$$(\theta - 3\alpha\Delta T) \approx f(g(\tau_{ij})) = f(\tau_{ij}) \quad (I-1)$$

where "f" is a non-linear algebraic function of the quantity "g", $g(\tau_{ij})$ is in turn a non-linear function of the stress invariants. The stress invariants are defined by the equations

Aerojet Solid Propulsion Company
Report 1341-26F

Appendix I

$$\Theta_1 = \tau_{11} + \tau_{22} + \tau_{33} \quad (I-2)$$

$$\Theta_2 = \begin{vmatrix} \tau_{22} & \tau_{23} \\ \tau_{32} & \tau_{33} \end{vmatrix} + \begin{vmatrix} \tau_{11} & \tau_{31} \\ \tau_{31} & \tau_{33} \end{vmatrix} + \begin{vmatrix} \tau_{11} & \tau_{12} \\ \tau_{12} & \tau_{22} \end{vmatrix}$$

$$\Theta_3 = \begin{vmatrix} \tau_{11} & \tau_{12} & \tau_{13} \\ \tau_{12} & \tau_{22} & \tau_{23} \\ \tau_{13} & \tau_{23} & \tau_{33} \end{vmatrix}$$

For linear theory we have $g = \Theta_1$ and $f = \frac{K}{3} g$ i.e.,

$$(\Theta - 3\alpha\Delta T) = K \frac{\Theta_1}{3} \quad (I-3)$$

Appropriate forms of the functions "f" and "g" were determined in the following manner. For a uniaxial state of stress (i.e., $\tau_{ij} = 0$ except $\tau_{11} \neq 0$) noting that $\Theta_2 = \Theta_3 = 0$, it was assumed that

$$g(\Theta_1) \approx \Theta_1 = \tau_{11}, \text{ i.e.,}$$

$$(\Theta - 3\alpha\Delta T) \approx f(\tau_{11}) \quad (I-4)$$

Inspecting results from uniaxial tests (and uniaxial tests with small superimposed hydrostatic pressures) the form of the function "f" was determined. The form of the function "g" was determined by inspecting the results of uniaxial tests with various levels of superimposed hydrostatic pressures. Lastly, the forms of the functions "f" and "g" were appropriately modified so that the predictions for other stress states would intuitively agree with the physical explanation given in Reference (I-2) for the non-linear dilatation phenomenon.

Aerojet Solid Propulsion Company
Report 1341-26F

Appendix I

The experimental results presented in Figures 8, 9, 10, 12 and 14 of Reference (I-2) were plotted in the form $\theta \sim \tau_{11}$ in Figure I-1. Although these data certainly demonstrate a dependence upon temperature and strain rate (and of course a dependence upon "volume of loading"), insufficient data were available to permit a description of this dependence, hence, it was neglected. No data was available for compressive stress states, however, it was anticipated that for negative stresses the relationship would be relatively linear. The data presented in Figure I-1 (i.e., the function "f") was approximated by a hyperbola, i.e., the relationship between θ and the function "g" was written as:

$$\theta = \frac{P_2 + P}{2} + \frac{\beta_2 - \beta}{2} + B \quad (I-5)$$

where

$$\beta_1 = \theta_o + \frac{1}{K_T} (g_1 - g_o)$$

$$B = \frac{\beta_1 (\theta_o - g_o/K_c)}{1 - \frac{\beta_1 K_g}{g_1}}$$

$$\beta_2 = \frac{BK_T}{g_1} - \frac{g}{K_c}$$

$$\beta = \frac{1}{K_T} (g_1 - g)$$

The meaning of the parameters K_T , K_c , g_1 , g_o and θ_o is illustrated in

VOLUME CHANGE
(Data taken from Reference (7))

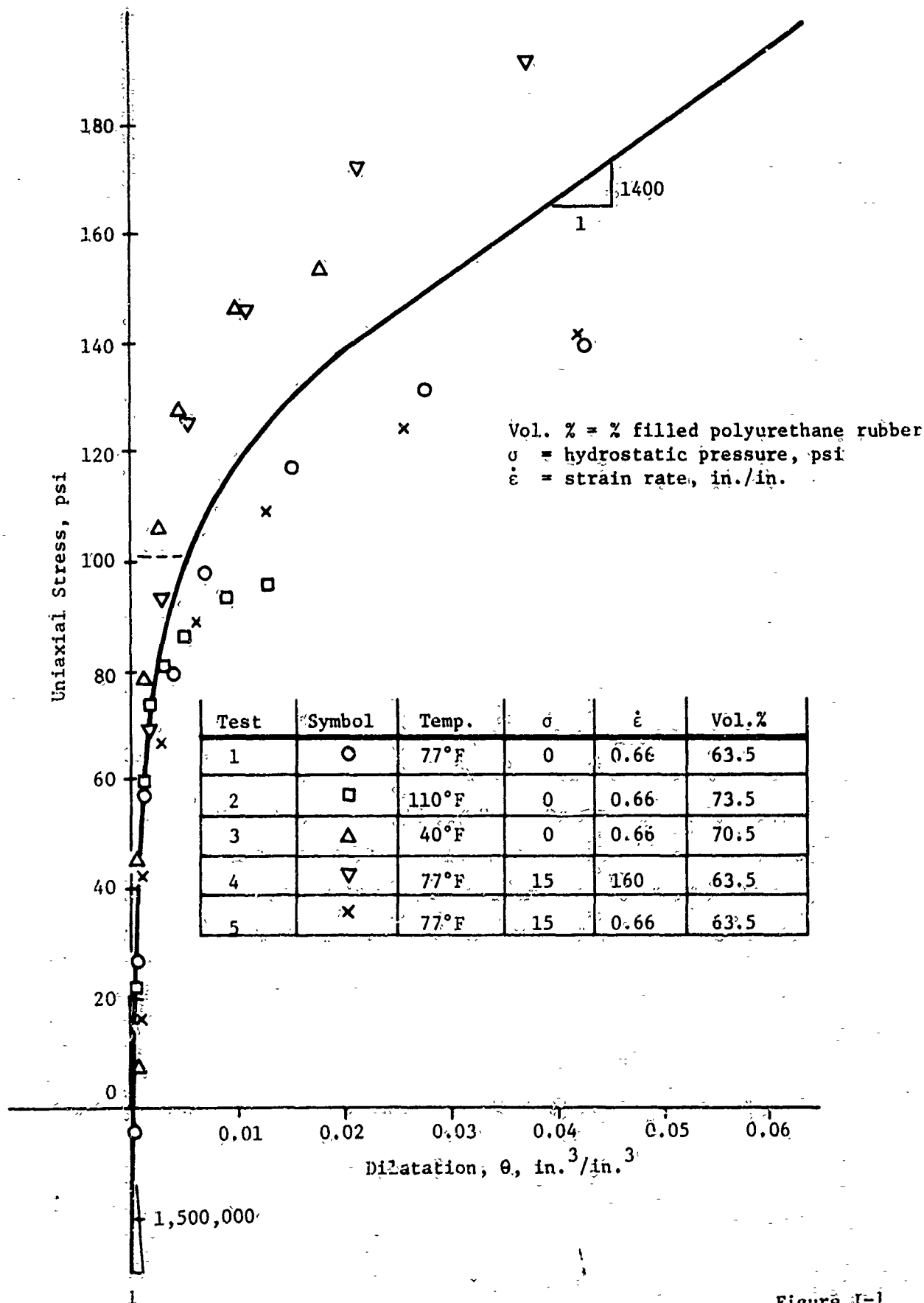


Figure I-1

Aerojet Solid Propulsion Company
Report 1341-26F

Appendix I

Figure I-2. The form of the function $g(\theta_1)$ was determined by considering the data presented in Figure 1 of Reference (I-2). A number of different functional forms were investigated from among which the following form was selected.

$$g(\theta_1) = \theta_1 - K_1 \theta_1^2 + K_2 \theta_1^3 + K_3 \theta_1^3 \quad (I-6)$$

The values of K_1 , K_2 , and K_3 were selected by noting that Equation (I-1) states that for a given amount of dilatation the value of "g" should be a constant. Thus for the different stress states (corresponding to different values of hydrostatic pressure) given in Figure 1 of Reference (I-2) an attempt was made to select the function "g" so that for a given value of θ all states would yield a common value of "g". The following values were found for the parameters

$$K_1 = 4.9 \times 10^{-3}$$

$$K_2 = 2.3 \times 10^{-5}$$

$$K_3 = 5.7 \times 10^{-6}$$

Using these parameters the following table was constructed

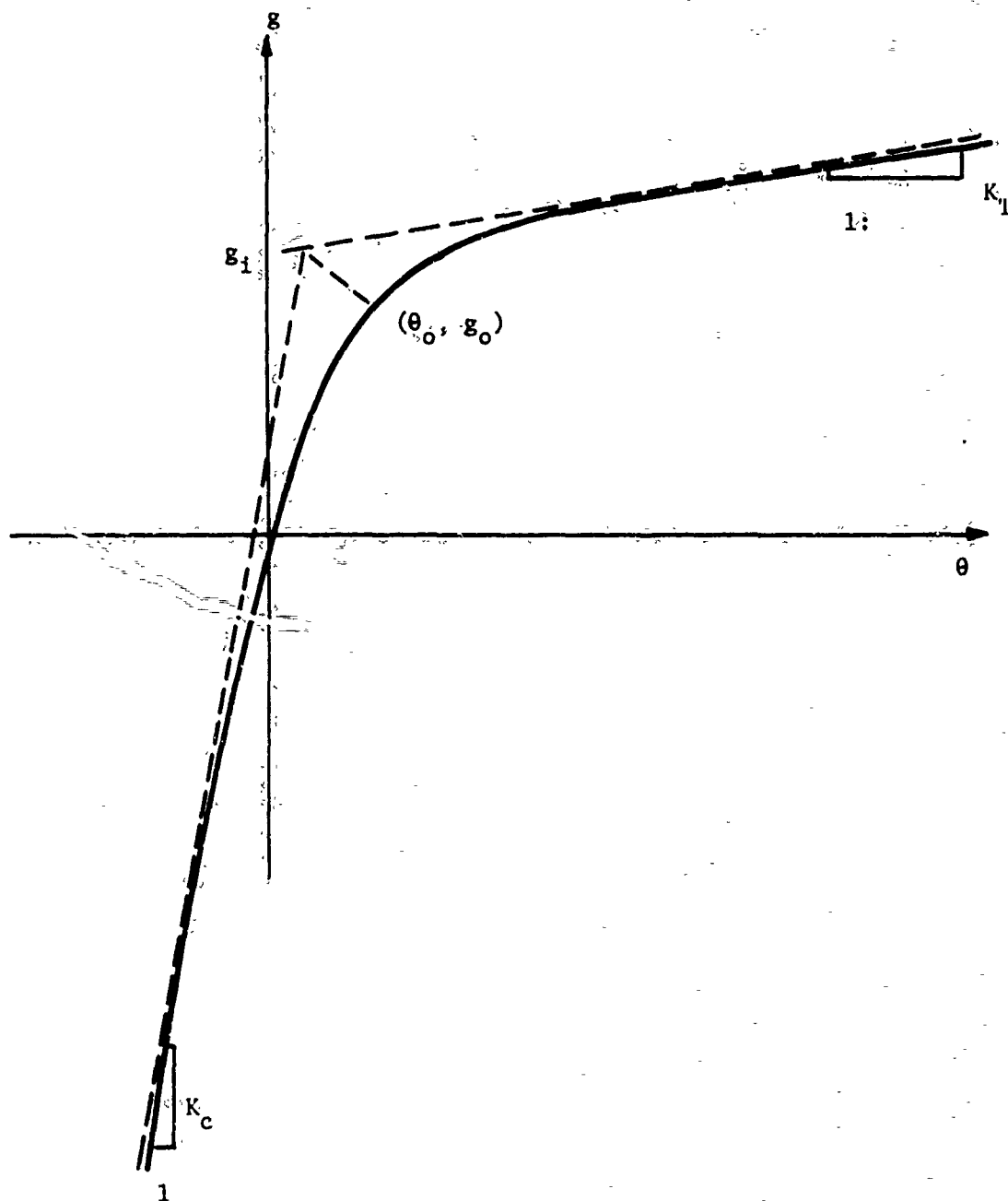
1	2	3	4	5
Hydrostatic Pressure, psi	$\theta = .005$		$\theta = .01$	
	g	$\theta/3$	g	$\theta/3$
15	66	54	84	68
65	66	-5	99	14
165	101	-150	125	-115

If the dilatational response could be described by a linear elastic law all the entries in Column 3 (and in Column 5) would need to be approximately equal, the extreme grossness of this approximation is evident. If the non-linear function "g" is to represent the experimental data all the entries in Column 2 (and in Column 4) would need to be

Aerojet Solid Propulsion Company
Report 1341-26F

Appendix I

PARAMETERS DEFINING HYPERBOLIC
DILATATIONAL RELATIONSHIP



Aerojet Solid Propulsion Company
Report 1341-26F

Appendix I

approximately equal, while this is not true, the very substantial improvement of the non-linear representation as compared to the linear representation is evident.

While no experimental information was available for stress states other than the uniaxial test with superimposed hydrostatic pressure, it is extremely important that the proposed model predicts reasonable results for other stress states as these stress states may occur in a given grain problem. Utilizing the proposed non-linear model dilatation was predicted for the following stress states:

- (a) Uniaxial stress with superimposed hydrostatic pressure (Figure I-3)
- (b) Hydrostatic pressure (Figure I-4)
- (c) Biaxial stress with superimposed hydrostatic pressure (Figure I-5)
- (d) Simple shear with superimposed hydrostatic pressure (Figure I-6)

The straight lines in Figure I-3 indicate the predictions of the linear model, the curved lines the predictions of the non-linear model. The predictions of the non-linear model qualitatively appear to be reasonable.

The incorporation of the non-linear dilatational relationship (Equation (I-1)) into the existing thermoviscoelastic analyses presented some difficulties. The existing thermoviscoelastic analysis employs the following incremental relationship for dilatation (for time increment N):

$$(\Delta\theta_N - 3\alpha\Delta T_N) = K_N \frac{\Delta\theta_N}{3} + \chi_N t_{N-1} \leq t \leq t_N \quad (I-7)$$

In the previous linear analysis K_N was considered to be a constant (the elastic bulk modulus) and $\chi_N = 0$. The utilization of Equation (I-7) as an approximation to Equation (I-1) was accomplished as follows:

Having obtained the solution for time t_{N-1} consider the utilization of Equation (I-7) for $t_{N-1} \leq t \leq t_N$. Symbolically denoting the stress state at time t_{N-1} as $\tau_{ij,N-1}$ and the incremental change in stress state for

$t_{N-2} \leq t_{N-1}$ as $\Delta\tau_{ij,N-1}$. The following two associated stress states are defined:

Appendix 1

DILATATIONAL PREDICTIONS FOR UNIAXIAL STRESS WITH SUPERIMPOSED HYDROSTATIC PRESSURE

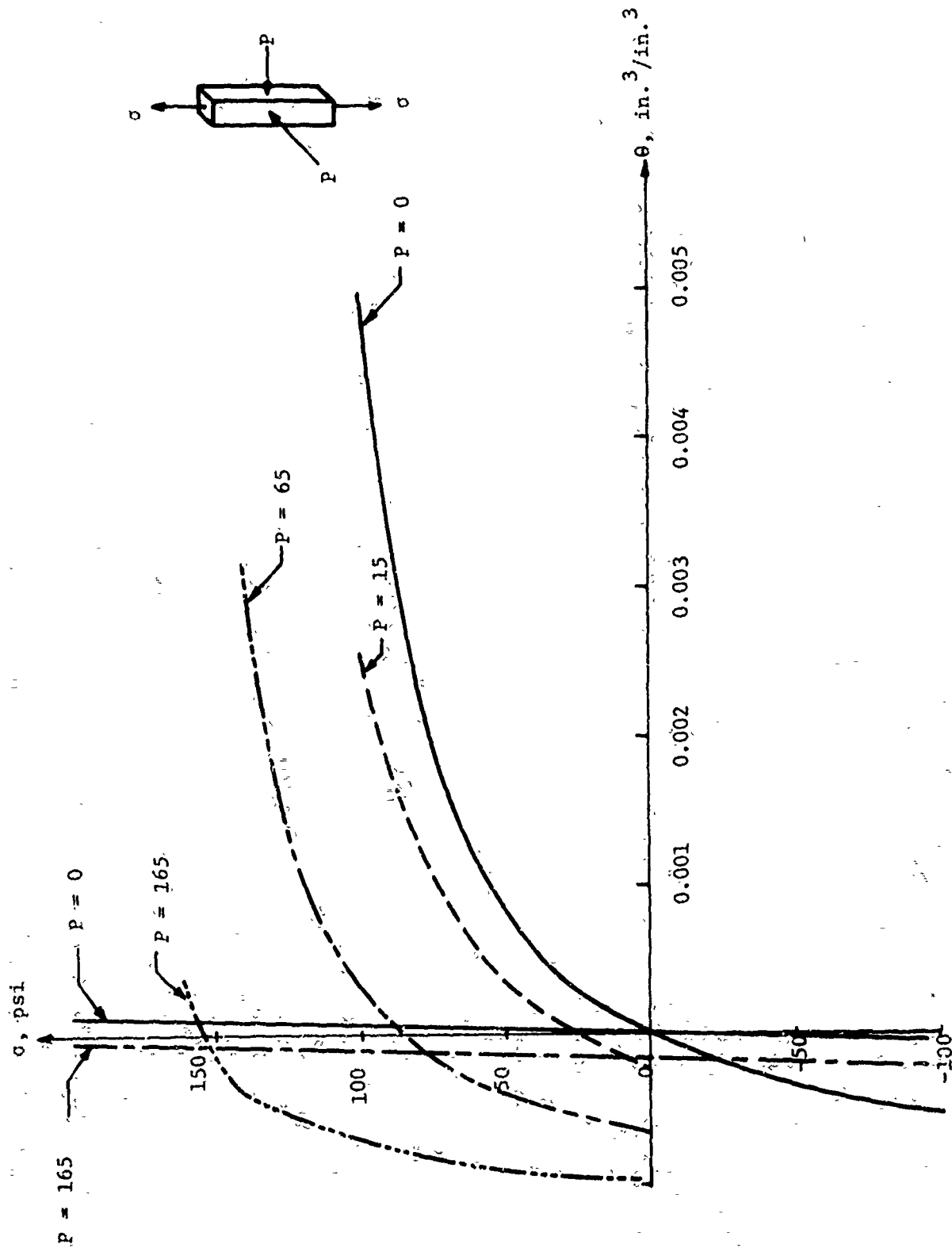
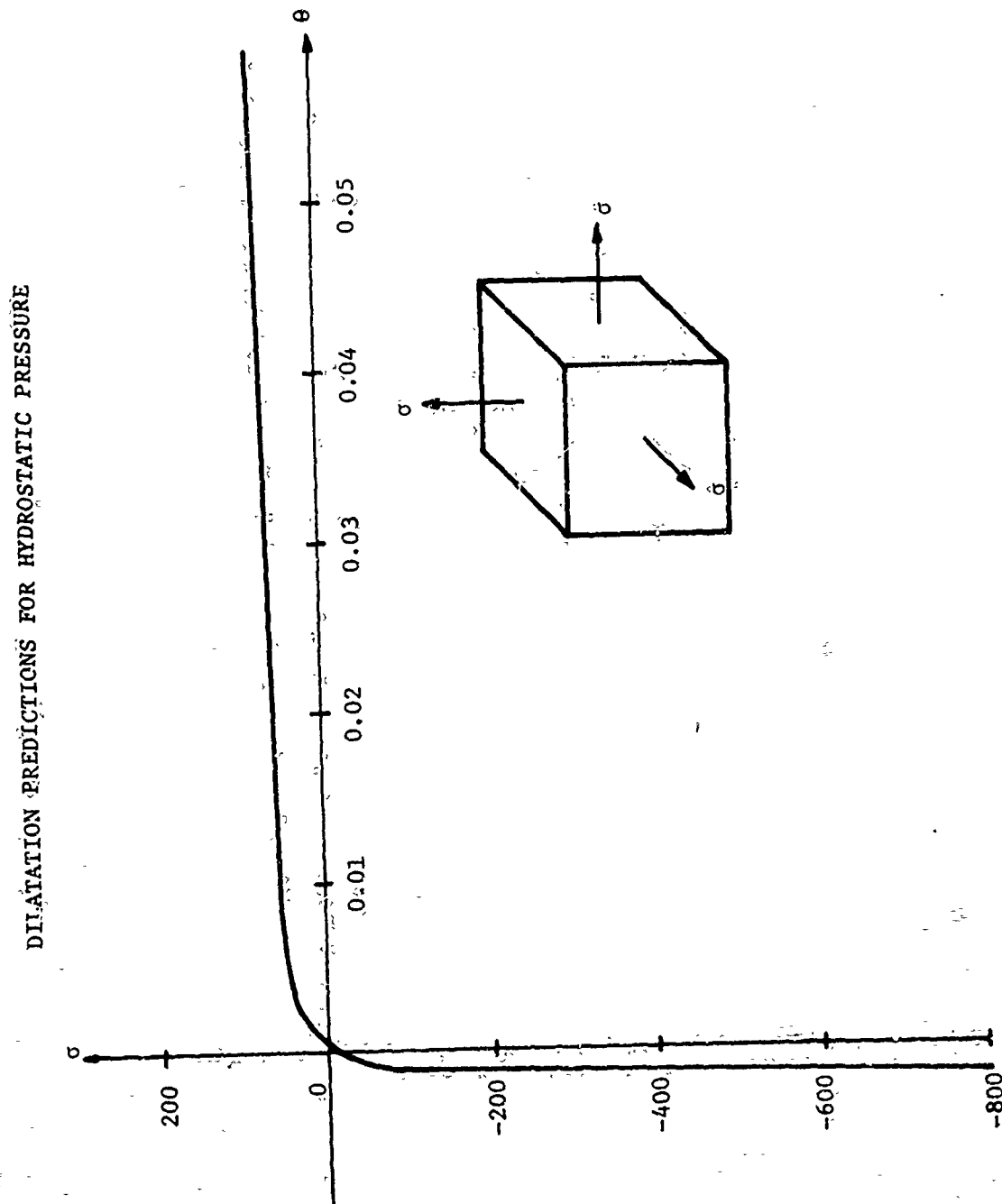
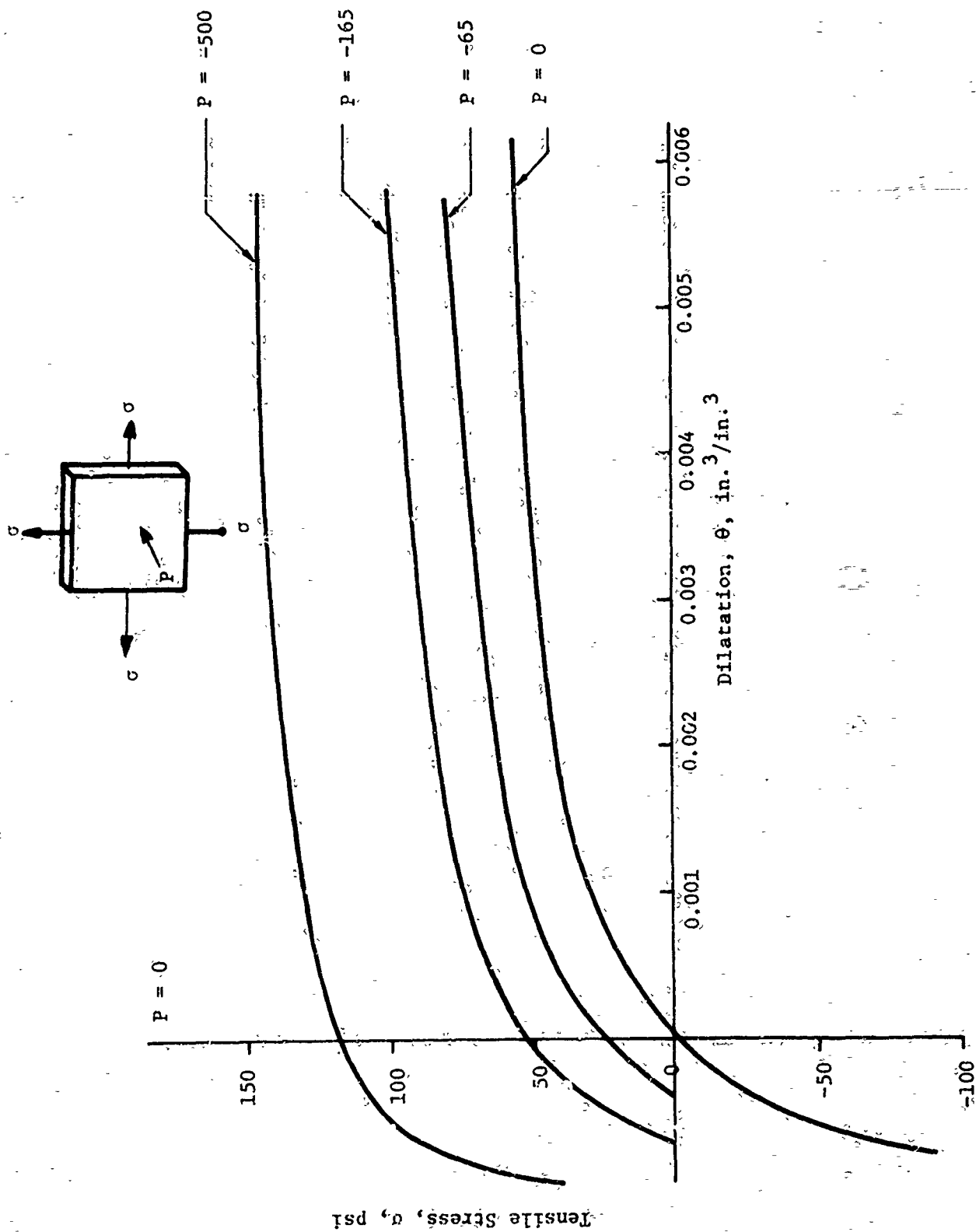


Figure I-3.





DILATATIONAL PREDICTIONS FOR BIAXIAL STRESS WITH SUPERIMPOSED HYDROSTATIC PRESSURE

Figure I-5

Aerojet Solid Propulsion Company
Report 1341-26F

Appendix 1

DILATATIONAL PREDICTIONS FOR SHEAR WITH SUPERIMPOSED HYDROSTATIC PRESSURE

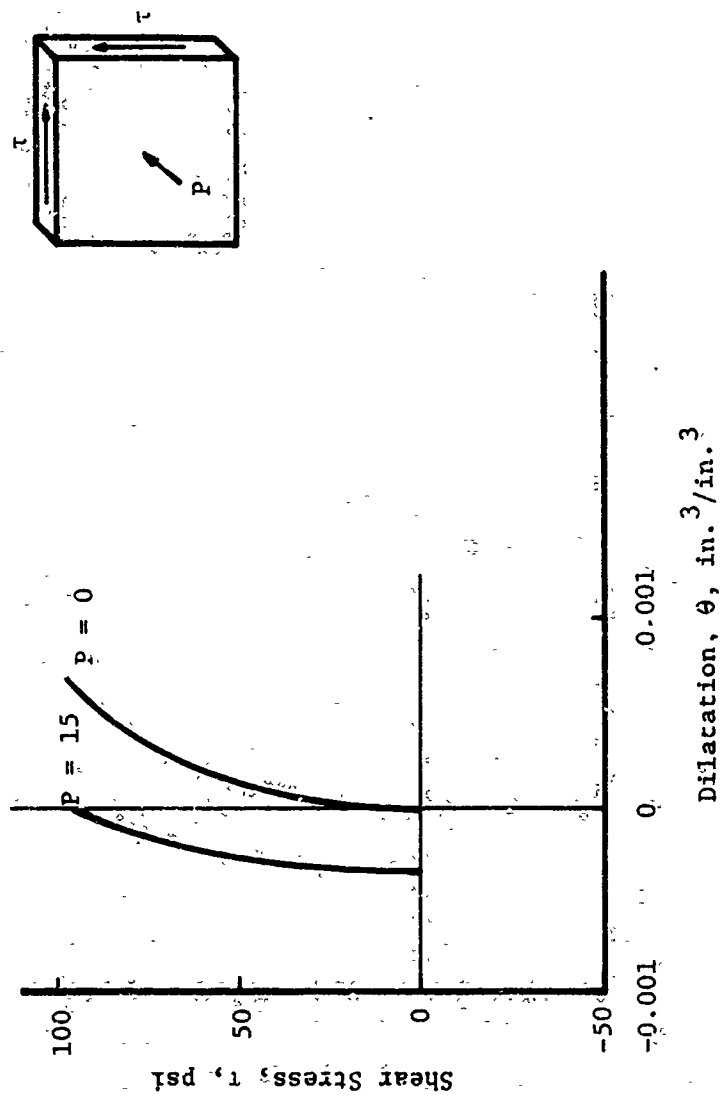


Figure I-6

Aerojet Solid Propulsion Company
Report 1341-26F

Appendix I

$$\tau_{ija} \equiv \tau_{ij_{N-1}} + \Delta \tau_{ij_{N-1}} \quad (I-8)$$

$$\tau_{ijb} \equiv \tau_{ij_{N-1}} + \Delta \tau_{ij_{N-1}} \quad (I-9)$$

Utilizing Equations (I-1), (I-2), (I-8), and (I-9), the following quantities are calculated θ_a , θ_b , θ_a and θ_b . The following approximate relationship is written for values of θ between θ_a and θ_b

$$\theta = \frac{\theta_a \theta_b - \theta_b \theta_a}{\theta_a - \theta_b} + \frac{\theta_a - \theta_b}{\theta_a - \theta_b} \theta \quad (I-10)$$

Assuming that the absolute value of the change in stress during the increment $\Delta \tau_N$ will be of the same order of magnitude as $|\Delta \tau_{ij_{N-1}}|$

(i.e., using Equation (I-10) and writing $\theta_N = \theta_{N-1} + \Delta \theta_N$ and $\theta_N = \theta_{N-1} + \Delta \theta_N$ yields

$$\theta_{N-1} + \Delta \theta_N = \frac{\theta_a \theta_b - \theta_b \theta_a}{\theta_a - \theta_b} + \frac{\theta_a - \theta_b}{\theta_a - \theta_b} (\theta_{N-1} + \Delta \theta_N) \quad (I-11)$$

Comparing the above expression to Equation (I-7) yields

$$K_N = \frac{\theta_a - \theta_b}{\theta_a - \theta_b}$$

$$X_N = \frac{\theta_a \theta_b - \theta_b \theta_a}{\theta_a - \theta_b} + \frac{\theta_a - \theta_b}{\theta_a - \theta_b} \theta_{N-1} - \theta_{N-1}$$

Because of the secant approximation to the non-linear function, in general, $X_N \neq 0$.

Aerojet Solid Propulsion Company
Report 1341-26F

Appendix I

References.

- I-1 Farris, R. J., "The Character of the Stress-Strain Function for Highly Filled Elastomers", Trans. of the Soc. of Rheology 12:2, 303-314 (1968).
- I-2 Farris, R. J., "The Influence of Vacuole Formation on the Response and Failure of Filled Elastomers", Trans. of the Soc. of Rheology 12:2, 315-334 (1968).

APPENDIX J

BASIC CUMULATIVE DAMAGE EQUATIONS

Aerojet Solid Propulsion Company
Report 1341-26F

APPENDIX J

BASIC CUMULATIVE DAMAGE EQUATIONS

The LCD relation merely states the manner in which damage can be added. To apply the relation in a three-dimensional stress field requires a time-dependent, stress failure criterion. An empirical approach showed that the applicable relation is a time-dependent, maximum principal stress, failure criterion (MPS).

Combining the LCD and MPS criteria leads to integral relations which take full account of the past stress-time-temperature history at a point in the grain.

1. Linear Cumulative Damage Relations

The very simple relation, applicable to solid propellant failures, is defined in terms of tests made under a constantly imposed "true" stress, σ_t . For a number, N, of discrete stress levels the accumulated damage fraction, ΣD , is given by the following linear relation:

$$\Sigma D = \frac{1}{P(n)} \sum_{i=1}^N \frac{\Delta t_i}{\bar{t}_{fi}} \quad (J-1)$$

where ΣD is the cumulative damage

$P(n)$ is a statistical distribution parameter and relates the n^{th} test specimen in the distribution to the mean of the population.

Δt_i is the increment of time the specimen is exposed to the i^{th} "true" stress level

\bar{t}_{fi} is the mean time-to-failure for the population of specimens if the specimens saw only the i^{th} "true" stress level.

The accumulated damage, ΣD , thus gives the fraction of that damage required to fail the specimen. Thus, by definition $\Sigma D = 1$ at failure.

The parameter, $P(n)$, is a highly useful term in that it provides the focal point for all the statistical studies pertinent to the cumulative damage relations. In its simplest form $P(n)$ defines the position of the individual failure with respect to the mean of the distribution of these failures. This is seen on considering specimens held under a single stress, where $P(n)$ equals the ratio of the time-to-failure, $t_f(n)$, for the n^{th} individual divided by the mean time-to-failure for the entire population, \bar{t}_f .

Aerojet Solid Propulsion Company

Report 1341-26F

Appendix J

Thus, we have

$$P(n) = t_f(n) / \bar{t}_f \quad (J-2)$$

The cumulative damage relation merely preserves this concept of $P(n)$ for conditions of complicated loading histories.

In Reference J-1, it was shown that $P(n)$ is independent of the stress level. This justifies placing the parameter outside the summation in Equation (J-1).

Statistical evaluations of $P(n)$ obtained from solid propellant failure testing, show the parameter to follow approximately a log normal distribution.

2. Time-Dependent Maximum Principal Stress Failure Criterion

The most general form of the MPS failure criterion for solid propellants appears to be a modified power-law relation. However, a simple power-law approximation to this criterion covers all of the practical motor problems that we have met to date. This power-law relation has the following form:

$$\bar{t}_f = t_o a_T \left(\frac{\sigma_t - \sigma_{cr}}{\sigma_{t_o} - \sigma_{cr}} \right)^{-B} \quad (J-3)$$

- where
- σ_t is the "true" stress applied to the specimen.
 - \bar{t}_f is the mean time-to-failure of specimens held under the constant true stress, σ_t .
 - t_o is the unit value of the time for whatever units are used in measuring t_f .
 - σ_{t_o} is the true stress required to fail the specimen in the time t_o .
 - σ_{cr} is the critical true stress below which no failures are observed.
 - a_T is the time-temperature shift relation.

Aerojet Solid Propulsion Company

Report 1341-26F

Appendix J

It has been found to apply to solid propellant behavior with correlation coefficients usually exceeding 0.98.

The limiting stress, σ_{cr} , is difficult to evaluate because it is usually not large compared with the relatively large variability typical of solid propellants. It appears to be negligibly small (except for the effects of pressure) for all the propellants tested to date.

The cumulative damage relation is generalized as follows. First, Equation (J-3) is combined with Equation (J-1) to obtain the cumulative damage relation in terms of discrete stress levels, loading time intervals, and test temperatures.

$$\Sigma D = \frac{1}{P(n)} \sum \left[\frac{\sigma_{ti} - \sigma_{cr}}{\sigma_{to} - \sigma_{cr}} \right]^B \frac{\Delta t_i}{t_o a_T} \quad (J-4)$$

where σ_{ti} is the i^{th} stress level.

For continuous changes in the stress and in the temperature, Equation (J-4) becomes:

$$\Sigma D \approx \frac{1}{P(n) (\sigma_{to} - \sigma_{cr})^B t_o} \int_0^t \frac{(\sigma_t - \sigma_{cr})^B}{a_T(t)} dt \quad (J-5)$$

where σ_t , the true stress, is now a function of time.

$a_T(t)$ is the time-temperature shift relation with the temperature expressed as a function of time.

Equation (J-5) represents a general form of the linear cumulative damage relation for solid propellants. This equation permits the summation of damage for any type of thermal or mechanical loading history, provided the stresses, times and temperatures are known. Also, Equation (J-5) can be applied without change to three dimensional stress problems.

Aerojet Solid Propulsion Company

Report 1341-26F

Appendix J

REFERENCES

- J-1 Bills, K. W., Jr., Peterson, F. E., Steele, R. D., and Sampson, R. C.,
"Development of Criteria for Solid Propellant Screening and
Preliminary Engineering Design", Aerojet Report 1159-81F
(December 1968).

APPENDIX K

STUDY OF PROPELLANT FAILURE UNDER PRESSURE

Aerojet Solid Propulsion Company

Report 1341-26F

APPENDIX K

STUDY OF PROPELLANT FAILURE UNDER PRESSURE

A. FAILURE MECHANISMS

The basic mechanisms of propellant failure have been extensively studied under current and past research programs (K-1, K-2). Failure is considered to be a three step process beginning with vacuole formation. The vacuoles may initiate in the polymer or at the binder-filler interface. The associated volume change may be so negligible that the process is termed a "Mullin's Effect". The second step is the extension of the vacuoles until they overlap producing a thin membrane of polymer between them. The third and final step is the production of a critical, biaxial, stress field in one or more of the thin membranes. The resulting tears propagate very slowly relative to the speed of sound in the propellant. This failure mechanism is the basis of the considerations made later.

The maximum principal stress failure criterion, Equation (J-3), contains a simple stress difference term, $\sigma_t - \sigma_{cr}$. Some feel that this indicates a maximum shear stress criterion to be operative. In biaxial tension this is expressed by

$$\tau(\text{critical}) = (\sigma_1 - \sigma_2)/2 \quad (K-1)$$

where $\tau(\text{critical})$ is the maximum shear strength of the material
 σ_1 and σ_2 are principal stresses

Considering the stress difference terms only, for both failure criteria, leads to the tabulation in Table K-1. It is assumed that a maximum principal stress, σ , is imposed in tension. The remaining stresses are tabulated.

Table K-1 shows that the two criteria give identical results for simple uniaxial and strip-biaxial tensile data from which the MPS criterion was derived. However, the two criteria differ greatly when applied to the triaxial, tensile, stress field of the poker chip specimen. In this case, the stress difference for the maximum shear stress criterion is dependent upon $1-k$, which is very small, indicating that very large axial stresses, σ , would be required to fail the specimen. On the other hand, the MPS criterion gives a relatively large value for the stress difference term, $\sigma_t - \sigma_{cr}$. This difference, like those for the uniaxial and biaxial tensile data, equals the axial stress on the specimen. Tests on poker chip specimens showed the MPS criterion to hold, (K-2) while the maximum shear stress criterion is grossly in error.

Aerojet Solid Propulsion Company
Report 1341-26F

Appendix X

TABLE K-1

STRESS DIFFERENCES AT ATMOSPHERIC PRESSURE

Test Mode	MPS Criterion			Maximum Shear Stress Criterion		
	σ_t	σ_{cr}^*	$\sigma_t - \sigma_{cr}$	σ_1	σ_2	$\sigma_1 - \sigma_2$
Uniaxial Tensile Test	σ	0	σ	σ	0	σ
Strip-Biaxial Tensile Test	σ	0	σ	σ	0	σ
Poker Chip Tensile Test	σ	0	σ	σ	$k\sigma$	$(1-k)\sigma$

* σ_{cr} is set equal to zero, which appears to be the case for many composite propellants.

** The maximum tensile stress at the center of the specimen.

*** k is a proportionality factor which, in this case, is close to one.

Aerojet Solid Propulsion Company

Report 1341-26F

Appendix K

This result is not surprising in view of the failure mechanisms summarized above. Tensile failures in uniaxial, biaxial, and poker chip specimens follow the same mechanism. Once the vacuoles are produced all three test modes become equivalent, in that failure is produced by extension of a foam-like material until the biaxial stress in the membranes exceeds the critical value and tearing starts.

B. EVALUATING THE TIME-PRESSURE SHIFT FACTOR

The time-pressure shift factor for propellants is best understood on referring to the foam-like failure behavior mentioned above. Before the vacuoles are formed, or when they are still quite small, a_p equals one (up to about 1500 psi pressure). This was shown for tensile moduli by Wiegand, (K-3) Hazelton (K-4) and Lim and Tshoegel (K-5). At this point, the a_p values are those for the solid binder which requires large pressure changes to effect significant changes in a_p . (K-6 to 14). On the other hand, propellant failure data are sensitive to relatively small pressure changes. Dilatation constitutes the only physical difference in the propellant between the points where initial tensile moduli and failure data are obtained. At failure, this dilatation is extensive and can be partially suppressed by superimposed hydrostatic pressures. As shown by Farris (K-15) and Lim and Tshoegel (K-5), the dilatation at failure is positive, even at the higher pressure levels.

Taken together these observations indicate that a_p provides a measure of the suppression of vacuole formation. But, σ_{cr} is also a measure of the same effect. That is, σ_{cr} is the stress level at which dilatation is completely suppressed; or, conversely, the stress level where vacuoles are first formed. Also, σ_{cr} is pressure dependent, defining the point of vacuole formation over the pressure range. Thus, a_p must be a simple function of σ_{cr} . That is,

$$a_p = f(\sigma_{cr}) \quad (K-2)$$

Equation (K-2) tells us how to evaluate a_p deep in the grain. The critical stress acts in the same direction as the maximum principal stress, σ_t , and it includes that portion of the inner-bore pressure that is effective deep within the grain and which acts in the same direction as σ_t . The fraction, f , of the inner-bore pressure that acts within the grain can be obtained directly from existing stress analyses. Using this fraction the critical stress becomes, on using Equation (14) of the text,

$$\sigma_{cr} = (F/A)_{cr} = fP_i \quad (K-3)$$

where P_i is the inner-bore pressure

Aerojet Solid Propulsion Company

Report 1341-26F

Appendix K

The appropriate values of a_p for use in Equation (K-2) are obtained from empirically obtained curve of a_p versus pressure, the desired value of a_p read from the curve at a pressure numerically equal to σ_{cr} , the latter being obtained from Equation (K-3).

Aerojet Solid Propulsion Company

Report 1341-26F

Appendix K

REFERENCES

- K-1 Bills, K. W., Jr., Campbell, D. M., Sampson, R. C., and Steele, R. D., "Failures in Grains Exposed to Rapid Changes of Environmental Temperatures", Aerojet Report 1236-81F (Contract No. N00017-68-C-4415) (April 1969).
- K-2 Bills, K. W., Jr., et. al, "Solid Propellant Cumulative Damage Program", Final Report No. AFRPL-TR-63-131, Contract No. FO4611-67-C-0102, (October 1968).
- K-3 Wiegand, J. H., "Study of Mechanical Properties of Solid Propellants", Report No. 0411-10F, Aerojet-General Corporation, 1962.
- K-4 Hazelton, I. G., and Planck, R. W., "Propellant Characterization for Firing and Flight", Bulletin of 45th Meeting of ICRPG Working Group on Mechanical Behavior, p. 287 (Nov. 16-19, 1965).
- K-5 Lim, C. K., and Tschoegel, N. W., "The Effect of Pressure on the Mechanical and Ultimate Properties of Filled Elastomers", Bulletin of the Eighth Meeting of the JANNAF Mechanical Behavior Working Group, p. 153 (March 1970).
- K-6 Hughes, D. S., et al, J. App. Phys. 21, 294 (1950).
- K-7 Masuoka, S., and Maxwell, B., J. Poly. Sci, 32, 131 (1958).
- K-8 J. Res. Nat. Bur. Stds., 50, 311 (1953).
- K-9 J. Appl. Phys., 30, 337 (1959).
- K-10 Bull. Amer. Phys. Soc. II, 5, 203 (1960).
- K-11 Modern Plastics, 35, 174 (1957).
- K-12 Trans. Soc. Rheol., 4, 347 (1960).
- K-13 J. Chem. Phys., 26, 196 (1957).
- K-14 Proc. Roy. Soc., A253, 52 (1959).
- K-15 Farris, R. J., "The Influence of Vacuole Formation on the Response and Failure of Filled Elastomers", Trans. of the Soc. of Rheology, 12:2, 315-334 (1968).

APPENDIX L
EFFECTS OF PREVIOUS DAMAGE

Aerojet Solid Propulsion Company

Report 1341-26F

APPENDIX L

EFFECTS OF PREVIOUS DAMAGE

The cumulative damage relations can be used to evaluate the effects of previous damage upon propellant failure data. This may be done using the LCD analysis of a single test-to-failure curve which duplicates a given failure condition in the motor. When considering the inner-bore failure of a grain on motor pressurization we use a high rate, uniaxial tensile test performed under a superimposed hydrostatic pressure.

The cumulative damage relation appropriate to this analysis is derived here, starting with Equation (16) from the text. For this analysis, considerations are simplified by assuming the pressure and temperature to be held constant. Thus a_p and a_T become constants and may be taken outside the integral in Equation (16).

For the previously undamaged specimen the time-to-break, t_b , and the maximum true stress become normalizing parameters for the integral term, as originally shown in Reference (L-1). Thus, we let

$$A = \int_0^{t_b/t_b} \frac{(\sigma_t - \sigma_{cr})^B}{(\sigma_{tM} - \sigma_{cr})^B} d(t/t_b) \quad (L-1)$$

Equation (16) after normalization by substituting A, gives

$$\Sigma D = 1 = \frac{(\sigma_{tM} - \sigma_{cr})^B t_b A}{P(n) (\sigma_{to} - \sigma_{cr})^B t_o a_T a_p} \quad (L-2)$$

Prior to failure we can use the same normalization terms, t_b and $(\sigma_{tM} - \sigma_{cr})^B$, but take the quantity A prior to failure with the upper integration limit the time $(t < t_b)$ at which we wish to assess the damage. Thus,

$$A(t) = \int_0^{t/t_b} \frac{(\sigma_t - \sigma_{cr})^B}{(\sigma_{tM} - \sigma_{cr})^B} d(t/t_b) \quad (L-3)$$

and

$$\Sigma D(t) = \frac{(\sigma_{tM} - \sigma_{cr})^B t_b A(t)}{P(n) (\sigma_{to} - \sigma_{cr})^B t_o a_p a_p} \quad (L-4)$$

This relation is greatly simplified on dividing Equation (L-4) by (L-2) to give

$$\Sigma D(t) = A(t)/A \quad (L-5)$$

Considering Equation (L-5), if the specimen which had been previously damaged fails at the time t , then the total damage on the specimen, by definition, must equal one. Since $\Sigma D(t)$ is less than one, the difference must be accounted for by the previous damage, ΣD_p . Thus, $\Sigma D(t)$ becomes

$$\Sigma D(t) = 1 - \Sigma D_p \quad (L-6)$$

The values of A and $A(t)$ can be obtained by integration of the data from a single uniaxial test record, from which the ratio $A(t)/A$ and hence ΣD_p can be plotted versus testing time. From the original test record we can make a plot of the stress versus time and the strain versus the time. Using these three plots then for failure at any given testing time, t , corresponding values for the stress, the strain and ΣD_p can be read off. Plotting the values of σ and ϵ versus ΣD_p gives the desired failure curves and shows the reduction in the undamaged^p values ϵ_b and σ_b caused by the previous damage.

APPENDIX M
INPUT DATA FOR PRESSURIZATION TESTS
ON A PBAN PROPELLANT

Aerojet Solid Propulsion Company

Report 1341-26F

APPENDIX M

INPUT DATA FOR PRESSURIZATION TESTS ON A PBAN PROPELLANT

The data input procedures follow those shown in Appendix A. The Prony Series constants are tabulated in Table M-1. The time-temperature and the time-pressure shift factors are tabulated in Table M-2.

The cumulative damage parameters for this propellant are as follows:

$$B = 8.75$$

$$\sigma_{to} = 71 \text{ psi}$$

$$t_o = 1 \text{ min.}$$

For reference purposes we have provided a master relaxation curve, Figure M-1, and the curves for a_T and a_p , Figures M-2 and M-3, respectively.

Aerofjet Solid Propulsion Company

Report 1341-26F

Appendix M

TABLE M-1

MODULUS INPUT FOR PBAN PROPELLANT

<u>log t/a_T, min.</u>	<u>E(T) psi</u>	<u>B_T min.⁻¹</u>	<u>A_T/3</u>	<u>i</u>
			8	0
-11	11,000	5 x 10 ¹⁰	3241.4	1
-10	6,600	5 x 10 ⁸	1187.7	2
-9	3,700	5 x 10 ⁶	287.07	3
-8	1,850	5 x 10 ⁴	108.14	4
-7	1,200	5 x 10 ²	45.09	5
-6	750	5 x 10 ⁰	32.153	6
-5	550	5 x 10 ⁻²	18.209	7
-4	398	5 x 10 ⁻⁴	14.289	8

Aerojet Solid Propulsion Company

Report 1341-26F

Appendix M

TABLE M-2
SHIFT FACTORS FOR PBAN PROPELLANT

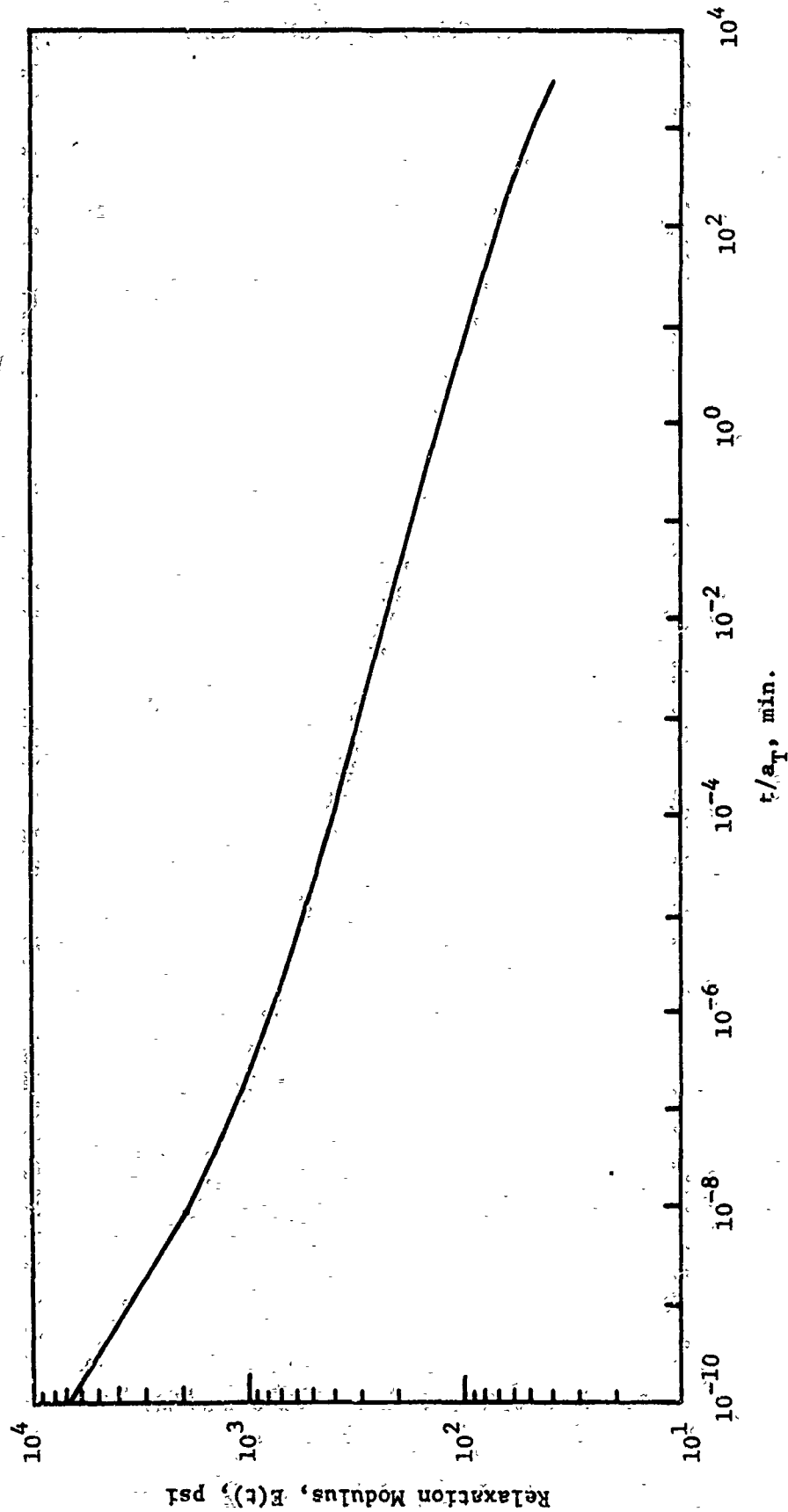
TIME-TEMPERATURE SHIFT FACTORS

<u>Temp., °F</u>	<u>$\log_{10} a_T$</u>
180	-2.508
150	-1.903
110	-0.876
77	0
40	2.097
0	4.057
-40	7.008
-75	10.528

TIME-PRESSURE SHIFT FACTOR

<u>Press., psig.</u>	<u>a_p</u>	<u>$\log_{10} a_p$</u>
0	1	0
200	51	1.71
600	150	2.176
1000	250	2.398

RELAXATION MODULUS FOR PBAN PROPELLANT



Aerojet Solid Propulsion Company
Report 1341-26F

Appendix M

TIME-TEMPERATURE SHIFT FACTOR FOR PBAN PROPELLANT

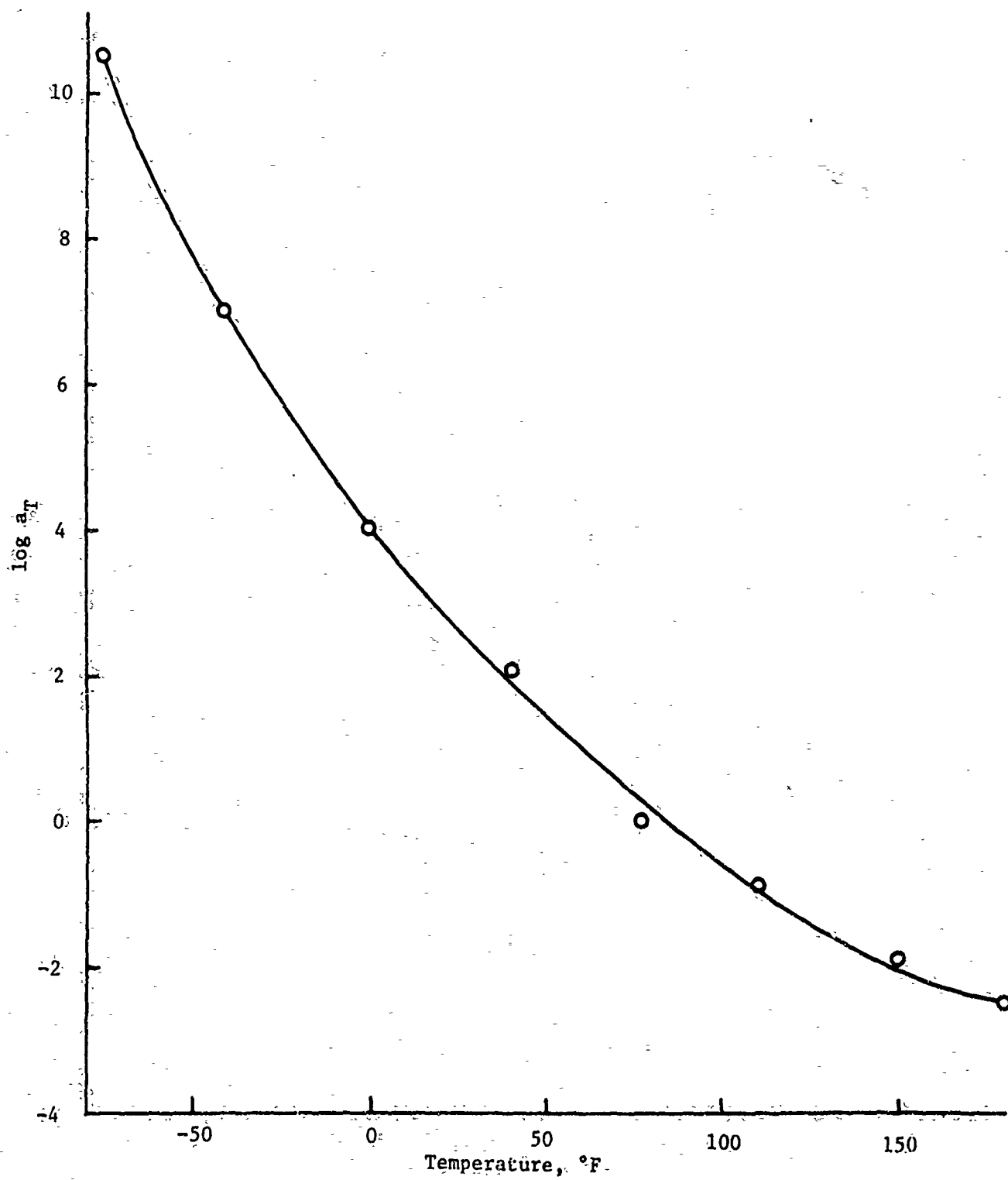
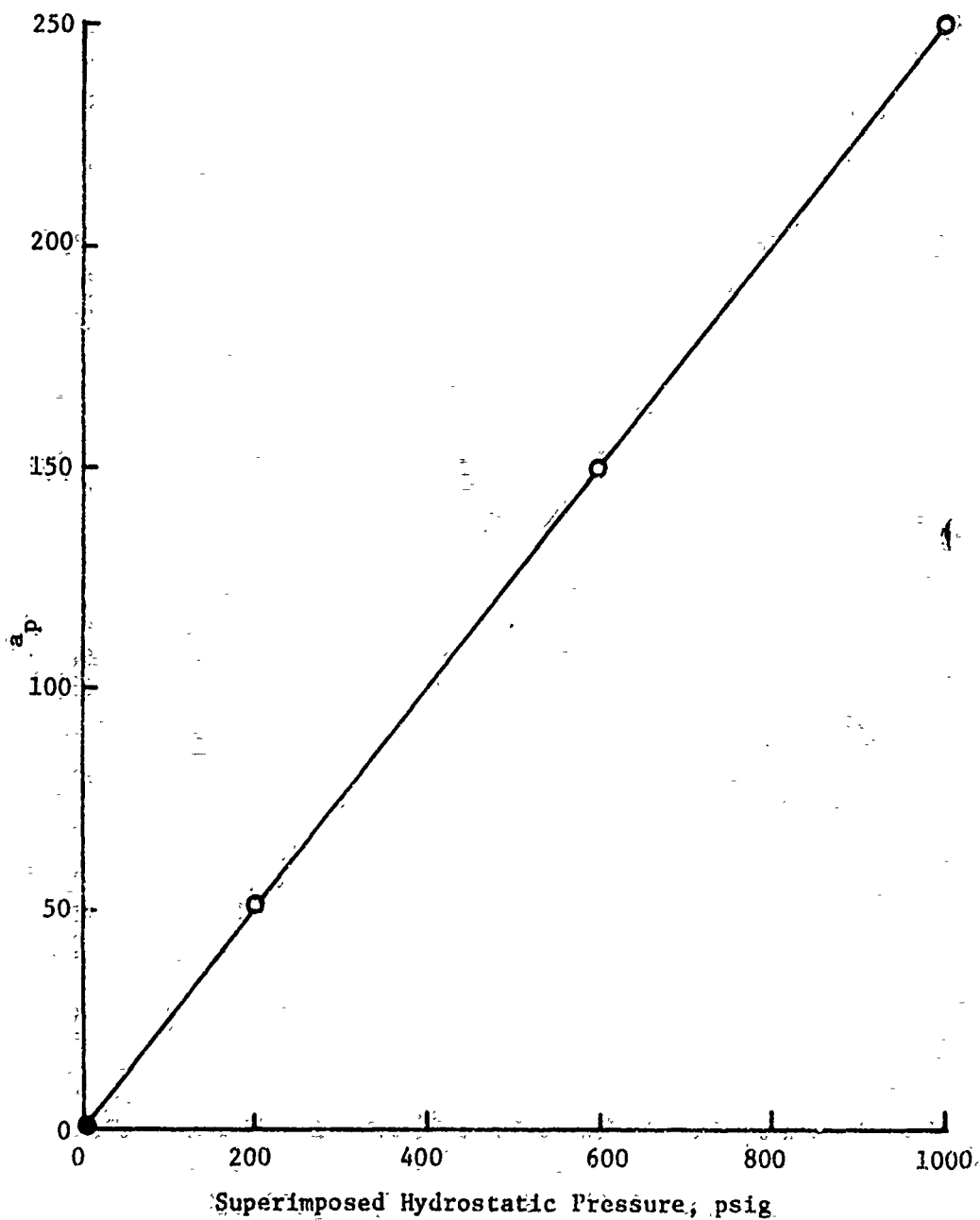


Figure M-2

Aerojet Solid Propulsion Company
Report 1341-26F

Appendix M

TIME-PRESSURE SHIFT FACTOR FOR PBAN PROPELLANT



Superimposed Hydrostatic Pressure, psig

Figure M-3